NASA
Technical Memorandum 4264

AVSCOM
Technical Report 91-B-003

Aerodynamic Characteristics of a Rotorcraft Airfoil Designed for the Tip Region of a Main Rotor Blade

Kevin W. Noonan

MAY 1991

NASA

US ARMY
AVIATION
SYSTEMS COMMAND
AVIATION R&T ACTIVITY

NASA
Technical Memorandum 4264

AVSCOM
Technical Report 91-B-003

Aerodynamic Characteristics of a Rotorcraft Airfoil Designed for the Tip Region of a Main Rotor Blade

Kevin W. Noonan
Aerostructures Directorate
U.S. Army-AVSCOM
Langley Research Center
Hampton, Virginia

National Aeronautics and
Space Administration
Office of Management
Scientific and Technical
Information Division

1991

Summary

A wind-tunnel investigation has been conducted to determine the two-dimensional aerodynamic characteristics of a new rotorcraft airfoil designed for application to the tip region (stations outboard of 85 percent radius) of a helicopter main rotor blade. The new airfoil, the RC(6)-08, and a baseline airfoil, the RC(3)-08, were investigated in the Langley 6- by 28-Inch Transonic Tunnel at Mach numbers from 0.37 to 0.90. The Reynolds number varied from 5.2×10^6 at the lowest Mach number (M) to 9.6×10^6 at the highest Mach number. Some comparisons have been made between the experimental data for the new airfoil and the predictions of a transonic, viscous analysis code.

The results of this investigation indicate that the RC(6)-08 airfoil met the design goals of attaining higher maximum lift coefficients than the baseline airfoil while maintaining drag divergence characteristics at low lift and pitching-moment characteristics nearly the same as those of the baseline airfoil. The maximum lift coefficients of the RC(6)-08 varied from 1.07 at $M = 0.37$ to 0.94 at $M = 0.52$, while those of the RC(3)-08 varied from 0.91 to 0.85 over the same Mach number range. At lift coefficients of -0.1 and 0, the drag-divergence Mach number of both the RC(6)-08 and the RC(3)-08 was 0.86. The pitching-moment coefficients of the RC(6)-08 were less negative than those of the RC(3)-08 for Mach numbers and lift coefficients typical of those that would occur on a main rotor blade tip at high forward speeds on the advancing side of the rotor disk.

Introduction

The performance requirements for the next generation of military helicopters include both higher forward flight speeds and more maneuverability, requiring higher lift loads on the retreating main rotor blade. Higher loading can be accommodated by increasing the airfoil section maximum lift coefficients and/or increasing the rotor solidity. Increasing the airfoil section lift capability is the more efficient approach to take since higher rotor solidity typically results in greater blade weight and drag. Two series of rotorcraft (RC) airfoils, the RC(4)-series and the RC(5)-series, were successfully designed for high maximum lift coefficients and applicability to the inboard region (stations ≤ 85 percent radius) of the rotor blade (ref. 1). Thus, an effort was undertaken to design an airfoil section for the blade tip region (stations ≥ 85 percent radius) that had improved maximum lift coefficients relative to a good baseline airfoil, the RC(3)-08. The RC(3)-series of airfoils was designed primarily for high drag-divergence Mach number and low pitching-moment characteristics (ref. 2). The design criteria for the new airfoil also included drag-divergence and pitching-moment characteristics that were nearly the same as for the RC(3)-08 airfoil. Prior experience indicated that it would be difficult to maintain the drag-divergence and pitching-moment characteristics of the RC(3)-08 in the new design since the airfoil geometry required for high maximum lift coefficients is inevitably in conflict with that needed for low pitching-moment coefficients and high drag-divergence Mach numbers.

An experimental investigation was conducted in the Langley 6-by 28-Inch Transonic Tunnel (6×28TT) to determine the two-dimensional aerodynamic characteristics of a new rotorcraft airfoil, the RC(6)-08, at Mach numbers from 0.37 to 0.90 and at chord Reynolds numbers from 5.2×10^6 to 9.6×10^6, respectively. The RC(3)-08 airfoil was tested in the same facility at the same conditions to ensure the best evaluation of the performance of the new airfoil. The RC(3)-08 airfoil was selected for the baseline since it was known to be a good airfoil for the rotor blade tip region (ref. 2), it had been successfully applied to several model rotors tested at Langley (refs. 3–5), and a wind-tunnel model of it was available.

The lift and pitching-moment coefficients were determined from measurements of airfoil surface static pressures, and the drag coefficients were determined from measurements of wake total and static pressures. For the new airfoil, some comparisons between the experimental data and the predictions of a transonic, viscous theory were made.

Symbols

The units used for the physical quantities in this paper are given in U.S. Customary Units. The measurements and calculations were also made in U.S. Customary Units.

c	airfoil chord, in.
c_d	section profile drag coefficient, $\sum_{\text{Wake}} c'_d \frac{\Delta h}{c}$
c'_d	point drag coefficient (ref. 10)
$c_{d,o}$	section profile drag coefficient at zero lift
c_l	section lift coefficient
c_m	section pitching-moment coefficient about quarter-chord from integration of airfoil surface pressure coefficients
$c_{m,o}$	section pitching-moment coefficient at zero lift

c_n	section normal force coefficient from integration of airfoil surface pressure coefficients
C_p	static-pressure coefficient, $(p_l - p_\infty)/q_\infty$
d	section drag force, lb
h	height of wake-survey probe tubes from given reference plane, in.
l	section lift force, lb
l/d	ratio of section lift force to section drag force
M	Mach number
M_{dd}	Mach number for drag divergence, $(dc_d/dM) = 0.1$
p	static pressure, psf
q	dynamic pressure, $\frac{1}{2}\rho V^2$, psf
R	Reynolds number, $\rho V_\infty c/12\mu$
t	airfoil thickness, in.
V	velocity, ft/sec
x	airfoil abscissa, in.
z_c	ordinate of airfoil camber line, in.
α	angle of attack, angle between airfoil chord line and airstream direction, deg
Δ	incremental change in parameter
μ	absolute viscosity, lb-sec/ft^2
ρ	density, slugs/ft^3

Subscripts:

c	wind-tunnel corrections applied
l	local
max	maximum
sep	boundary-layer separation occurred
sonic	Mach number equal to 1
∞	free stream

Abbreviation:

6×28TT	6- by 28-Inch Transonic Tunnel

Airfoil Designation

Rotorcraft airfoils designed at the U.S. Army Aerostructures Directorate at Langley Research Center are designated according to the following convention (ref. 2): RC(x)-xx, where "RC" means rotorcraft; (x) is the airfoil series number; and -xx is the maximum thickness of the airfoil in percent of airfoil chord. Thus, the RC(6)-08 is a member of the sixth series of rotorcraft airfoils, and its maximum thickness is 8 percent of the chord. A difference in the series number indicates that, as a minimum, the camber line or the thickness distribution differs between the airfoils. Both the camber line and the thickness distribution of the RC(6)-08 differ from the previous series of airfoils.

Airfoil Design

The requirements for an airfoil designed to operate at the rotor tip are driven by three main considerations. The airfoil must have high maximum lift coefficients in the Mach number range from 0.35–0.50 to sustain lift when the rotor blade is on the retreating side of the rotor disk. The airfoil must have a high drag-divergence Mach number at low lift coefficients to reduce the rotor power required when the rotor blade is on the advancing side of the rotor disk. For all conditions encountered around the rotor disk, but particularly for $M \geq 0.80$, the airfoil pitching moment must be kept low to reduce the torsional twist of the rotor blade and the control loads.

The design goals for the new airfoil were based on the measured performance (in the 6×28TT) of a good tip airfoil section, the RC(3)-08. In general, the design goals were to improve the maximum lift coefficients at $M = 0.35$–0.50 without substantially degrading the drag-divergence characteristics at low lift coefficients and the pitching-moment characteristics, especially at $M > 0.80$ and c_l near zero. The specific goals for the new airfoil were the following:

(1) $c_{l,\max} \geq 1.00$ at $M = 0.40$ and $R \approx 5.0 \times 10^6$

(2) $M_{dd} \geq 0.85$ at $c_l = 0$ and -0.1

(3) $c_{m,o} \leq -0.02$ at $0.80 \leq M \leq 0.85$

(4) $c_{l,\max} \geq 0.95$ at $M = 0.50$ and $R \approx 7.0 \times 10^6$

Major emphasis was placed on attaining the first three design goals. If the maximum lift coefficient of the new airfoil at $M = 0.4$ was increased but M_{dd} at low values of c_l was substantially reduced compared with the RC(3)-08, then the new airfoil would not be applicable to the rotor tip region. Also, if the pitching-moment coefficients of the new airfoil at high Mach numbers were substantially higher (more nose-down) than those of the RC(3)-08, then the new airfoil would not be an improvement. The $c_{l,\max}$ design goals at $M = 0.4$ and 0.5 represent a minimum improvement of about 11 percent. If the new airfoil attained the drag-divergence design goal, then the maximum reduction in M_{dd} (if any) compared with

that of the RC(3)-08 would be 0.01. The pitching-moment design goal represents a level which, at the upper limit, is not significantly higher than that of the RC(3)-08. The maximum thickness of the new airfoil was restricted to 8 percent chord so that it would be in the same airfoil class as that of the RC(3)-08.

The airfoil design process was the same as that successfully used for other rotor airfoils (ref. 1). This approach involved combining a camber line tailored to the approximate load distribution and a thickness distribution to result in an airfoil shape which was subsequently evaluated with a transonic analysis code (ref. 6). An iteration process of modifying the airfoil shape by changing the camber line and/or thickness distribution and then evaluating the new airfoil was used to converge on the design goals. However, it was known that the transonic analysis code does not adjust the airfoil pressure distribution to account for separated flow when boundary-layer separation is predicted, so the code could not quantify the maximum lift coefficient of an airfoil.

With this knowledge, the code was used to try to develop an airfoil shape that achieved the maximum lift coefficient goals with the indicated upper surface boundary-layer separation point at or aft of the 95-percent-chord station. Previous correlation of the analysis code results with experimental data on existing airfoils (ref. 1) had indicated that the prediction of the upper surface boundary-layer separation point was generally conservative; i.e., the theory generally predicted the separation point to be farther toward the airfoil leading edge than indicated by the test data for the same α. If the predicted lift coefficient of an airfoil was close to the $c_{l,\max}$ design goal and the predicted boundary-layer separation point was not forward of $x/c = 0.95$, then that airfoil would be expected to attain the design $c_{l,\max}$ experimentally.

Models and Wind Tunnel

Models

The airfoil profiles are shown in figure 1, and the airfoil thickness and camber distributions are shown in figure 2. The maximum thickness of both the RC(6)-08 and the RC(3)-08 is 8 percent chord and is also located at the 38-percent-chord station for both airfoils (fig. 2(a)). Comparing the thickness distributions of these two airfoils with each other, the thickness of the RC(6)-08 is greater from near the airfoil leading edge to about the 20-percent-chord station, and it is less from about the 40-percent-chord station to the airfoil trailing edge. The maximum positive camber of the RC(6)-08 is 0.7 percent chord and is located at the 48-percent-chord station, whereas that of the RC(3)-08 is 1.1 percent chord and is located at the 34-percent-chord station (fig. 2(b)). The RC(6)-08 camber line has a leading-edge droop of 0.6 percent chord and is below that of the RC(3)-08 except near the airfoil trailing edge. The camber line of both airfoils is reflexed the same amount, and the reflex starts at the same station (95 percent chord). The design coordinates for the RC(6)-08 and the RC(3)-08 are given in tables I and II, respectively.

The models of the RC(6)-08 and the RC(3)-08 are of identical construction, and each was machined from a heat-treated stainless steel block with a finished span of 6.010 in. and a chord of 6.000 in. (fig. 3). The coordinates of the RC(6)-08 were measured at three spanwise stations, and the measured values differ from the design values by no more than ± 0.0011 in. The measured coordinates of the RC(3)-08 were mostly within ± 0.001 in. of the design values. Each model has a total of 45 orifices: 1 on the leading edge, 22 on the upper surface, and 22 on the lower surface. The upper and lower surface orifices are located in single chordwise rows on the respective surfaces, and the rows are positioned 12.6 percent span on opposite sides of the midspan (see tables III and IV). Channels were milled in the airfoil surface, and tubes were placed in the channels and then covered with an epoxy filler material (fig. 3(b)). The orifices were then drilled from the metal side of the model to the embedded tubes to minimize surface irregularities near the orifices. The orifices have a diameter of 0.020 in. and were drilled perpendicular to the local surface contour. The surface of each model was polished by hand until it was aerodynamically smooth ($\approx$32 μin. rms surface finish).

Wind Tunnel

The Langley 6- by 28-Inch Transonic Tunnel is a blowdown wind tunnel with a slotted floor and ceiling (5.0 percent openness ratio and slot spacing of 6.0 in.) and is generally operated at stagnation pressures from about 30 to 90 psia and at Mach numbers from 0.35 to 0.90 (refs. 7 and 8). The slot geometry is described in detail in reference 9. Mach number is controlled by hydraulically actuated choker doors downstream of the test section. The airfoil model spans the 6.010-in. width of the tunnel (fig. 3(a)) and is rigidly attached by mounting tangs to circular end plates driven by a hydraulic actuator to position the airfoil at the desired angle of attack. A run sequence usually consists of an angle-of-attack sweep at constant Mach number and Reynolds number.

Apparatus

Wake-Survey Probe

A traversing wake-survey probe is cantilevered from one tunnel sidewall to measure the profile drag of the airfoils (fig. 3(a)). The vertical sweep rate of the probe was about 1.0 in/sec, consistent with previous investigations. The probe was located 1.67 chords (based on a 6.00-in-chord model) downstream of the airfoil trailing edge and has a maximum vertical travel of about ±11.0 in. from the tunnel centerline. Data are measured with four stainless steel total pressure tubes having an outside diameter of 0.060 in. and an inside diameter of 0.040 in., and the tubes are spaced 0.375 in. apart laterally as shown in figure 4.

Instrumentation

All measurements made during the test program were obtained with the use of a high-speed, computer-controlled digital data acquisition system and were recorded by a high-speed tape recording unit (ref. 7). The airfoil surface static pressures and the airfoil wake pressures were measured with individual variable-capacitance-type pressure transducers. The free-stream stagnation and static reference pressures were also measured with the same type of pressure transducers. The geometric angle of attack was determined from the output of a digital shaft encoder attached to a pinion engaging a rack on one model support end plate.

Repeatability

The overall precision of the data was determined by examination of the repeatability of the data. The repeat points for the two airfoils were mostly measured at nominally zero geometric angle of attack, and those points considered to be valid repeat points differed by no more than 0.05°. An examination of these 27 repeat points measured at Mach numbers up to 0.84 (below M_{dd} for these airfoils) indicated that the average of the differences between 27 pairs of data points was 0.0004 in drag coefficient (that is, $(1/27)\sum|c_{d,2}-c_{d,1}|$) and 0.0005 in pitching-moment coefficient. For the three pairs of data points with $\Delta\alpha = 0°$, the average of the differences in lift coefficient was 0.0012.

The RC(3)-08 data reported herein were compared with that of reference 2. The agreement between these two data sets was very close except at $M = 0.88$, the highest Mach number data reported in reference 2. At this Mach number, the drag coefficients of this investigation were generally higher than those of reference 2.

Methods and Corrections

Methods

For both airfoils, data were taken for an angle-of-attack sweep at a stagnation pressure of 60 psia at Mach numbers from about 0.37 to 0.90 to obtain Reynolds numbers typical of full-scale main rotor blades ($\approx 5\times10^6$–10×10^6). In addition, both airfoils were investigated at a stagnation pressure less than 60 psia at three Mach numbers to evaluate the effect of Reynolds number on the maximum lift coefficients. At the lower test Mach numbers, the geometric angle of attack ranged from about −4° to 13°; the angle-of-attack sweep was stopped when the wake of the airfoil became very large, indicating that the airfoil was either stalled or near stall. This range of angle of attack was decreased with increasing Mach number.

Section lift and pitching-moment coefficients were calculated from the airfoil surface pressures by a trapezoidal integration of the pressure coefficients. The pressure coefficient at the most rearward orifice on each surface was applied from that station to the airfoil trailing edge in the integration. Each of the pressure coefficients represents the average of five measurements obtained in a 1.0-sec interval.

The point-drag coefficients were calculated (ref. 10) from the measured wake pressures, and a trapezoidal integration of the point-drag coefficients was used to calculate the drag coefficient. The static pressures used in the point-drag calculation were measured with tunnel sidewall orifices located at the same longitudinal tunnel station as the tips of the tubes on the wake-survey probe. The drag coefficients represent the average of the measurements made with the four total pressure tubes on the wake-survey probe in one sweep through the wake of an airfoil.

Corrections

The corrections for lift interference, which have been applied to the angles of attack, were obtained from references 9 and 11. The maximum correction for the angle of attack is about 1.3°. The basic equations for the α-correction (ref. 11) are

$$\alpha_c = \alpha + \Delta\alpha$$

where

$$\Delta\alpha = \frac{-c_n}{8}\left(\frac{c}{14.250}\right)\left(\frac{1}{k+1}\right)\left(\frac{180}{\pi}\right)$$

and

$$k = (a/h_s)K$$

In the equation for the slotted-wall boundary-condition coefficient k, a is the slot spacing (6.0 in.), and h_s is the semiheight of the tunnel (14.250 in.). A value of 3.5 was selected for the slotted-wall performance coefficient K, based on the data and discussion presented in reference 9. This substitution results in a correction given by the equation

$$\Delta\alpha = -c_n c(0.2032)$$

where $\Delta\alpha$ is the angle-of-attack correction in degrees, c is the airfoil chord in inches, c_n is the section normal force coefficient, and the constant (0.2032) is in degrees per inch.

No correction for blockage was made since the 6×28TT slot geometry was designed to yield a relatively blockage-free flow (ref. 9). Although a similarity-rule type of correction for tunnel sidewall boundary-layer effects has been reported for cases of fully attached flow on an airfoil model (ref. 12), the state of the art does not presently permit a general correction applicable to the entire range of the lift, drag, and pitching-moment curves important to rotorcraft airfoils, i.e., one which applies with or without separated flow on the model. Additionally, the existing 6×28TT data base of two-dimensional airfoil data is extensive and does not include corrections for sidewall boundary-layer effects. For these reasons, no correction for tunnel sidewall boundary-layer influences has been made to the data presented herein, and the emphasis is placed on a comparison of the performance of the new airfoil with that of the baseline airfoil, the RC(3)-08.

Presentation of Results

The results of this investigation have been reduced to coefficient form and are presented as follows:

Results	Airfoil	Figure
Experimental results		
Basic aerodynamic characteristics: c_l against α_c; c_m and c_d against c_l; l/d against α_c	RC(6)-08 RC(3)-08	5 6
$c_{l,\max}$ against M	RC(6)-08 RC(3)-08	7 7
$c_{m,o}$ against M	RC(6)-08 RC(3)-08	8 8
c_d against M	RC(6)-08 RC(3)-08	9 9
c_l against M_{dd}	RC(6)-08 RC(3)-08	10 10
Comparison of experiment and theory		
Basic aerodynamic characteristics: c_l against α; c_m and c_d against c_l	RC(6)-08	11
$c_{m,o}$ against M	RC(6)-08	12
$c_{d,o}$ against M	RC(6)-08	13
Experimental pressure distributions		
C_p against x/c	RC(6)-08 RC(3)-08	14 15

The basic data plotted in figures 5 and 6 are also presented in tables V and VI.

Discussion of Results

Lift

The lift coefficients for Mach numbers from 0.37 to 0.90 are presented as a function of angle of attack in figures 5(a) and 6(a) for the RC(6)-08 and RC(3)-08 airfoils, respectively.

Reduction of $c_{l,\max}$ in 6×28TT. The results of a previous investigation of rotorcraft airfoils in the Langley 6×28TT (ref. 1) have shown that the measured maximum lift coefficient at Mach numbers less than 0.38 is reduced by tunnel sidewall boundary-layer influences. This reduction is characteristic of two-dimensional wind tunnels without proper sidewall boundary-layer control and is the result of initial flow separation beginning at the sidewall/airfoil juncture instead of in the center span of the model. The $c_{l,\max}$ reduction indicated in reference 1 for the RC(4)-10 airfoil at $M = 0.37$ is only 0.02. Since the minimum Mach number of the present investigation is 0.37, the $c_{l,\max}$ data presented herein for the RC(6)-08 and RC(3)-08 airfoils are believed to be only slightly degraded at the lowest test Mach number and unaffected at $M \geq 0.38$.

Maximum lift coefficient. The maximum lift coefficients determined from figures 5(a) and 6(a) are presented as a function of Mach number in figure 7. The $c_{l,\max}$ value of the RC(6)-08 airfoil has much greater sensitivity to changes in Mach number than that of the RC(3)-08 airfoil. The $c_{l,\max}$ value of the RC(6)-08 decreases from 1.07 at $M = 0.38$ to 0.89 at $M = 0.57$ whereas that of the RC(3)-08 only decreases from 0.91 to 0.87 for the same change in Mach number. The RC(6)-08 airfoil attained a maximum lift coefficient of 1.05 at $M = 0.40$ and 0.96 at $M = 0.50$, thus meeting two of the design goals for the new airfoil. These values at $M = 0.40$ and 0.50 represent an improvement of about 19 percent and 12 percent, respectively, over those of the RC(3)-08 airfoil.

Varying Reynolds number had only a small effect on the maximum lift coefficients of both airfoils (figs. 5(a) and 6(a)). The largest change in the maximum lift coefficient of the RC(6)-08 due to Reynolds number is 0.05. The differences in $c_{l,\max}$ of the RC(3)-08 airfoil due to changes in Reynolds number are less than 0.02, or about the amount typical of the repeatability of this parameter.

Both airfoils have a trailing-edge type of stall as indicated by the characteristic rounding of the lift curves near $c_{l,\max}$ (figs. 5(a) and 6(a)). This rounding of the lift curve is caused by a gradual movement of the upper surface turbulent-boundary-layer separation point toward the airfoil leading edge. The pressure distributions of the RC(6)-08 at angles of attack near $c_{l,\max}$ exhibit the loss in pressure recovery near the upper surface trailing edge that is characteristic of turbulent-boundary-layer separation (figs. 14(a)–(e)).

Pitching Moment

The pitching-moment coefficients are presented as a function of the lift coefficient in figures 5(b) and 6(b) for the RC(6)-08 and RC(3)-08 airfoils, respectively. Both airfoils have very low pitching-moment levels (nearly zero) for a broad range of c_l for Mach numbers up to about 0.67. At Mach numbers above 0.67, the range of c_l for low c_m is reduced due to compressibility effects. At Mach numbers up to 0.63, the RC(6)-08 airfoil has less of a pitch-up tendency than the RC(3)-08 airfoil for values of c_l near $c_{l,\max}$. In general, the Mach numbers and lift coefficients important to the rotor blade tip region on the advancing side of the rotor disk in high-speed forward flight are $M \geq 0.80$ and $-0.1 \leq c_l \leq 0.1$. For such values of M and c_l, the pitching-moment coefficients of the RC(6)-08 are less nose-down than those of the RC(3)-08. A rotor blade that used the new airfoil in place of the RC(3)-08 would be expected to have a reduced torsional twist in high-speed forward flight. Changes in Reynolds number had no appreciable effect on the pitching-moment coefficients of either airfoil.

The pitching-moment coefficients at $c_l = 0$ for both airfoils are presented as a function of Mach number in figure 8. The pitching-moment level is unchanged by variation in Mach number until $M = 0.65$ for the RC(3)-08 and $M = 0.70$ for the RC(6)-08, and then $c_{m,o}$ for both airfoils becomes more negative (nose down) with increasing Mach number. The $c_{m,o}$ for the new airfoil is less negative than that of the RC(3)-08 for the entire range of Mach numbers investigated. For the RC(6)-08, $c_{m,o}$ is less negative than -0.02 for $M \leq 0.87$, thus meeting the design goal for pitching moment.

Drag

The drag coefficients at constant Mach numbers are plotted against the lift coefficient in figure 5(c) for the RC(6)-08 and in figure 6(c) for the RC(3)-08. Data in these figures were cross-plotted to obtain the variation of c_d with M for a constant c_l and to determine the drag-divergence Mach number (fig. 9). The lift coefficient is presented as a function of the drag-divergence Mach number in figure 10.

Minimum drag. For lift coefficients from −0.1 to 0.2 and Mach numbers less than 0.80, the drag level of the RC(6)-08 airfoil is equal to or higher than that of the RC(3)-08 airfoil (fig. 9). The drag level of the RC(6)-08 airfoil for these conditions ranges from about 0.0060 to 0.0075 whereas that of the RC(3)-08 ranges from about 0.0060 to 0.0065. For both airfoils at low lift coefficients (−0.2 to 0.3), the average change in the drag level due to a variation in Reynolds number is within the repeatability of the drag measurements (figs. 5(c) and 6(c)).

Drag divergence. The drag-divergence Mach number is nearly the same for both airfoils for lift coefficients from −0.1 to 0.1 (fig. 10). For the RC(6)-08 airfoil, M_{dd} is 0.86 for $c_l = -0.1$ and 0, thus meeting the design goals for this parameter. At lift coefficients from 0.3 to 0.5, M_{dd} for the RC(6)-08 airfoil exceeds that of the RC(3)-08 airfoil, but this new airfoil also has a significant amount of drag creep prior to M_{dd} (fig. 9). The RC(3)-08 airfoil has a drag-divergence Mach number that exceeds that of the new airfoil for c_l values above about 0.52, and it has no significant drag creep except at $c_l = 0.8$.

Lift-to-drag ratio. The lift-to-drag ratios of the two airfoils were calculated from the measured data, and they are presented as a function of angle of attack in figures 5(d) and 6(d). For the RC(6)-08 airfoil, $(l/d)_{\max}$ varies from a high of 97 at $M = 0.42$ to a low of 8 at $M = 0.90$. For Mach numbers greater than 0.42, $(l/d)_{\max}$ of the RC(6)-08 airfoil decreases continuously with increasing Mach number. The maximum lift-to-drag ratio of the RC(3)-08 airfoil ranges from 87 at $M = 0.63$ to 6 at $M = 0.90$. For this airfoil, $(l/d)_{\max}$ generally decreases with increasing Mach number for $M > 0.63$. For both airfoils, the differences in $(l/d)_{\max}$ due to Reynolds number are small (nearly within the repeatability) for the Mach numbers presented.

Comparison With Theory

The basic aerodynamic characteristics of the RC(6)-08 airfoil at selected Mach numbers are compared with theory in figure 11. Data/theory comparisons of the variation of $c_{m,o}$ with Mach number and of $c_{d,o}$ with Mach number for the RC(6)-08 airfoil are presented in figures 12 and 13, respectively. The theory used for all comparisons was the Korn-Garabedian-Bauer (KGB) theory (ref. 6).

The KGB code is a viscous, transonic analysis applicable to airfoils with turbulent boundary layers. For all conditions calculated with the KGB code (i.e., M, R, and α or c_l), the turbulent boundary layer was forced to start at the 5-percent-chord station on both surfaces of the airfoil since the code could not determine where the turbulent boundary layers would naturally begin, and the turbulent boundary layers on the model in the 6×28TT would be expected to begin near the airfoil leading edge due to the high turbulence level in the tunnel. This code does not make the appropriate adjustment to the pressure distribution when boundary-layer separation is predicted to occur ahead of the airfoil trailing edge. The pressure coefficients aft of the predicted boundary-layer separation point calculated by the KGB code continue to recover to a positive value at the airfoil trailing edge that is close to that of fully attached flow. Thus, the predicted lift coefficients continue to vary almost linearly with α even though separation has occurred.

A qualitative summary of the agreement of the KGB theory relative to the experimental data is given in the table below:

		Agreement of KGB theory versus experiment			
Airfoil	M	$dc_l/d\alpha$	$(x/c)_{\text{sep}}$	c_m	c_d
RC(6)-08	0.37	Good	High	Poor	High at $c_l < 0.7$; low at $c_l > 0.7$
	0.42	Good	High	Poor	High at $c_l < 0.8$; low at $c_l > 0.8$
	0.52	High	High	Poor	Good at $c_l \geq -0.2$ and < 0.7; low at $c_l < -0.2$ and ≥ 0.7
Airfoil	M	$c_{m,o}$			$c_{d,o}$
RC(6)-08	0.37–0.90	More negative at all M; trend with M good			High at $M > 0.73$ and < 0.88; M_{dd} low

Conclusions

A wind-tunnel investigation has been conducted to determine the two-dimensional aerodynamic characteristics of a new rotorcraft airfoil designed for application to the tip region (stations outboard of 85 percent radius) of a helicopter main rotor blade. The new airfoil, the RC(6)-08, and a baseline airfoil, the RC(3)-08, were investigated in the Langley 6- by 28-Inch Transonic Tunnel at Mach numbers (M) from 0.37 to 0.90. The Reynolds number varied from

5.2×10^6 at the lowest Mach number to 9.6×10^6 at the highest Mach number. Several design goals were established for the new airfoil to improve (relative to the RC(3)-08) the maximum lift coefficients at $M = 0.35$–0.50 without substantially degrading the drag-divergence characteristics at low lift coefficients and the pitching-moment characteristics, especially at $M > 0.80$ and lift coefficients near zero. Some comparisons have been made between the experimental data for the new airfoil and the predictions of a transonic, viscous analysis code. The conclusions are summarized as follows:

1. The RC(6)-08 airfoil attained a maximum lift coefficient $c_{l,\max}$ of 1.05 at $M = 0.40$ and of 0.96 at $M = 0.50$, thus meeting the two $c_{l,\max}$ design goals for the new airfoil. These values at $M = 0.40$ and 0.50 represent an improvement of about 19 percent and 12 percent, respectively, over those of the RC(3)-08 airfoil. For the RC(6)-08, $c_{l,\max}$ decreased from 1.07 at $M = 0.38$ to 0.89 at $M = 0.57$ whereas that of the RC(3)-08 only decreased from 0.91 to 0.87 for the same change in Mach number.

2. Both airfoils had very low pitching-moment c_m levels (nearly zero) for a broad range of lift coefficient c_l for Mach numbers up to about 0.67. At Mach numbers above 0.67 for both airfoils, the range of c_l for low c_m was reduced by compressibility effects. The pitching-moment coefficient at zero lift $c_{m,o}$ for the RC(6)-08 airfoil was less negative than that of the RC(3)-08 airfoil for the entire range of Mach numbers investigated. For the RC(6)-08, $c_{m,o}$ was less negative than -0.02 for $M \leq 0.87$. Thus the RC(6)-08 airfoil met the design goal for pitching moment.

3. The drag-divergence Mach number M_{dd} was nearly the same for both airfoils for lift coefficients from -0.1 to 0.1. For the RC(6)-08 airfoil, M_{dd} was 0.86 for lift coefficients of -0.1 and 0, thus meeting the design goals for this parameter. At lift coefficients from 0.3 to 0.5, the drag-divergence Mach number of the RC(6)-08 airfoil exceeded that of the RC(3)-08 airfoil, but this new airfoil also had a significant amount of drag creep prior to M_{dd}.

4. For lift coefficients from -0.1 to 0.2 and Mach numbers less than 0.80, the drag level of the RC(6)-08 airfoil was equal to or higher than that of the RC(3)-08 airfoil. The drag level of the RC(6)-08 airfoil for these conditions ranged from about 0.0060 to 0.0075 whereas that of the RC(3)-08 ranged from about 0.0060 to 0.0065.

5. The airfoil performance predictions of the Korn-Garabedian-Bauer (KGB) theory were compared with the experimental data for the RC(6)-08 airfoil. When the upper surface turbulent boundary layer was predicted to separate, the predicted separation point was farther aft on the airfoil than the separation point indicated by the experimental data. In general, the pitching-moment coefficient values were poorly predicted for most lift coefficients and Mach numbers. However, the trend of $c_{m,o}$ with Mach number was well predicted. The predicted M_{dd} at zero lift was low compared with the experimental value because of an overprediction of the wave drag.

NASA Langley Research Center
Hampton, VA 23665-5225
March 12, 1991

References

1. Noonan, Kevin W.: *Aerodynamic Characteristics of Two Rotorcraft Airfoils Designed for Application to the Inboard Region of a Main Rotor Blade.* NASA TP-3009, AVSCOM TR-90-B-005, 1990.

2. Bingham, Gene J.; and Noonan, Kevin W.: *Two-Dimensional Aerodynamic Characteristics of Three Rotorcraft Airfoils at Mach Numbers From 0.35 to 0.90.* NASA TP-2000, AVRADCOM TR 82-B-2, 1982.

3. Kelley, Henry L.: *Effect of Planform Taper on Hover Performance of an Advanced AH-64 Model Rotor.* NASA TM-89145, AVSCOM TM 87-B-10, 1987.

4. Yeager, William T., Jr.; Mantay, Wayne R.; Wilbur, Matthew L.; Cramer, Robert G., Jr.; and Singleton, Jeffrey D.: *Wind-Tunnel Evaluation of an Advanced Main-Rotor Blade Design for a Utility-Class Helicopter.* NASA TM-89129, AVSCOM TM 87-B-8, 1987.

5. Althoff, Susan L.: *Effect of Advanced Rotorcraft Airfoil Sections on the Hover Performance of a Small-Scale Rotor Model.* NASA TP-2832, AVSCOM TP-88-B-001, 1988.

6. Bauer, Frances; Garabedian, Paul; Korn, David; and Jameson, Antony: *Supercritical Wing Sections II. Volume 108 of Lecture Notes in Economics and Mathematical Systems*, M. Beckmann and H. P. Kuenzi, eds., Springer-Verlag, 1975.

7. Ladson, Charles L.: *Description and Calibration of the Langley 6- by 28-Inch Transonic Tunnel.* NASA TN D-8070, 1975.

8. Sewall, William G.: *Description of Recent Changes in the Langley 6- by 28-Inch Transonic Tunnel.* NASA TM-81947, 1981.

9. Barnwell, Richard W.: *Design and Performance Evaluation of Slotted Walls for Two-Dimensional Wind Tunnels.* NASA TM-78648, 1978.

10. Baals, Donald D.; and Mourhess, Mary J.: *Numerical Evaluation of the Wake-Survey Equations for Subsonic Flow Including the Effect of Energy Addition.* NACA WR L-5, 1945. (Formerly NACA ARR L5H27.)

11. Davis, Don D., Jr.; and Moore, Dewey: *Analytical Study of Blockage- and Lift-Interference Corrections for Slotted Tunnels Obtained by the Substitution of an Equivalent Homogeneous Boundary for the Discrete Slots.* NACA RM L53E07b, 1953.

12. Sewall, William Grier: *Application of a Transonic Similarity Rule To Correct the Effects of Sidewall Boundary Layers in Two-Dimensional Transonic Wind Tunnels.* M.S. Thesis, George Washington Univ., Aug. 1982. (Available as NASA TM-84847.)

Table I. Design Coordinates for RC(6)-08 Airfoil

[Stations and ordinates given in percent airfoil chord]

Upper surface		Lower surface	
Station	Ordinate	Station	Ordinate
0.00	−0.40	0.00	−0.40
.10	.05	.40	−1.10
.30	.40	.70	−1.28
.99	1.11	1.51	−1.56
2.21	1.87	2.79	−1.82
4.76	2.76	5.24	−2.14
7.48	3.29	7.52	−2.34
9.88	3.59	10.12	−2.52
12.45	3.81	12.55	−2.65
14.93	3.98	15.07	−2.76
17.46	4.13	17.54	−2.86
20.00	4.26	20.00	−2.94
22.48	4.36	22.52	−3.02
24.99	4.44	25.01	−3.09
30.01	4.57	29.99	−3.21
34.99	4.65	35.01	−3.29
37.49	4.68	37.51	−3.30
40.00	4.68	40.00	−3.30
42.50	4.66	42.50	−3.28
45.00	4.61	45.00	−3.23
47.50	4.54	47.50	−3.16
50.00	4.44	50.00	−3.06
52.51	4.32	52.46	−2.96
55.03	4.17	54.97	−2.85
57.52	4.01	57.48	−2.73
60.02	3.82	59.98	−2.62
62.55	3.60	62.45	−2.49
65.04	3.38	64.96	−2.37
67.56	3.13	67.44	−2.23
70.03	2.88	69.97	−2.10
72.56	2.61	72.44	−1.96
75.09	2.34	74.91	−1.81
77.54	2.07	77.46	−1.66
80.04	1.81	79.96	−1.51
82.53	1.56	82.46	−1.35
85.03	1.30	84.97	−1.18
87.52	1.06	87.48	−1.02
90.01	.82	89.99	−.85
92.50	.61	92.50	−.67
95.00	.43	95.00	−.48
97.50	.28	97.50	−.27
100.00	.10	100.00	−.02

Table II. Design Coordinates for RC(3)-08 Airfoil

[Stations and ordinates given in percent airfoil chord]

Station	Upper surface	Lower surface
0.00	0.00	0.00
.31	.67	−.66
1.17	1.31	−1.10
2.53	1.90	−1.45
4.37	2.46	−1.73
6.51	2.95	−1.95
8.89	3.39	−2.13
11.47	3.77	−2.28
14.24	4.10	−2.40
17.19	4.38	−2.51
20.30	4.61	−2.61
23.56	4.79	−2.69
26.96	4.93	−2.79
30.48	5.02	−2.85
34.12	5.08	−2.88
37.84	5.09	−2.91
41.61	5.05	−2.93
45.40	4.99	−2.94
49.20	4.88	−2.93
52.98	4.73	−2.90
56.77	4.53	−2.86
60.55	4.30	−2.80
64.37	4.02	−2.71
68.24	3.70	−2.61
72.15	3.34	−2.47
76.06	2.94	−2.30
79.84	2.53	−2.10
83.46	2.11	−1.87
86.93	1.69	−1.60
90.28	1.27	−1.29
93.54	.86	−.94
96.78	.49	−.51
100.00	.13	−.05

Table III. Static-Pressure Orifice Locations for RC(6)-08 Airfoil

[Locations given in percent airfoil chord]

Upper surface station	Lower surface station
0.00	
1.25	1.20
2.48	2.50
5.00	5.00
7.50	7.50
10.00	10.01
15.00	15.01
20.00	20.00
25.00	25.00
29.99	30.00
34.97	35.00
40.02	40.00
45.00	45.00
50.00	50.00
55.00	55.00
59.97	60.00
64.98	65.00
69.95	70.00
75.00	75.00
80.00	80.00
85.00	85.00
90.03	90.00
95.00	95.00

Table IV. Static-Pressure Orifice Locations for RC(3)-08 Airfoil

[Locations given in percent airfoil chord]

Upper surface station	Lower surface station
0.00	
1.17	1.17
2.60	2.43
4.92	4.99
7.46	7.48
10.00	10.00
15.03	15.02
20.04	20.01
25.02	24.98
30.06	30.00
35.05	34.98
39.99	40.02
45.00	45.04
50.05	50.00
55.02	55.01
60.05	60.01
65.01	65.04
70.02	70.03
75.01	75.01
79.97	80.01
84.96	85.08
89.98	90.03
94.99	95.04

Table V. Force and Moment Coefficients for the RC(6)-08 Airfoil

$M = 0.37; R = 5.2 \times 10^6$

α_c, deg	c_d	c_l	c_m	l/d
−3.65	0.00749	−0.3705	0.0060	−49.47
−2.74	.00661	−.2694	.0051	−40.76
−1.80	.00615	−.1644	.0032	−26.73
−1.04	.00568	−.0691	.0022	−12.17
−.12	.00783	.0298	.0016	3.81
−.09	.00649	.0336	.0011	5.18
1.84	.00543	.2495	−.0022	45.95
3.51	.00588	.4409	−.0036	74.98
5.29	.00797	.6379	−.0066	80.04
6.11	.00905	.7334	−.0072	81.04
6.99	.00987	.8205	−.0083	83.13
7.85	.01207	.8962	−.0090	74.25
8.84	.01250	1.0028	−.0090	80.22
9.65	.01364	1.0395	−.0077	76.21
10.68	.02728	1.0648	−.0142	39.03
11.73	(a)	1.0732	−.0469	(a)

$M = 0.42; R = 5.9 \times 10^6$

α_c, deg	c_d	c_l	c_m	l/d
−3.51	0.00783	−0.3624	0.0050	−46.28
−2.69	.00680	−.2679	.0045	−39.40
−1.85	.00623	−.1717	.0031	−27.56
−1.06	.00640	−.0779	.0025	−12.17
−.11	.00591	.0329	.0010	5.57
−.10	.00539	.0351	.0010	6.51
1.74	.00645	.2442	−.0024	37.86
3.79	.00693	.4831	−.0049	69.71
5.15	.00796	.6367	−.0066	79.99
5.20	.00783	.6388	−.0061	81.58
6.09	(a)	.7405	−.0074	(a)
6.14	.00763	.7421	−.0080	97.26
6.92	.00982	.8259	−.0085	84.10
7.92	.01242	.9303	−.0085	74.90
8.84	.01609	.9781	−.0062	60.79
9.80	.03064	1.0050	−.0080	32.80
10.76	.04628	1.0165	−.0163	21.96
11.89	(a)	1.0321	−.0384	(a)

[a]Data unavailable.

Table V. Continued

$M = 0.43; R = 3.8 \times 10^6$

α_c, deg	c_d	c_l	c_m	l/d
−3.64	0.00861	−0.3607	0.0027	−41.89
−2.75	.00641	−.2589	.0027	−40.39
−1.89	.00636	−.1627	.0017	−25.58
−.96	.00707	−.0548	.0013	−7.75
−.06	.00711	.0452	−.0013	6.36
−.01	.00710	.0524	−.0003	7.38
1.65	.00709	.2270	−.0023	32.02
3.53	.00767	.4398	−.0043	57.34
5.24	.00777	.6313	−.0068	81.25
6.99	.01010	.8206	−.0099	81.25
7.94	.01048	.9075	−.0097	86.59
8.73	.01827	.9558	−.0080	52.32
9.94	.03423	.9810	−.0097	28.66
10.73	.05481	.9831	−.0181	17.94

$M = 0.47; R = 6.5 \times 10^6$

α_c, deg	c_d	c_l	c_m	l/d
−3.60	0.01043	−0.3741	0.0012	−35.87
−2.75	.00709	−.2802	.0038	−39.52
−1.78	.00607	−.1664	.0032	−27.41
−1.03	.00608	−.0769	.0020	−12.65
−.08	.00677	.0373	.0006	5.51
−.07	.00754	.0364	.0007	4.83
2.26	.00607	.3085	−.0030	50.82
3.54	.00642	.4593	−.0044	71.54
5.19	.00759	.6541	−.0066	86.18
6.02	.00784	.7435	−.0074	94.83
6.98	.01243	.8391	−.0070	67.51
7.80	.01802	.8977	−.0036	49.82
8.76	.03144	.9468	−.0024	30.11
9.86	.05248	.9739	−.0089	18.56
10.75	.06932	.9847	−.0260	14.20

Table V. Continued

$M = 0.52; R = 7.0 \times 10^6$

α_c, deg	c_d	c_l	c_m	l/d
−3.59	0.01531	−0.3749	−0.0015	−24.49
−2.73	.00999	−.2767	.0029	−27.70
−1.86	.00760	−.1709	.0029	−22.49
−.92	.00647	−.0596	.0015	−9.21
−.12	.00667	.0382	.0005	5.73
−.06	.00691	.0413	.0004	5.98
1.64	.00664	.2425	−.0022	36.52
3.42	.00770	.4642	−.0046	60.29
5.12	.00817	.6652	−.0058	81.42
6.16	.01302	.7750	−.0025	59.53
7.05	.02314	.8418	−.0008	36.38
8.01	.04146	.8772	−.0029	21.16
8.79	.05934	.9098	−.0089	15.33
9.70	(a)	.9443	−.0188	(a)

$M = 0.53; R = 4.7 \times 10^6$

α_c, deg	c_d	c_l	c_m	l/d
−3.53	0.01427	−0.3618	−0.0028	−25.35
−2.73	.00784	−.2751	.0006	−35.09
−1.80	.00686	−.1649	.0014	−24.04
−1.20	.00658	−.0927	.0012	−14.09
−1.02	(a)	−.0715	.0013	(a)
−.10	.00738	.0383	−.0002	5.19
−.08	.00688	.0412	−.0001	5.99
2.44	.00694	.3303	−.0032	47.59
3.10	.00745	.4073	−.0036	54.67
4.33	.00755	.5511	−.0045	72.99
5.16	.00841	.6458	−.0052	76.79
6.19	.01300	.7531	−.0027	57.93
6.98	.02089	.8193	−.0018	39.22
7.84	.03173	.8589	−.0014	27.07
8.82	.05349	.8979	−.0081	16.79
9.81	.07547	.9282	−.0178	12.30

[a]Data unavailable.

Table V. Continued

$M = 0.57; R = 7.1 \times 10^6$

α_c, deg	c_d	c_l	c_m	l/d
−3.66	0.01666	−0.3872	−0.0043	−23.24
−3.04	.01141	−.3206	−.0019	−28.10
−1.91	.00763	−.1827	.0022	−23.94
−.92	.00706	−.0632	.0017	−8.95
−.09	.00680	.0406	.0002	5.97
−.07	.00675	.0424	.0003	6.28
1.83	.00696	.2720	−.0024	39.08
3.37	.00680	.4659	−.0038	68.51
5.09	.01438	.6750	−.0002	46.94
5.21	.01406	.6886	−.0002	48.98
5.89	.01905	.7469	.0012	39.21
6.26	.02582	.7775	.0017	30.11
7.12	.03642	.8336	.0018	22.89
7.87	.05178	.8550	−.0078	16.51
8.98	.07685	.8865	−.0222	11.54

$M = 0.63; R = 7.9 \times 10^6$

α_c, deg	c_d	c_l	c_m	l/d
−3.63	0.01832	−0.4027	−0.0085	−21.98
−2.73	.01098	−.2969	−.0039	−27.04
−1.78	.00752	−.1810	−.0006	−24.07
−.94	.00694	−.0647	.0008	−9.32
−.08	.00615	.0426	−.0004	6.93
−.06	.00692	.0457	−.0002	6.60
1.90	.00694	.2969	−.0031	42.78
3.32	.00864	.4860	−.0016	56.25
4.21	.01458	.6093	.0034	41.79
5.19	.02666	.7065	.0042	26.50
6.13	.03966	.7785	.0025	19.63
6.93	.05260	.8247	−.0002	15.68

Table V. Continued

$M = 0.63; R = 5.8 \times 10^6$

α_c, deg	c_d	c_l	c_m	l/d
−4.05	0.02279	−0.4229	−0.0085	−18.56
−3.07	.01412	−.3246	−.0058	−22.99
−1.88	.00778	−.1803	−.0014	−23.17
−1.01	.00669	−.0646	.0000	−9.66
−.09	.00653	.0523	−.0006	8.01
−.09	.00623	.0463	−.0005	7.43
1.63	.00614	.2548	−.0023	41.50
3.45	.00892	.4877	−.0007	54.67
5.07	.02217	.6910	.0060	31.17
6.84	.05112	.8218	−.0005	16.08
8.07	.07637	.8515	−.0243	11.15
9.04	(a)	.8587	−.0419	(a)
9.96	(a)	.8773	−.0525	(a)

$M = 0.67; R = 8.1 \times 10^6$

α_c, deg	c_d	c_l	c_m	l/d
−3.85	0.02366	−0.4473	−0.0116	−18.91
−2.77	.01328	−.3158	−.0068	−23.78
−1.83	.00787	−.1854	−.0022	−23.56
−1.04	.00723	−.0857	.0001	−11.85
−.12	.00732	.0464	−.0010	6.34
−.08	.00646	.0486	−.0002	7.52
1.84	.00698	.3032	−.0017	43.44
2.64	.00916	.4164	.0003	45.46
4.30	.02566	.6516	.0070	25.39
5.18	.03797	.7482	.0076	19.71
6.08	.05710	.8123	.0027	14.23
7.04	.08103	.8351	−.0169	10.31

[a]Data unavailable.

Table V. Continued

$M = 0.72; R = 8.7 \times 10^6$

α_c, deg	c_d	c_l	c_m	l/d
−3.63	0.02878	−0.4937	−0.0167	−17.15
−2.82	.01725	−.3620	−.0113	−20.99
−1.78	.00946	−.1964	−.0040	−20.76
−.93	.00702	−.0691	−.0011	−9.84
−.09	.00661	.0541	−.0011	8.18
−.09	.00666	.0531	−.0005	7.97
1.68	.00819	.3074	−.0005	37.53
3.37	.02389	.5881	.0061	24.62
4.28	.04085	.7155	.0050	17.52
4.95	.05859	.7793	.0000	13.30
6.01	.07654	.8284	−.0137	10.82

$M = 0.78; R = 8.8 \times 10^6$

α_c, deg	c_d	c_l	c_m	l/d
−3.40	0.04185	−0.5684	−0.0109	−13.58
−2.62	.02433	−.4128	−.0146	−16.97
−1.84	.01145	−.2498	−.0103	−21.82
−1.08	.00774	−.1073	−.0055	−13.86
−.15	.00644	.0639	−.0022	9.92
−.10	.00592	.0652	−.0020	11.01
1.43	.01051	.3174	.0025	30.20
2.29	.01918	.5028	−.0034	26.21
3.33	.04518	.6596	−.0233	14.60
4.13	.07116	.7095	−.0387	9.97
5.15	(a)	.7533	−.0509	(a)

[a]Data unavailable.

Table V. Continued

$M = 0.83; R = 9.4 \times 10^6$

α_c, deg	c_d	c_l	c_m	l/d
−3.38	0.05333	−0.6146	0.0298	−11.52
−2.49	.02747	−.4727	.0037	−17.21
−1.66	.01346	−.2815	−.0097	−20.91
−1.66	.01334	−.2626	−.0115	−19.69
−.98	.00856	−.1012	−.0094	−11.82
−.94	.00835	−.0977	−.0087	−11.70
−.90	.00782	−.0747	−.0073	−9.55
−.17	.00708	.0731	−.0032	10.32
−.16	(a)	.0680	−.0032	(a)
−.13	.00646	.0707	−.0032	10.94
.79	.00997	.2822	−.0079	28.30
1.64	.01893	.4609	−.0283	24.35
2.33	.03415	.5525	−.0410	16.18
3.22	.05549	.6234	−.0502	11.23

$M = 0.86; R = 9.6 \times 10^6$

α_c, deg	c_d	c_l	c_m	l/d
−3.26	0.05026	−0.5998	0.0573	−11.93
−2.45	.03650	−.5068	.0448	−13.88
−1.73	.01766	−.3415	.0086	−19.34
−.94	.00740	−.1126	−.0114	−15.22
−.21	.00764	.0902	−.0151	11.81
−.10	.00757	.1011	−.0075	13.36
.66	.01474	.2867	−.0245	19.45
1.38	.02654	.4136	−.0380	15.58
2.28	.04130	.4876	−.0532	11.81
3.29	.06207	.5475	−.0558	8.82

[a]Data unavailable.

Table V. Concluded

$M = 0.88; R = 9.8 \times 10^6$

α_c, deg	c_d	c_l	c_m	l/d
−1.54	0.02059	−0.3055	0.0277	−14.84
−1.27	.01856	−.2334	.0133	−12.58
−.92	.01590	−.1252	−.0071	−7.87
−.57	(a)	−.0080	−.0223	(a)
−.18	.01741	.1076	−.0261	6.18
−.16	(a)	.1085	−.0242	(a)
.74	.02846	.2753	−.0511	9.67
1.61	.03433	.3729	−.0559	10.86
2.83	.04678	.4784	−.0546	10.23

$M = 0.90; R = 9.6 \times 10^6$

α_c, deg	c_d	c_l	c_m	l/d
−3.38	0.05415	−0.5088	0.0640	−9.40
−2.58	.04435	−.4215	.0547	−9.50
−1.63	.03381	−.3039	.0355	−8.99
−1.26	.03049	−.2379	.0235	−7.80
−.90	.02515	−.1346	.0037	−5.34
−.87	.02572	−.1374	.0044	−5.35
−.68	.02531	−.0696	−.0107	−2.75
−.13	.02705	.0779	−.0435	2.88
−.13	(a)	.0831	−.0447	(a)
.29	.02895	.1561	−.0473	5.39
.90	.03372	.2506	−.0538	7.43
1.11	.03568	.2717	−.0541	7.61

[a]Data unavailable.

Table VI. Force and Moment Coefficients for the RC(3)-08 Airfoil

$M = 0.38; R = 5.0 \times 10^6$

α_c, deg	c_d	c_l	c_m	l/d
−3.59	0.00724	−0.3367	−0.0008	−46.50
−2.84	.00632	−.2517	−.0014	−39.83
−1.92	.00643	−.1477	−.0010	−22.97
−1.02	.00659	−.0432	−.0011	−6.56
−.13	.00604	.0522	−.0009	8.64
−.07	.00591	.0605	−.0004	10.24
1.71	.00685	.2513	.0007	36.69
3.34	.00694	.4391	.0014	63.27
5.22	.00848	.6495	.0023	76.59
6.16	.01003	.7620	.0034	75.97
7.02	.01055	.8509	.0063	80.65
8.01	.01950	.9063	.0117	46.48
8.99	.04394	.9039	.0097	20.57
9.87	.07745	.9012	−.0069	11.64

$M = 0.43; R = 5.7 \times 10^6$

α_c, deg	c_d	c_l	c_m	l/d
−3.70	0.00730	−0.3513	−0.0037	−48.12
−2.70	.00717	−.2425	−.0028	−33.82
−2.02	.00678	−.1651	−.0024	−24.35
−1.56	.00634	−.1069	−.0024	−16.86
−.13	.00720	.0553	−.0014	7.68
−.10	.00653	.0587	−.0015	8.99
1.75	.00569	.2630	.0008	46.22
3.40	.00720	.4508	.0013	62.61
5.09	.00900	.6480	.0024	72.00
6.00	.01008	.7513	.0050	74.53
6.92	.01458	.8232	.0089	56.46
7.82	.02678	.8611	.0151	32.15
8.93	.04755	.8691	.0158	18.28
9.85	.07447	.8721	−.0027	11.71

Table VI. Continued

$M = 0.43; R = 3.9 \times 10^6$

α_c, deg	c_d	c_l	c_m	l/d
−3.63	0.00842	−0.3392	−0.0054	−40.29
−2.73	.00720	−.2365	−.0040	−32.85
−1.98	.00666	−.1509	−.0032	−22.66
−1.20	.00655	−.0637	−.0024	−9.73
−.24	(a)	.0419	−.0021	(a)
−.09	.00615	.0623	−.0023	10.13
1.64	.00642	.2504	.0007	39.00
3.59	.00659	.4578	.0019	69.47
5.14	.00782	.6432	.0022	82.25
6.05	.00865	.7380	.0048	85.32
7.22	.01548	.8086	.0115	52.24
8.01	.02484	.8578	.0150	34.53
8.91	.04314	.8619	.0169	19.98
9.82	.06633	.8858	.0065	13.35
11.06	(a)	.8843	−.0090	(a)

$M = 0.48; R = 6.5 \times 10^6$

α_c, deg	c_d	c_l	c_m	l/d
−3.69	0.00971	−0.3595	−0.0066	−37.02
−2.78	.00750	−.2594	−.0036	−34.59
−1.96	.00680	−.1614	−.0029	−23.74
−1.26	.00719	−.0794	−.0022	−11.04
−.14	.00603	.0556	−.0024	9.22
−.10	.00616	.0610	−.0020	9.90
1.81	.00702	.2863	−.0007	40.78
3.86	.00798	.5264	.0011	65.96
5.10	.00863	.6721	.0032	77.88
5.96	.01124	.7496	.0071	66.69
7.04	.01611	.8199	.0147	50.89
8.52	.04330	.8693	.0196	20.08
9.77	.06813	.8805	.0112	12.92

[a]Data unavailable.

Table VI. Continued

$M = 0.52; R = 6.9 \times 10^6$

α_c, deg	c_d	c_l	c_m	l/d
−3.69	0.01087	−0.3566	−0.0090	−32.81
−2.71	.00762	−.2525	−.0050	−33.14
−1.81	.00683	−.1456	−.0029	−21.32
−1.06	.00619	−.0528	−.0023	−8.53
−.11	.00602	.0666	−.0022	11.06
−.11	.00628	.0655	−.0020	10.43
1.68	.00640	.2702	−.0005	42.22
3.45	.00696	.4860	.0014	69.83
5.13	.00877	.6844	.0055	78.04
6.08	.01335	.7702	.0130	57.69
7.24	.02560	.8310	.0204	32.46
7.86	.03807	.8448	.0222	22.19
8.96	.06156	.8487	.0129	13.79
9.91	.08846	.8529	−.0032	9.64

$M = 0.53; R = 4.8 \times 10^6$

α_c, deg	c_d	c_l	c_m	l/d
−3.66	0.01242	−0.3454	−0.0098	−27.81
−2.71	.00634	−.2466	−.0061	−38.90
−1.99	.00705	−.1615	−.0043	−22.91
−1.15	.00663	−.0596	−.0033	−8.99
−.11	.00642	.0626	−.0024	9.75
−.11	.00637	.0641	−.0024	10.06
1.87	.00644	.2933	.0008	45.54
3.80	.00668	.5101	.0038	76.36
5.09	.00824	.6544	.0064	79.42
6.07	.01342	.7579	.0136	56.48
6.95	.02087	.7942	.0204	38.05
7.88	.03429	.8316	.0213	24.25
9.14	.06242	.8513	.0121	13.64
9.91	.08128	.8672	−.0029	10.67

Table VI. Continued

$M = 0.57; R = 7.4 \times 10^6$

α_c, deg	c_d	c_l	c_m	l/d
−3.58	0.01229	−0.3499	−0.0109	−28.47
−2.69	.00786	−.2528	−.0058	−32.16
−1.86	.00725	−.1576	−.0038	−21.74
−.91	.00601	−.0368	−.0028	−6.12
−.15	.00701	.0582	−.0020	8.30
−.11	.00643	.0664	−.0022	10.33
1.84	.00655	.3059	−.0006	46.70
3.48	.00760	.5088	.0022	66.95
5.11	.01047	.6944	.0107	66.32
6.12	.01400	.7717	.0181	55.12
7.04	.02161	.8313	.0258	38.47
8.07	.04072	.8552	.0235	21.00
8.84	.05727	.8724	.0154	15.23
9.96	.08317	.8740	−.0011	10.51

$M = 0.63; R = 7.9 \times 10^6$

α_c, deg	c_d	c_l	c_m	l/d
−3.60	0.01232	−0.3575	−0.0153	−29.04
−2.70	.00728	−.2640	−.0109	−36.26
−1.94	.00643	−.1687	−.0047	−26.24
−1.08	.00586	−.0576	−.0040	−9.83
−.13	.00563	.0693	−.0031	12.31
−.12	.00619	.0731	−.0031	11.81
1.66	.00572	.2955	−.0010	51.66
3.32	.00686	.5083	.0031	74.10
4.30	.00721	.6273	.0085	87.00
4.98	.01149	.7130	.0162	62.05
6.02	.02068	.8001	.0239	38.69
7.01	.03213	.8567	.0306	26.66
7.91	.04320	.8705	.0284	20.15
9.15	.07704	.8766	−.0040	11.38

Table VI. Continued

$M = 0.63; R = 5.9 \times 10^6$

α_c, deg	c_d	c_l	c_m	l/d
−3.66	0.01456	−0.3616	−0.0163	−24.84
−2.59	.00818	−.2462	−.0111	−30.10
−1.81	.00703	−.1476	−.0060	−21.00
−1.12	.00672	−.0593	−.0044	−8.82
−.14	.00606	.0668	−.0035	11.02
−.09	.00619	.0718	−.0031	11.60
1.72	.00676	.3026	−.0001	44.76
2.91	.00716	.4500	.0031	62.85
5.25	.01295	.7327	.0182	56.58
6.05	.02001	.7901	.0242	39.49
7.11	.03101	.8451	.0304	27.25
8.04	.04765	.8647	.0168	18.15
8.91	.06896	.8705	.0000	12.62

$M = 0.68; R = 8.3 \times 10^6$

α_c, deg	c_d	c_l	c_m	l/d
−3.49	0.01614	−0.3719	−0.0184	−23.04
−2.75	.00966	−.2797	−.0134	−28.95
−1.93	.00640	−.1763	−.0078	−27.55
−1.04	.00671	−.0541	−.0047	−8.06
−.13	.00647	.0742	−.0032	11.47
−.12	.00613	.0727	−.0034	11.86
1.59	.00621	.3065	−.0011	49.36
3.43	.00757	.5508	.0072	72.76
4.26	.01118	.6574	.0149	58.80
5.25	.01991	.7544	.0227	37.89
6.17	.02821	.7973	.0269	28.26
7.03	.03584	.8315	.0300	23.20
7.86	.04500	.8674	.0323	19.28

Table VI. Continued

$M = 0.72; R = 8.6 \times 10^6$

α_c, deg	c_d	c_l	c_m	l/d
−3.51	0.02019	−0.4079	−0.0216	−20.20
−2.69	.01246	−.3060	−.0177	−24.56
−1.93	.00730	−.1746	−.0104	−23.92
−1.11	.00721	−.0685	−.0065	−9.50
−.16	.00667	.0772	−.0047	11.57
−.11	.00629	.0831	−.0048	13.21
1.60	.00656	.3305	−.0010	50.38
3.36	.01217	.6019	.0096	49.46
4.18	.02401	.7150	.0141	29.78
5.07	.03009	.7700	.0185	25.59
6.00	.03581	.7933	.0217	22.15
7.03	.04419	.8292	.0243	18.76

$M = 0.78; R = 9.0 \times 10^6$

α_c, deg	c_d	c_l	c_m	l/d
−3.39	0.03449	−0.5026	−0.0201	−14.57
−2.64	.01958	−.3455	−.0212	−17.65
−1.89	.00987	−.2008	−.0164	−20.34
−1.02	.00617	−.0464	−.0108	−7.52
−.15	.00624	.0959	−.0072	15.37
−.13	.00590	.0988	−.0072	16.75
1.62	.00777	.3903	−.0019	50.23
3.35	.02489	.6461	−.0046	25.96
4.27	.03807	.7251	−.0025	19.05
5.19	.05326	.7905	−.0062	14.84
5.93	.06714	.8113	−.0132	12.08

Table VI. Continued

$M = 0.84; R = 9.1 \times 10^6$

α_c, deg	c_d	c_l	c_m	l/d
−3.36	0.03905	−0.5880	0.0047	−15.06
−2.57	.02246	−.4336	−.0066	−19.31
−1.78	.01272	−.2259	−.0181	−17.76
−1.72	.01240	−.2139	−.0177	−17.25
−.88	.00666	−.0239	−.0146	−3.59
−.22	.00674	.1199	−.0135	17.79
−.19	.00647	.1290	−.0146	19.94
−.17	.00677	.1194	−.0117	17.64
.82	.01078	.2995	−.0140	27.78
1.63	.01695	.4056	−.0201	23.93
2.41	.02537	.4928	−.0255	19.42
3.29	.03836	.5681	−.0355	14.81

$M = 0.86; R = 9.4 \times 10^6$

α_c, deg	c_d	c_l	c_m	l/d
−3.19	0.03971	−0.5453	0.0321	−13.73
−2.57	.02586	−.4686	.0201	−18.12
−1.63	.00825	−.2447	−.0090	−29.66
−1.02	.00733	−.0440	−.0225	−6.00
−.21	(a)	.1487	−.0325	(a)
−.21	.01088	.1509	−.0298	13.87
.73	.01971	.2967	−.0392	15.05
1.76	.02805	.3793	−.0364	13.52
2.54	.03593	.4509	−.0369	12.55
3.38	.04716	.5022	−.0346	10.65

[a]Data unavailable.

Table VI. Concluded

$M = 0.88; R = 9.6 \times 10^6$

α_c, deg	c_d	c_l	c_m	l/d
−2.90	0.03681	−0.4916	0.0297	−13.36
−2.40	.02697	−.4014	.0237	−14.88
−1.77	.01463	−.2914	.0078	−19.92
−1.38	.01156	−.1856	−.0106	−16.06
−1.35	(a)	−.1670	−.0144	(a)
−.96	.01253	−.0610	−.0342	−4.87
−.76	.01438	.0103	−.0435	.72
−.19	.01952	.1301	−.0485	6.66
.77	.02519	.2644	−.0439	10.50
1.76	.03165	.3367	−.0376	10.64
2.60	.03971	.3972	−.0334	10.00
3.61	.04691	.4416	−.0222	9.41

$M = 0.90; R = 9.5 \times 10^6$

α_c, deg	c_d	c_l	c_m	l/d
−3.44	0.04765	−0.4076	0.0117	−8.55
−2.57	.03611	−.3458	.0128	−9.58
−1.88	.02880	−.2518	.0021	−8.74
−1.69	(a)	−.2011	−.0103	(a)
−1.37	.02237	−.1613	−.0150	−7.21
−.93	.01925	−.0817	−.0310	−4.24
−.51	.02004	−.0158	−.0390	−.79
−.08	.02217	.0405	−.0397	1.83
.40	.02520	.1196	−.0351	4.75
1.27	.03171	.1933	−.0228	6.10
2.10	.04053	.2603	−.0125	6.42

[a]Data unavailable.

RC(6)-08

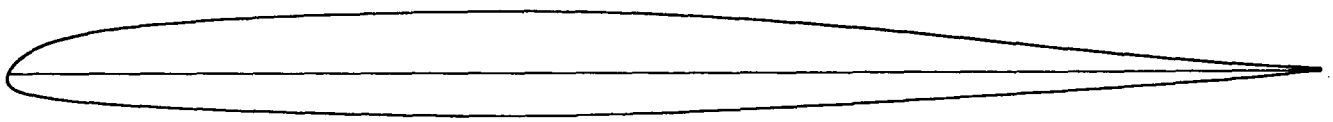

RC(3)-08

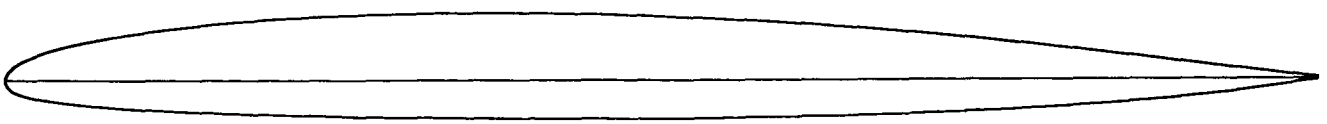

Figure 1. Airfoil profiles.

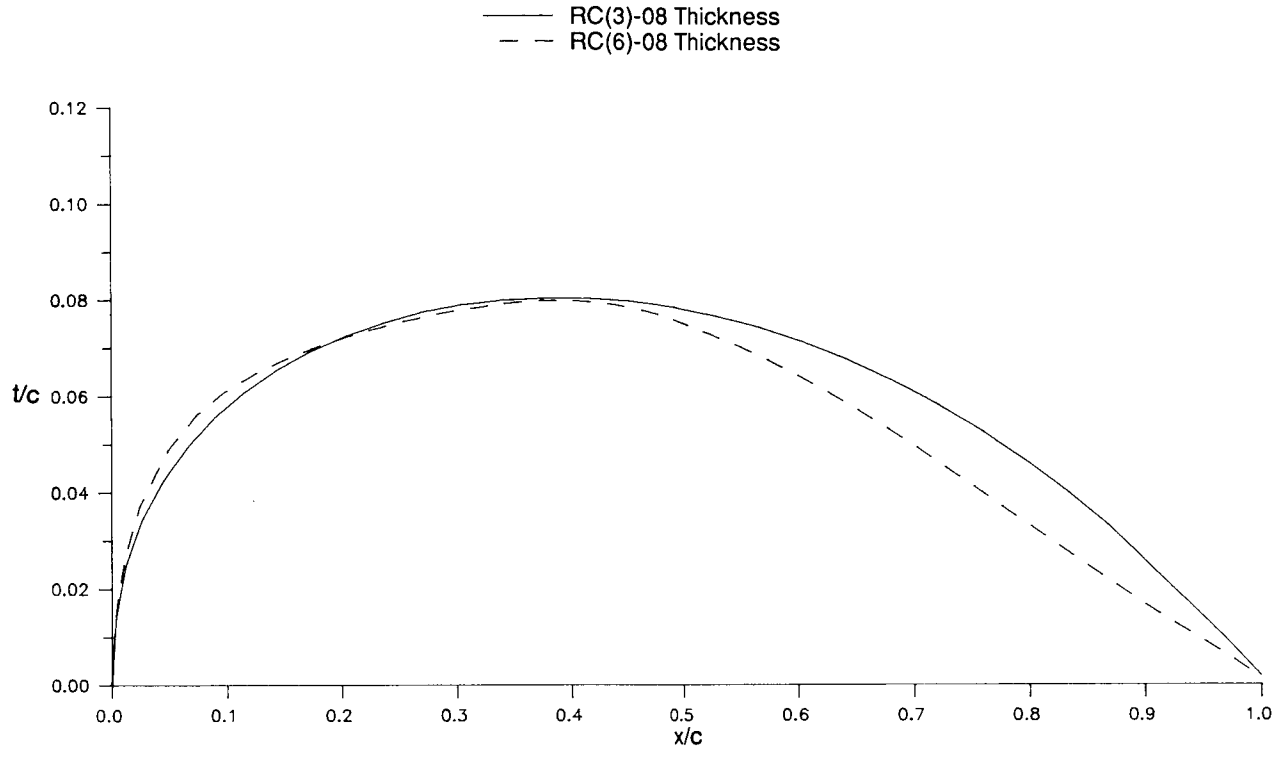

(a) Thickness distribution.

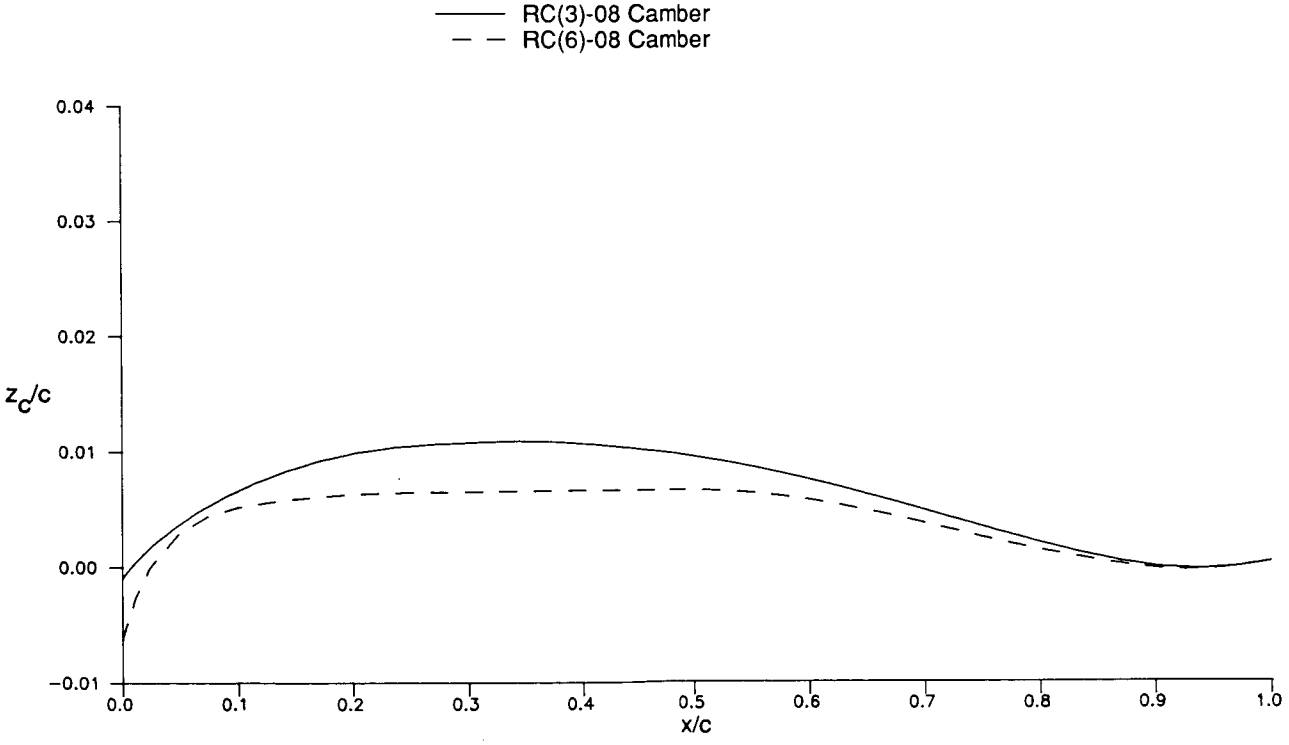

(b) Camber distribution.

Figure 2. Thickness and camber distributions of the RC(6)-08 and RC(3)-08 airfoils.

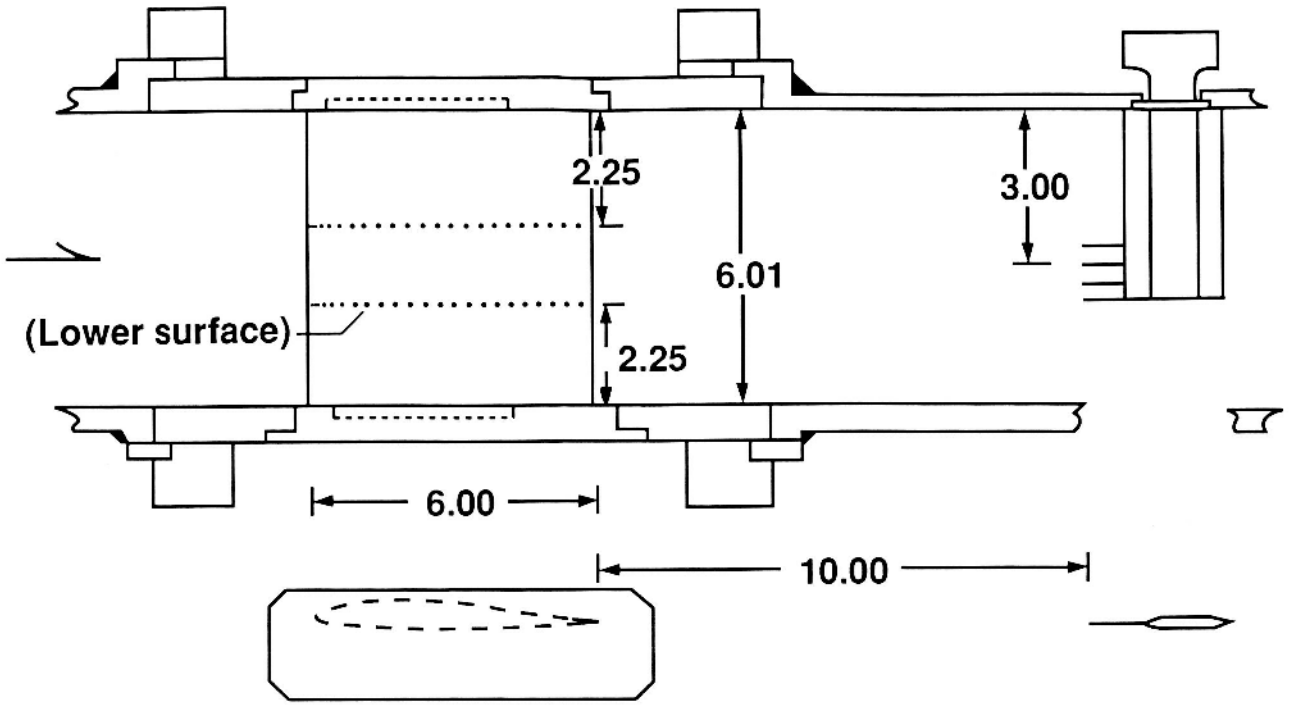

(a) Installation in wind tunnel.

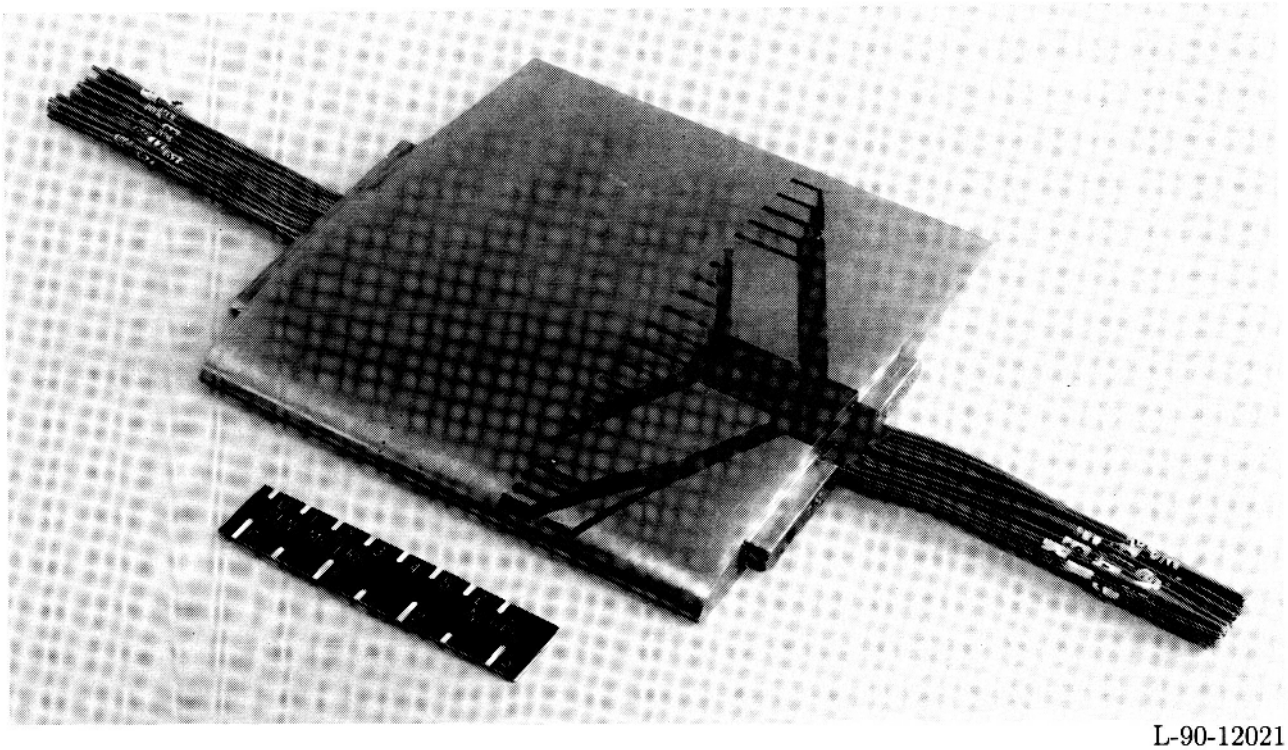

L-90-12021

(b) Typical airfoil model.

Figure 3. Model and wake-survey probe for Langley 6- by 28-Inch Transonic Tunnel. All dimensions are in inches.

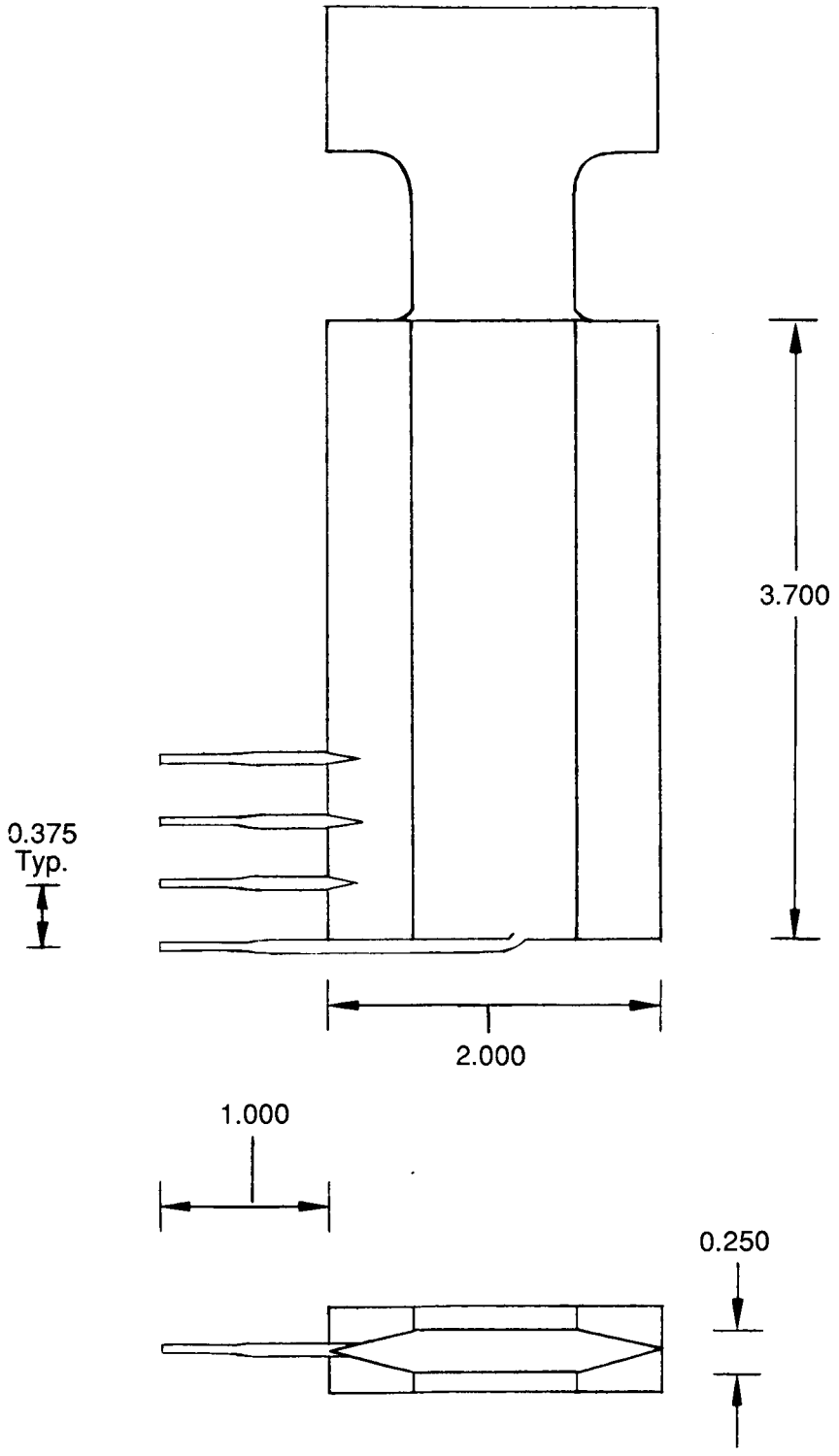

Figure 4. Wake-survey probe used in Langley 6- by 28-Inch Transonic Tunnel. All dimensions are in inches.

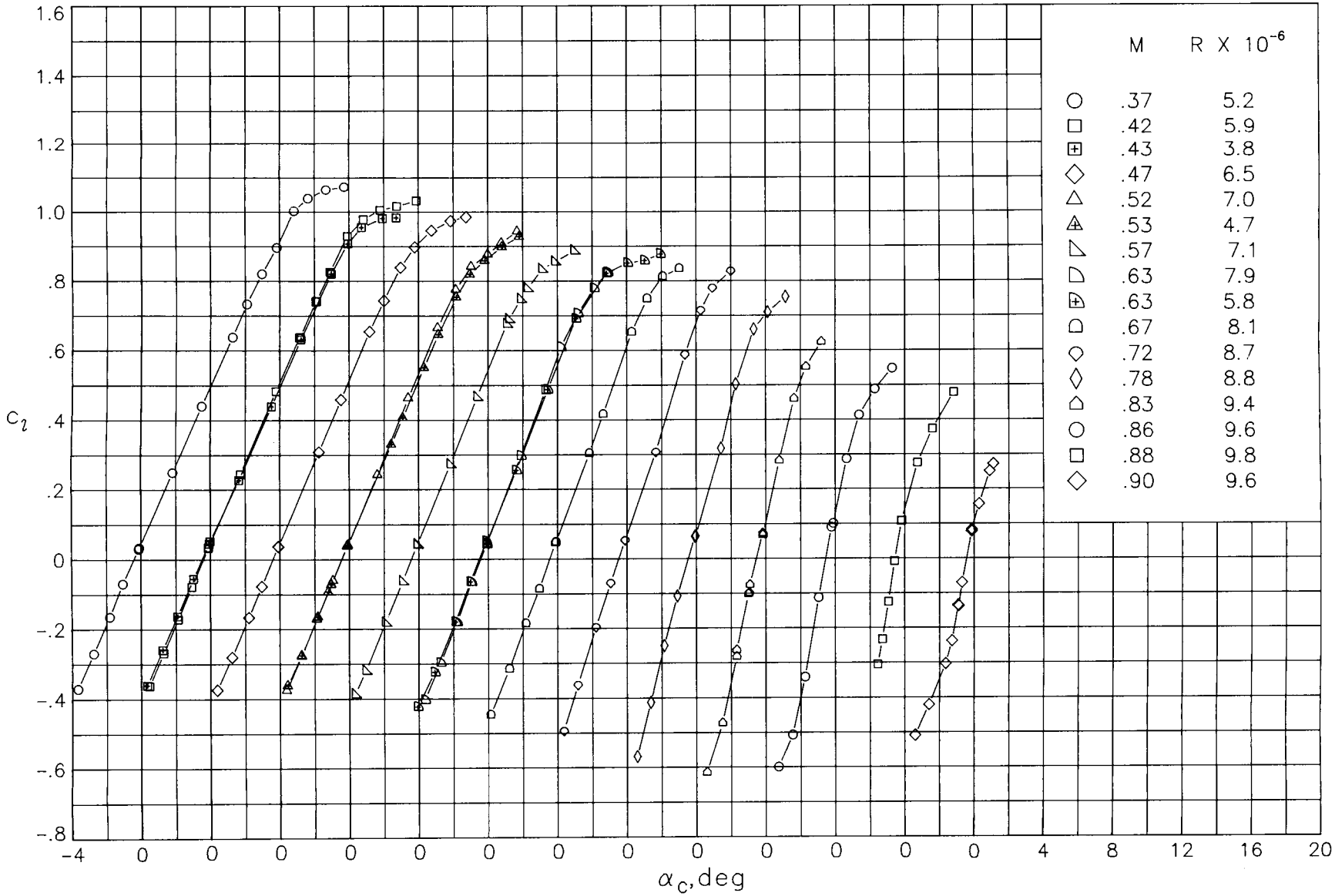

(a) Section lift coefficients.

Figure 5. Aerodynamic characteristics of RC(6)-08 airfoil measured in Langley 6- by 28-Inch Transonic Tunnel.

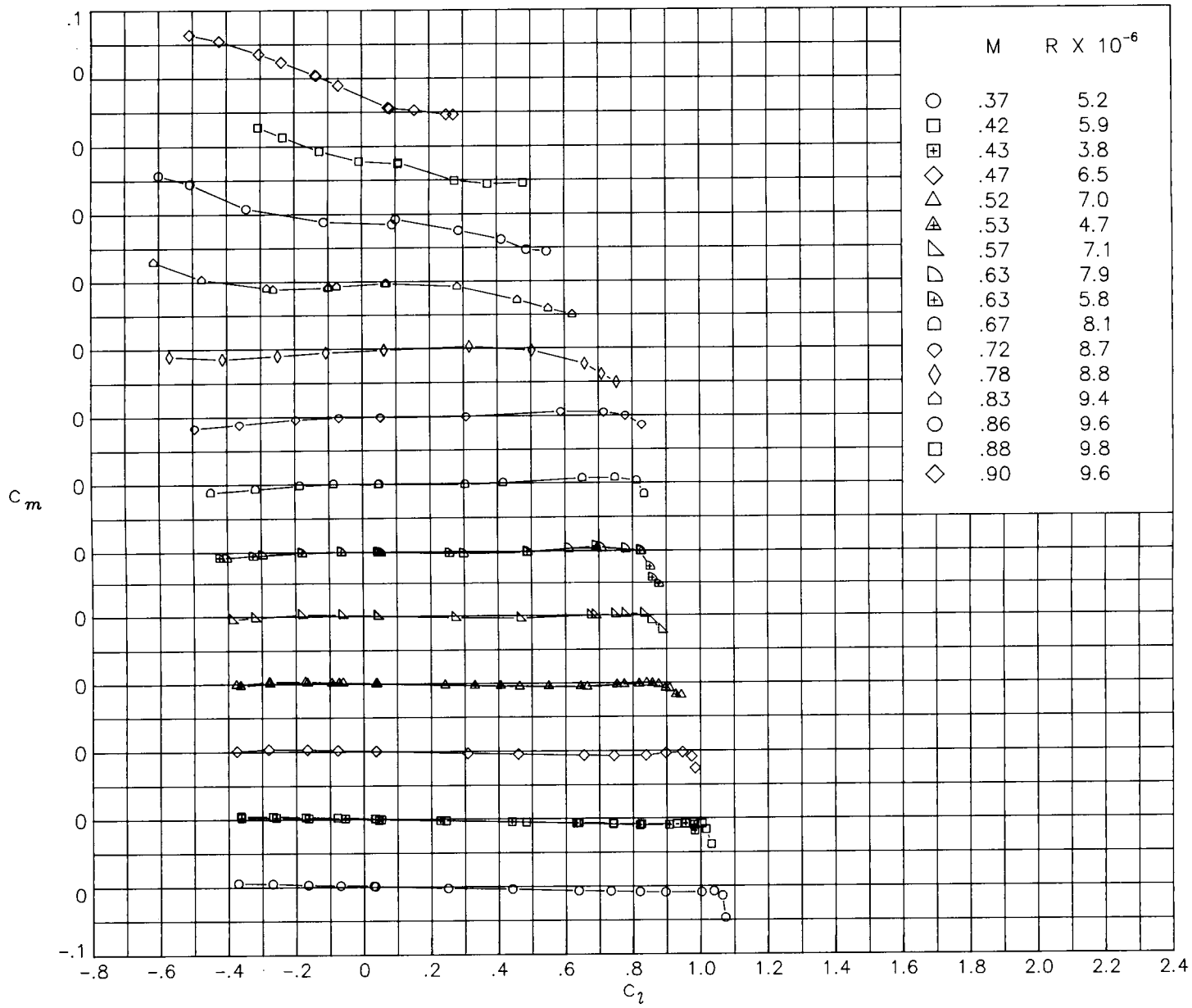

(b) Section pitching-moment coefficients.

Figure 5. Continued.

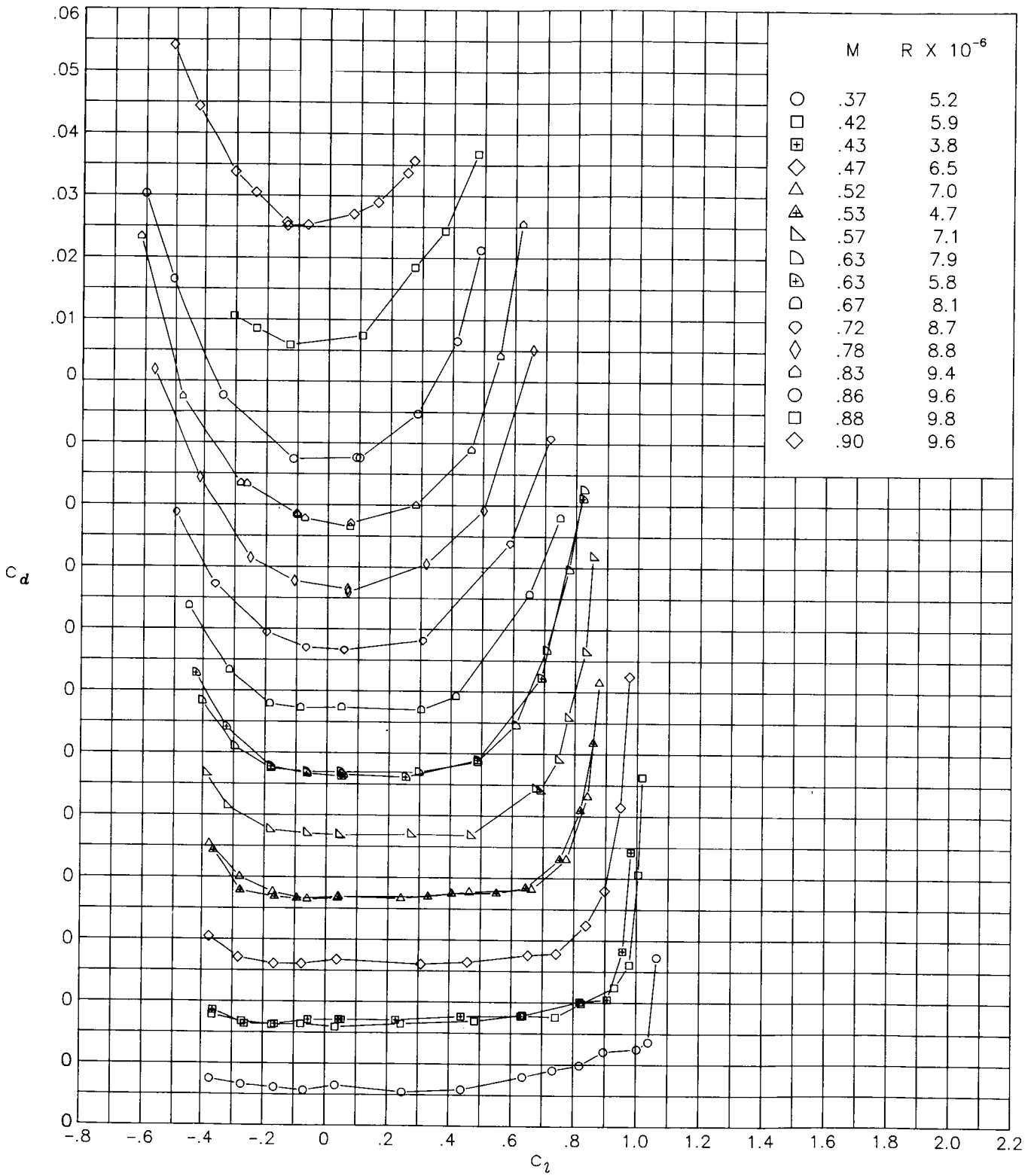

(c) Section drag coefficients.

Figure 5. Continued.

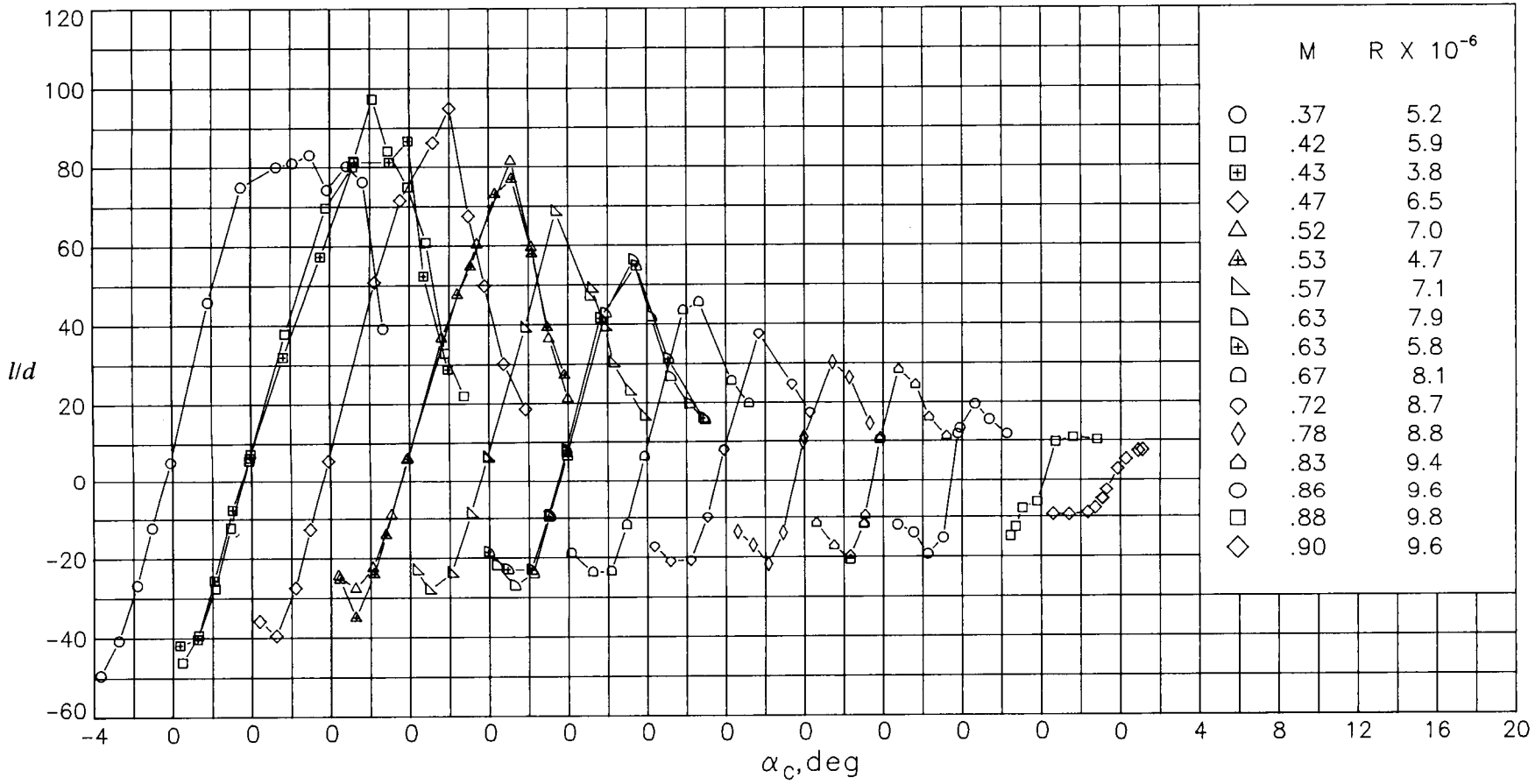

(d) Section lift-to-drag ratio.

Figure 5. Concluded.

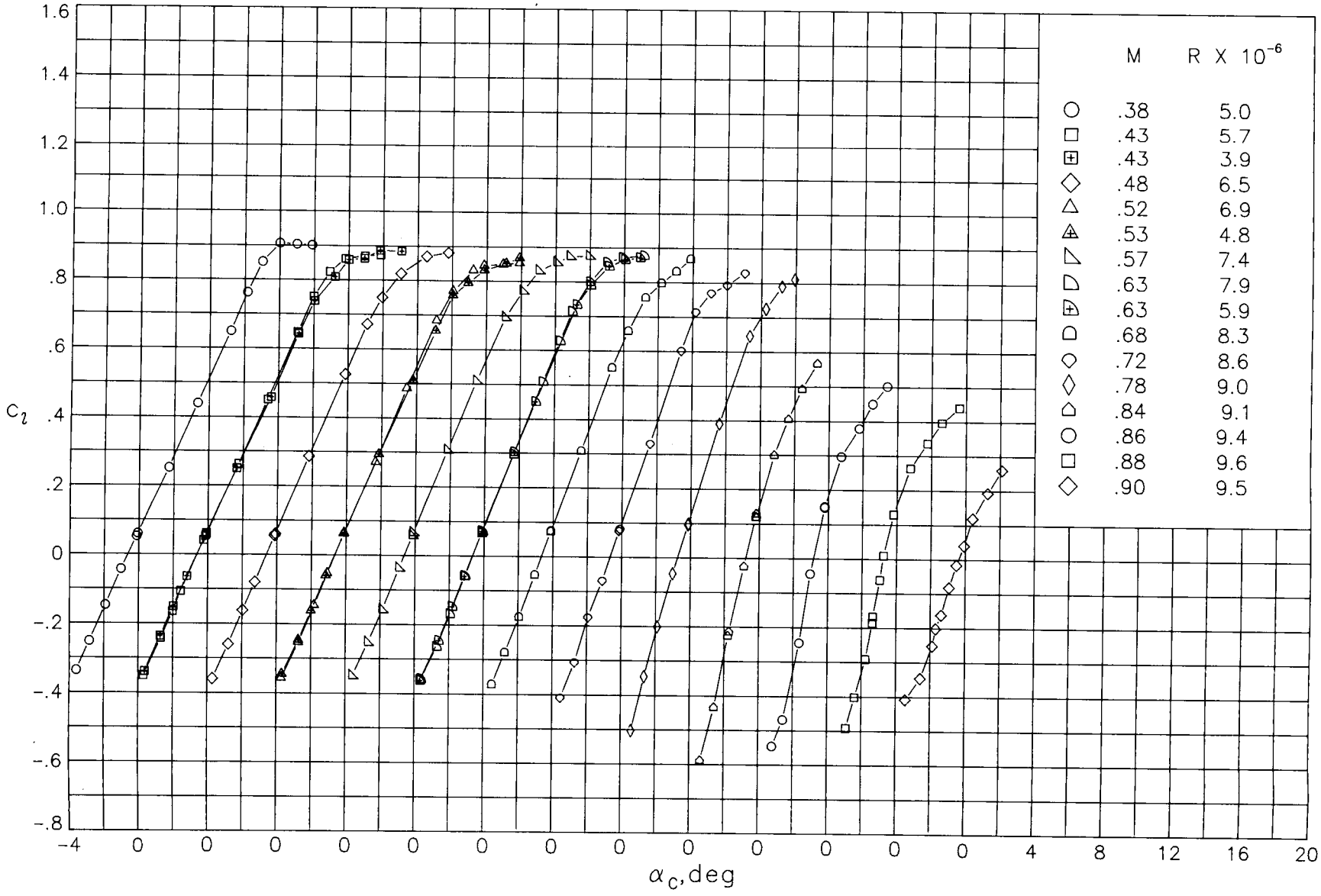

(a) Section lift coefficients.

Figure 6. Aerodynamic characteristics of RC(3)-08 airfoil measured in Langley 6- by 28-Inch Transonic Tunnel.

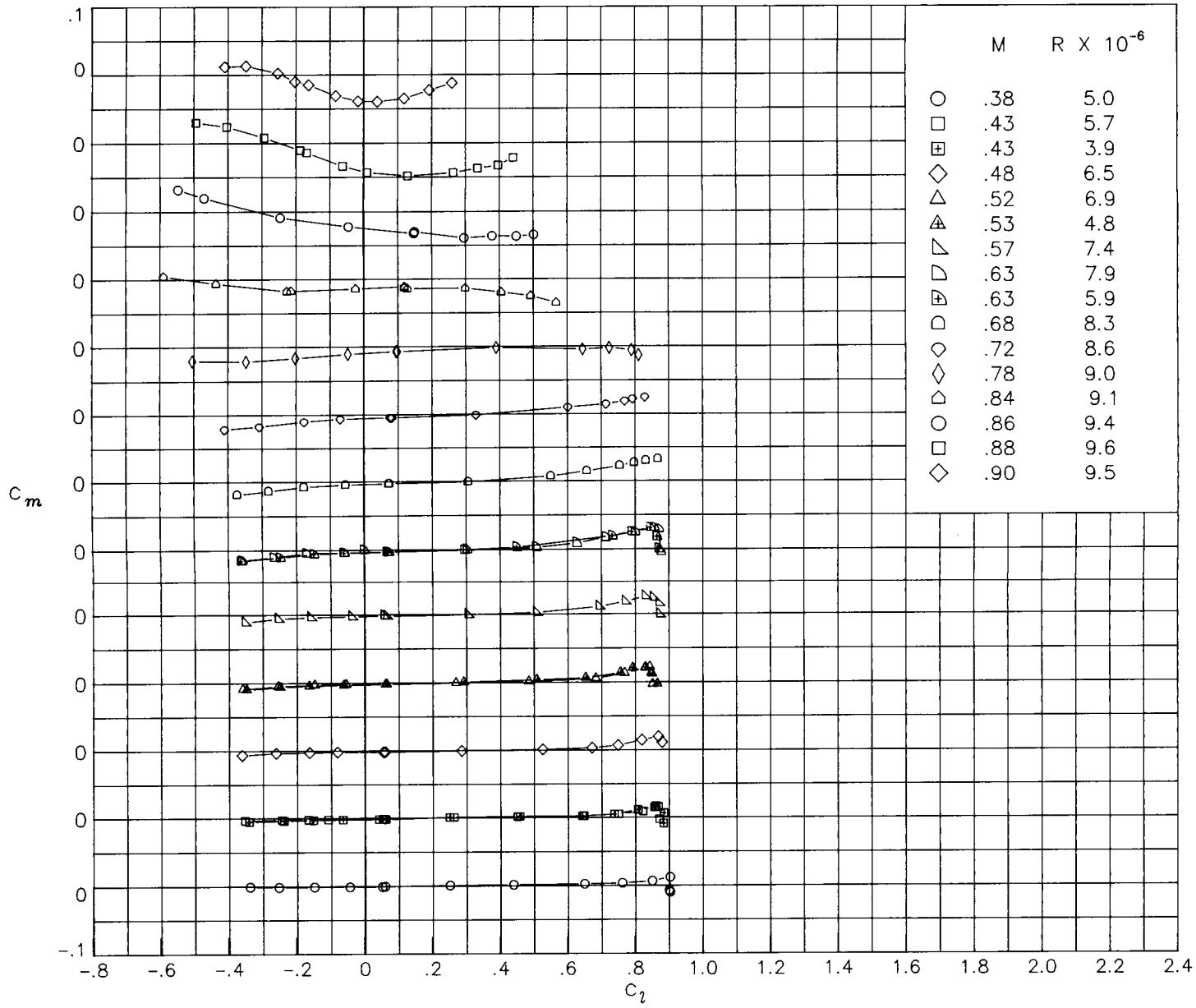

(b) Section pitching-moment coefficients.

Figure 6. Continued.

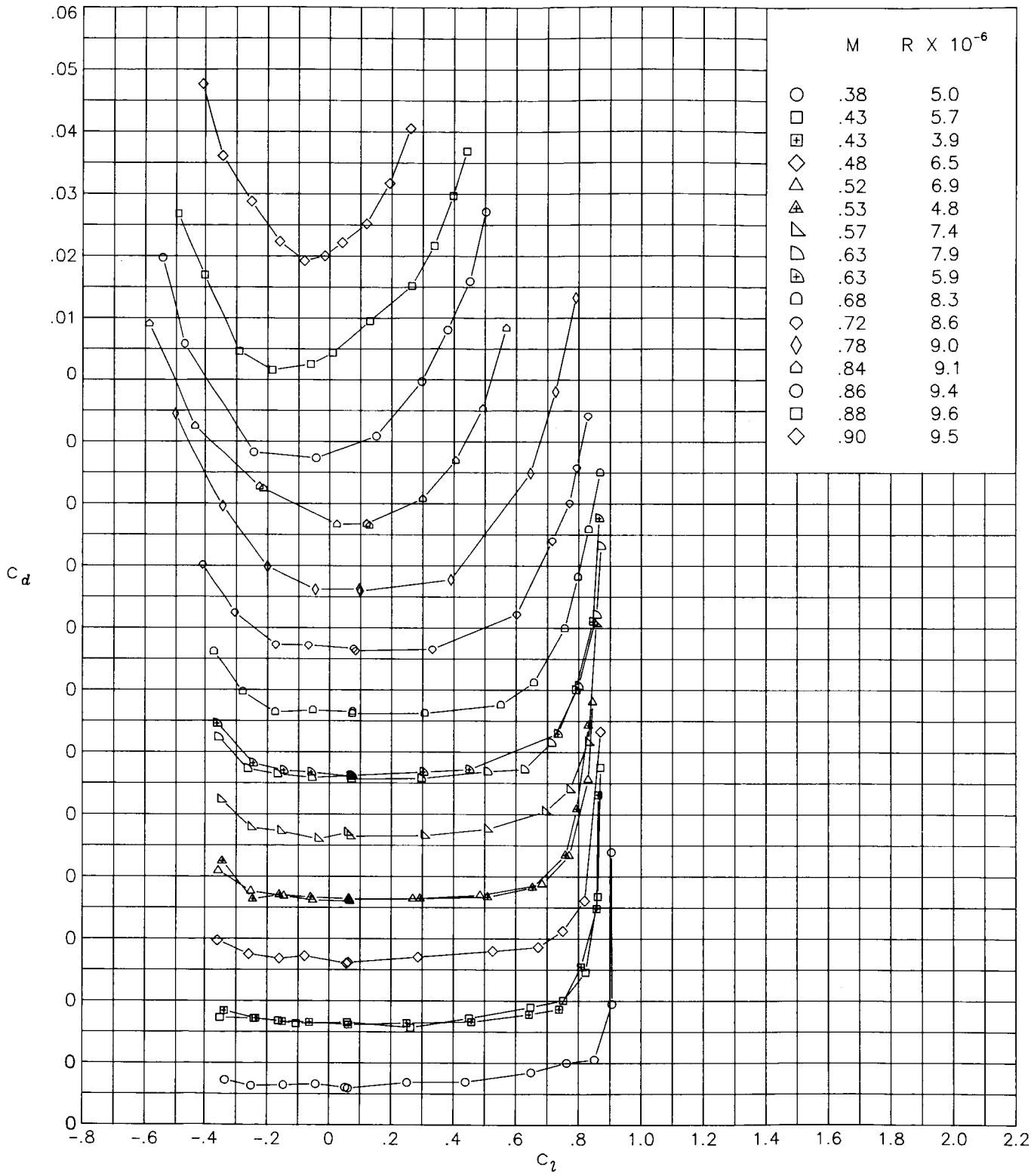

(c) Section drag coefficients.

Figure 6. Continued.

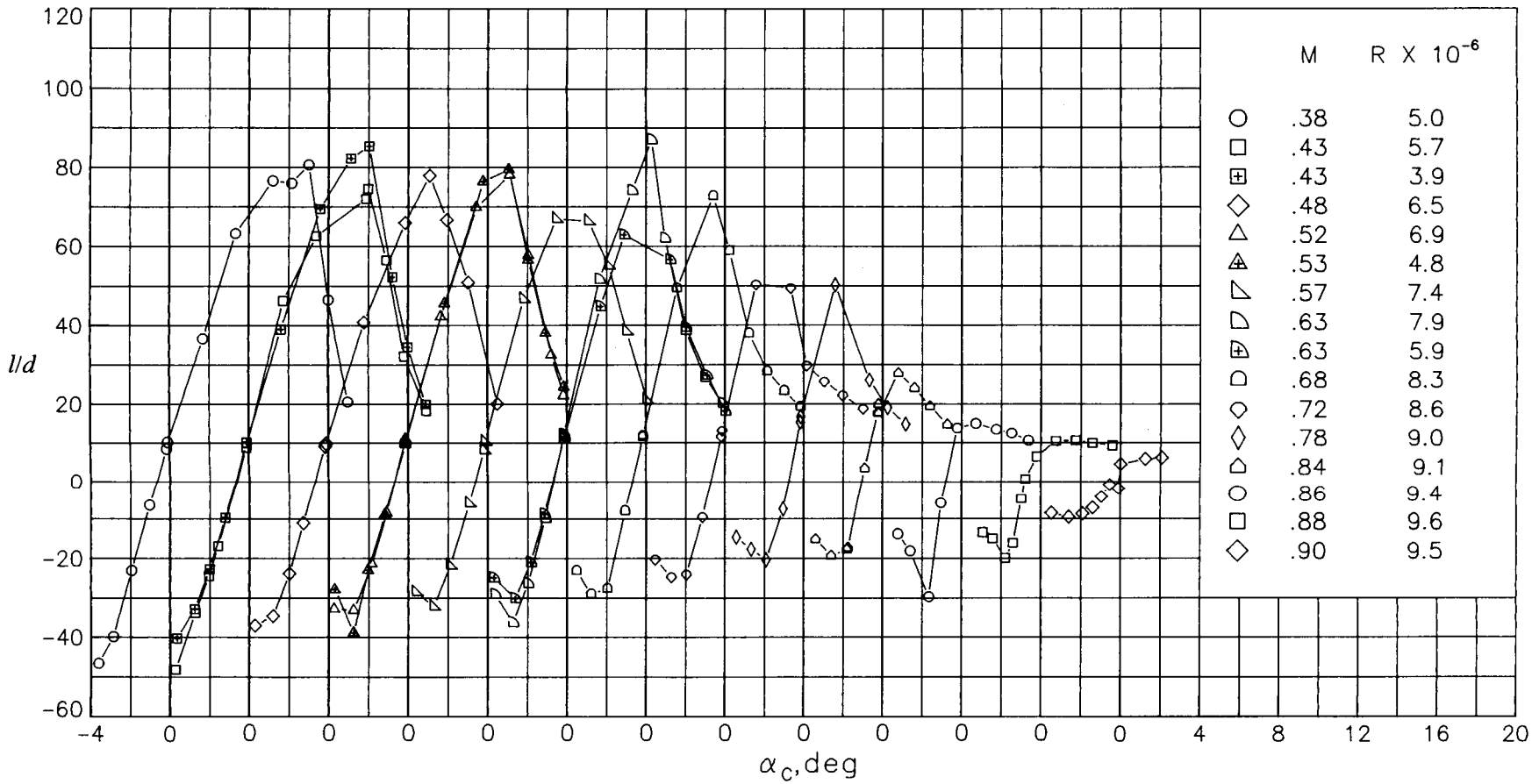

(d) Section lift-to-drag ratio.

Figure 6. Concluded.

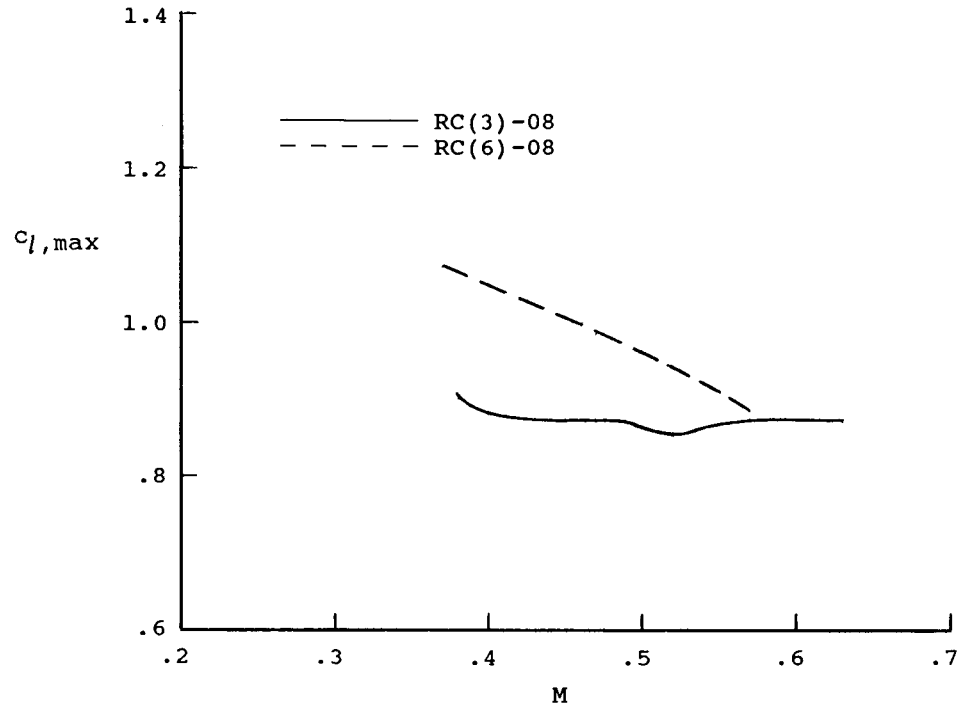

Figure 7. Variation in maximum lift coefficient with Mach number for the RC(6)-08 and RC(3)-08 airfoils.

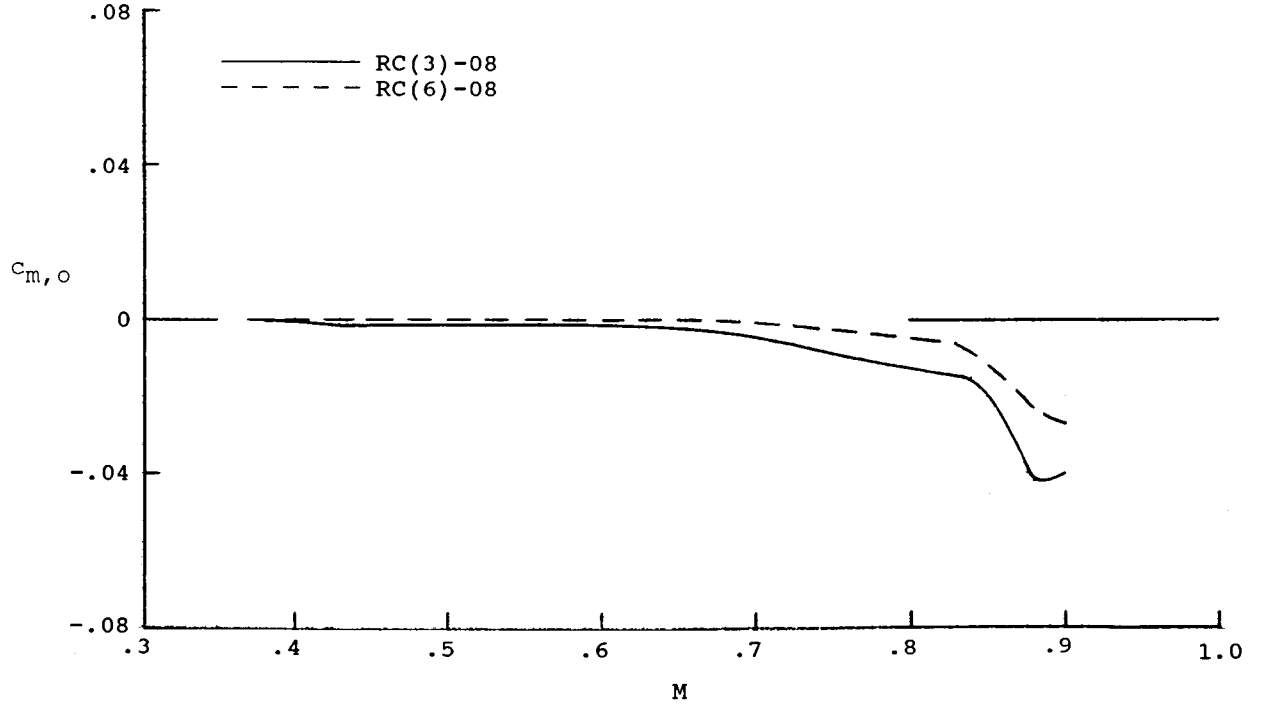

Figure 8. Variation in pitching-moment coefficient at $c_l = 0$ with Mach number for the RC(6)-08 and RC(3)-08 airfoils.

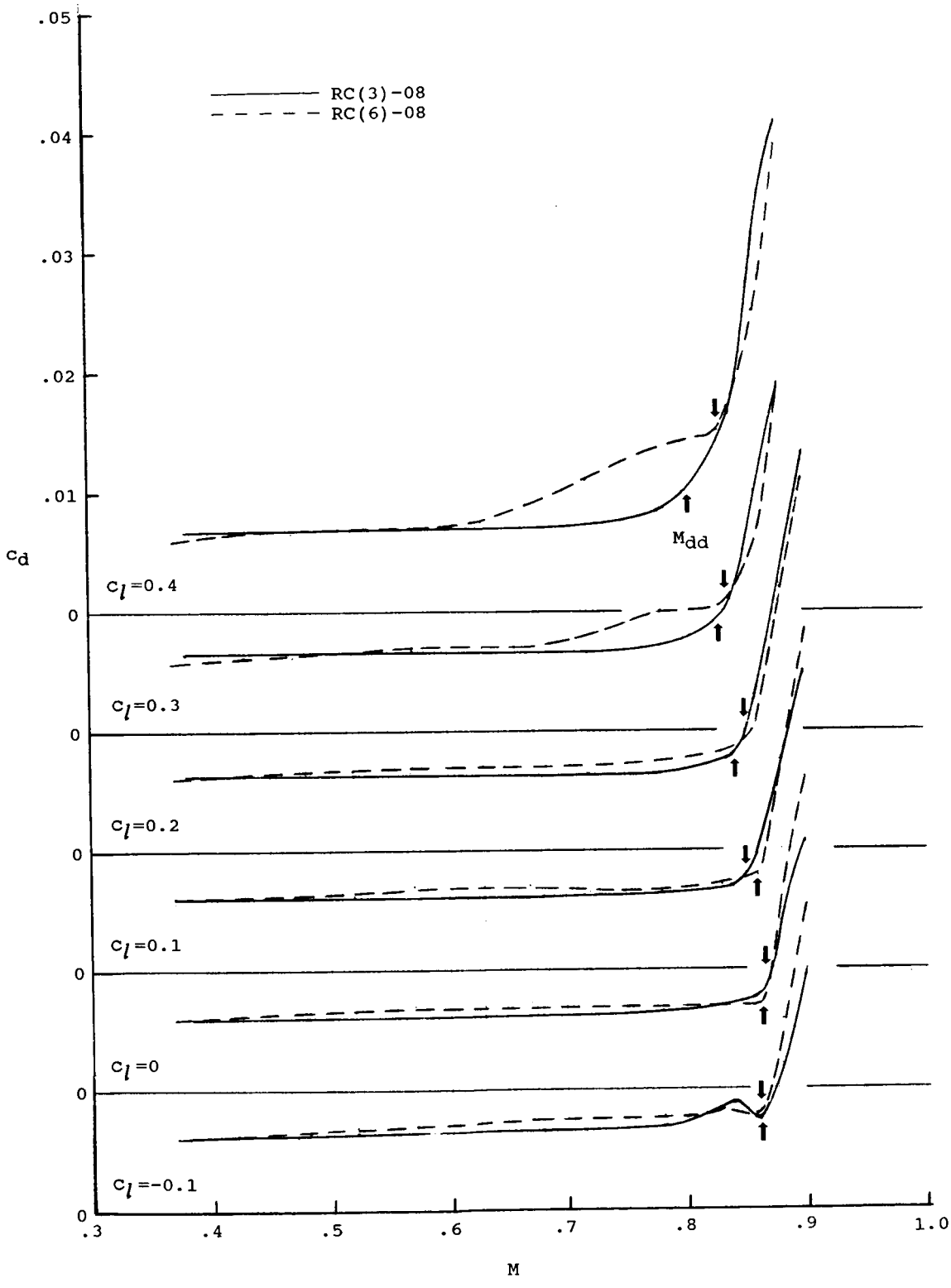

(a) $c_l = -0.1$ to 0.4.

Figure 9. Variation in drag coefficient with Mach number for the RC(6)-08 and RC(3)-08 airfoils.

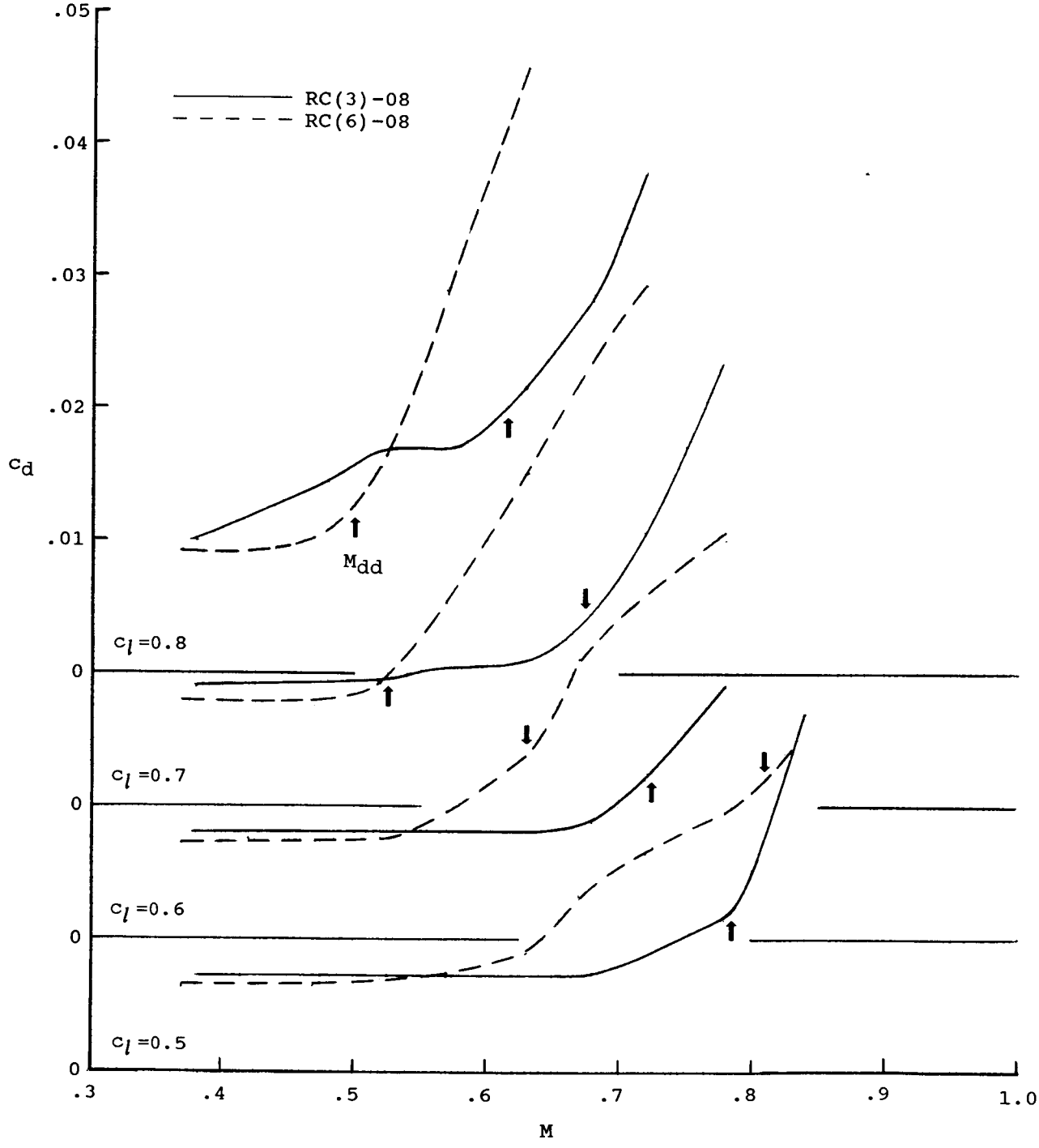

(b) $c_l = 0.5$ to 0.8.

Figure 9. Concluded.

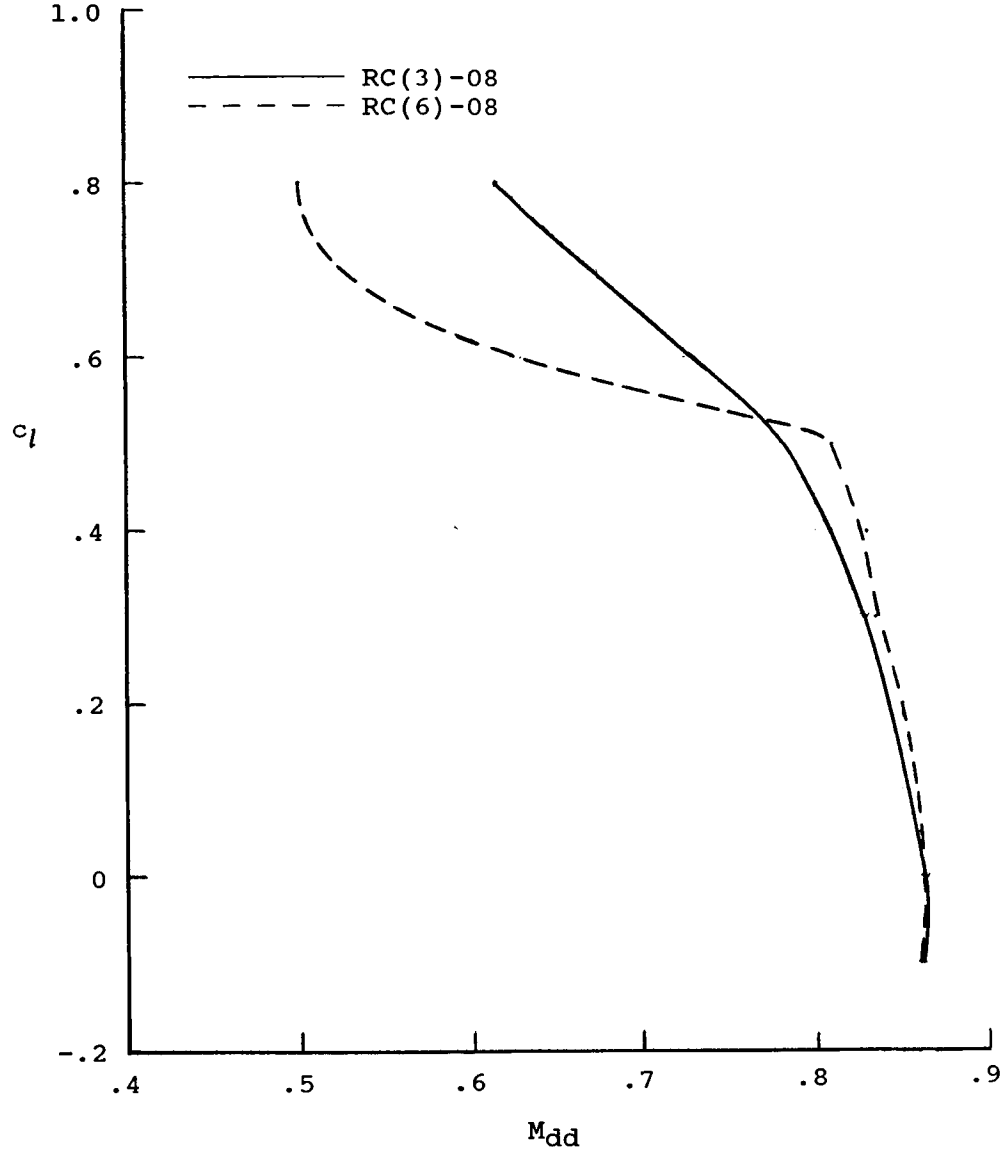

Figure 10. Variation in lift coefficient with drag-divergence Mach number for the RC(6)-08 and RC(3)-08 airfoils.

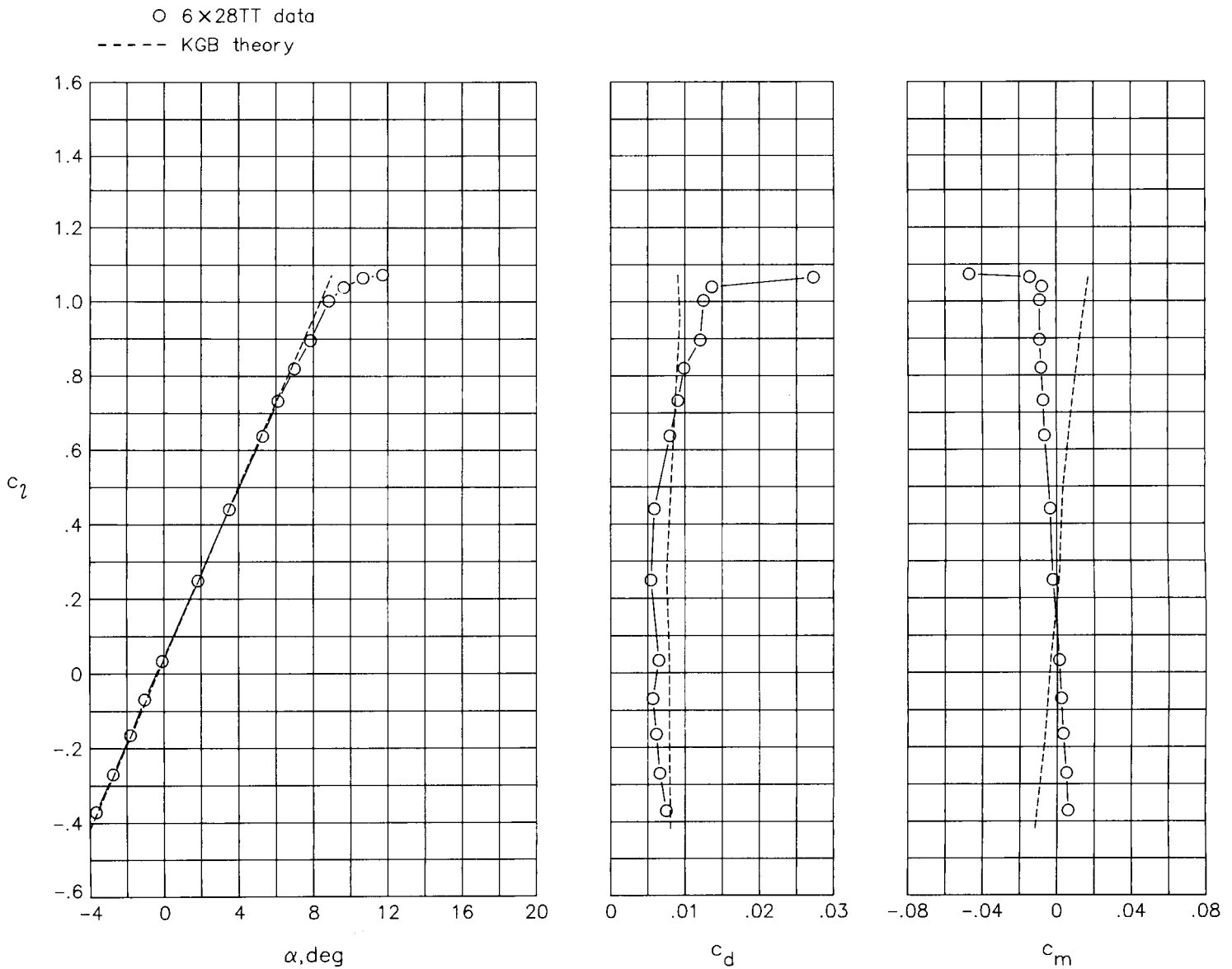

(a) $M = 0.37$; $R = 5.2 \times 10^6$.

Figure 11. Comparison of RC(6)-08 airfoil data measured in the 6×28TT with theory.

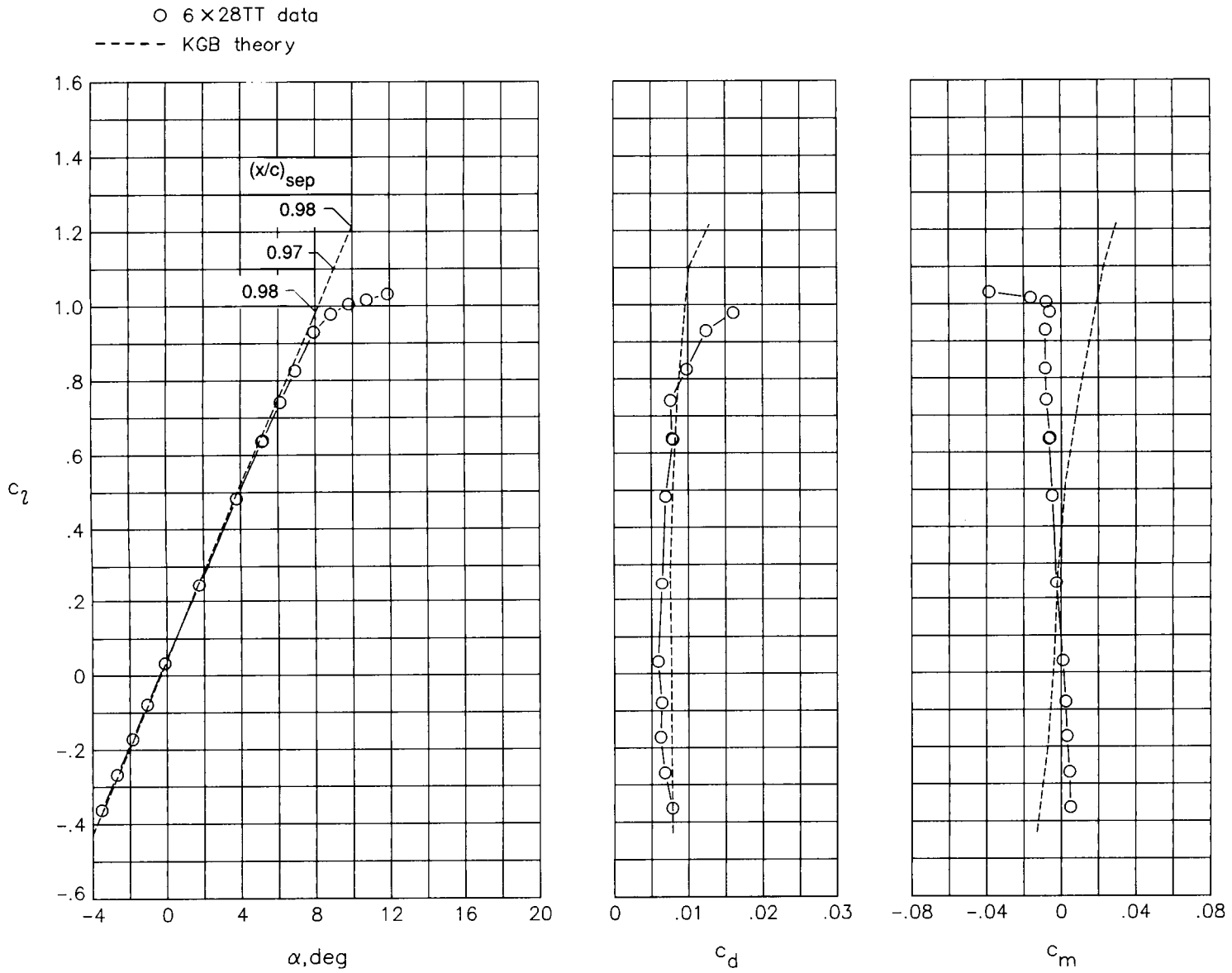

(b) $M = 0.42$; $R = 5.9 \times 10^6$.

Figure 11. Continued.

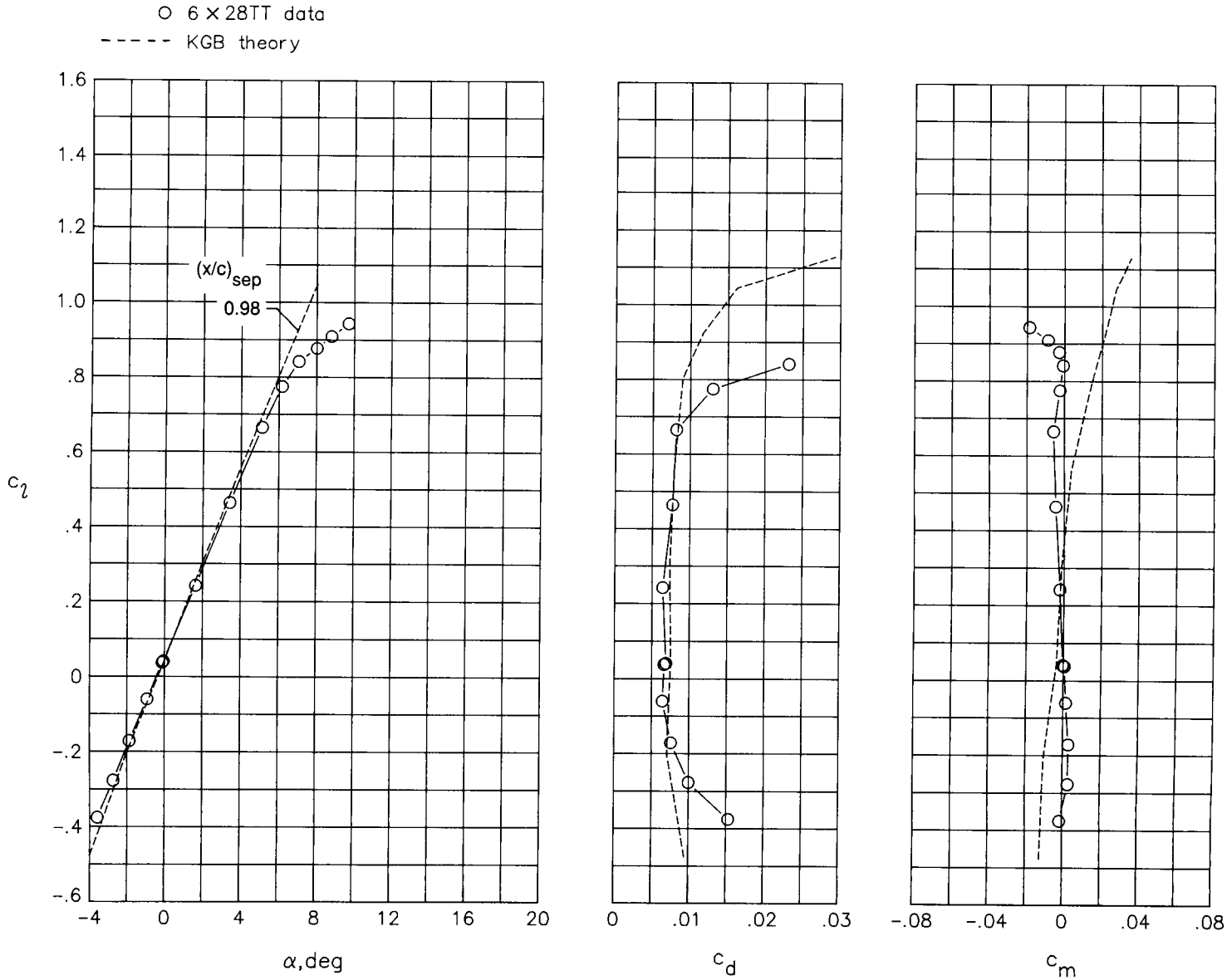

(c) $M = 0.52$; $R = 7.0 \times 10^6$.

Figure 11. Concluded.

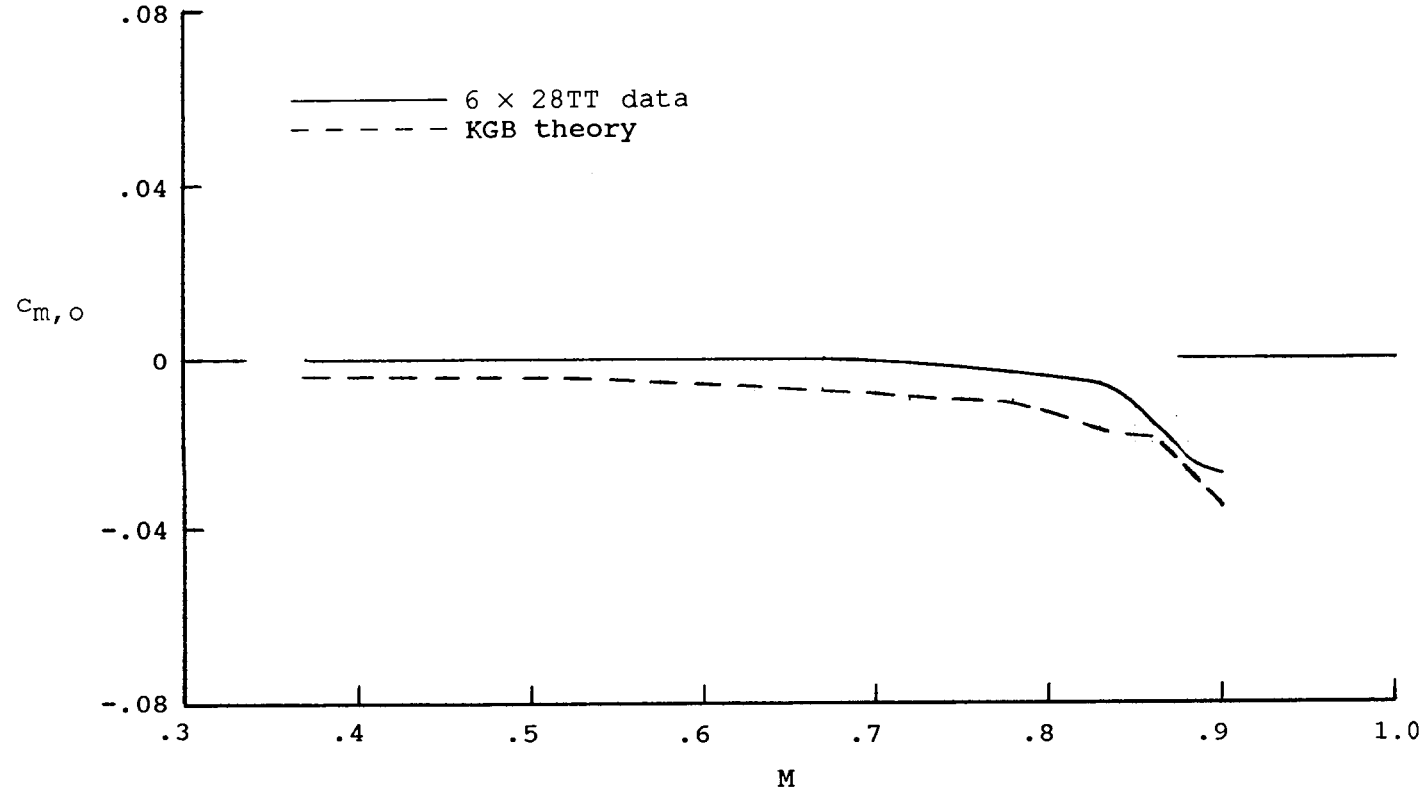

Figure 12. Comparison of experimental and theoretical variation of pitching-moment coefficient with Mach number for the RC(6)-08 airfoil; $c_l = 0$.

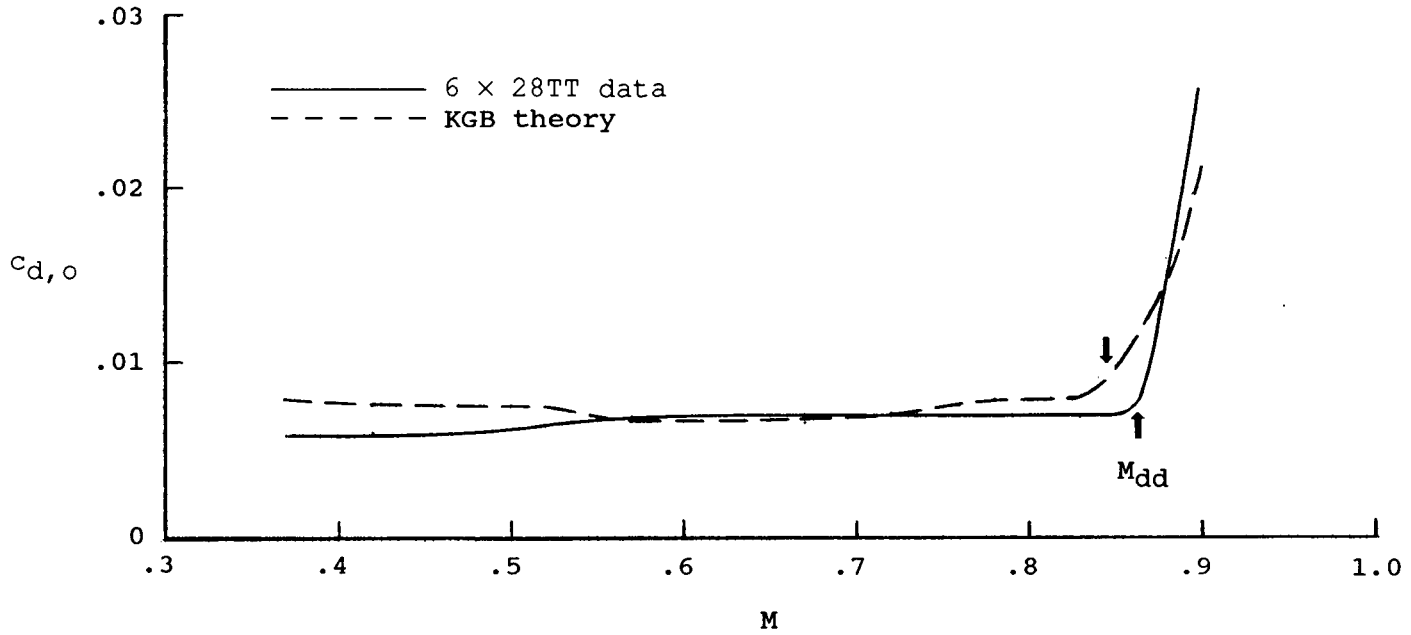

Figure 13. Comparison of experimental and theoretical variation of drag coefficient with Mach number for the RC(6)-08 airfoil; $c_l = 0$.

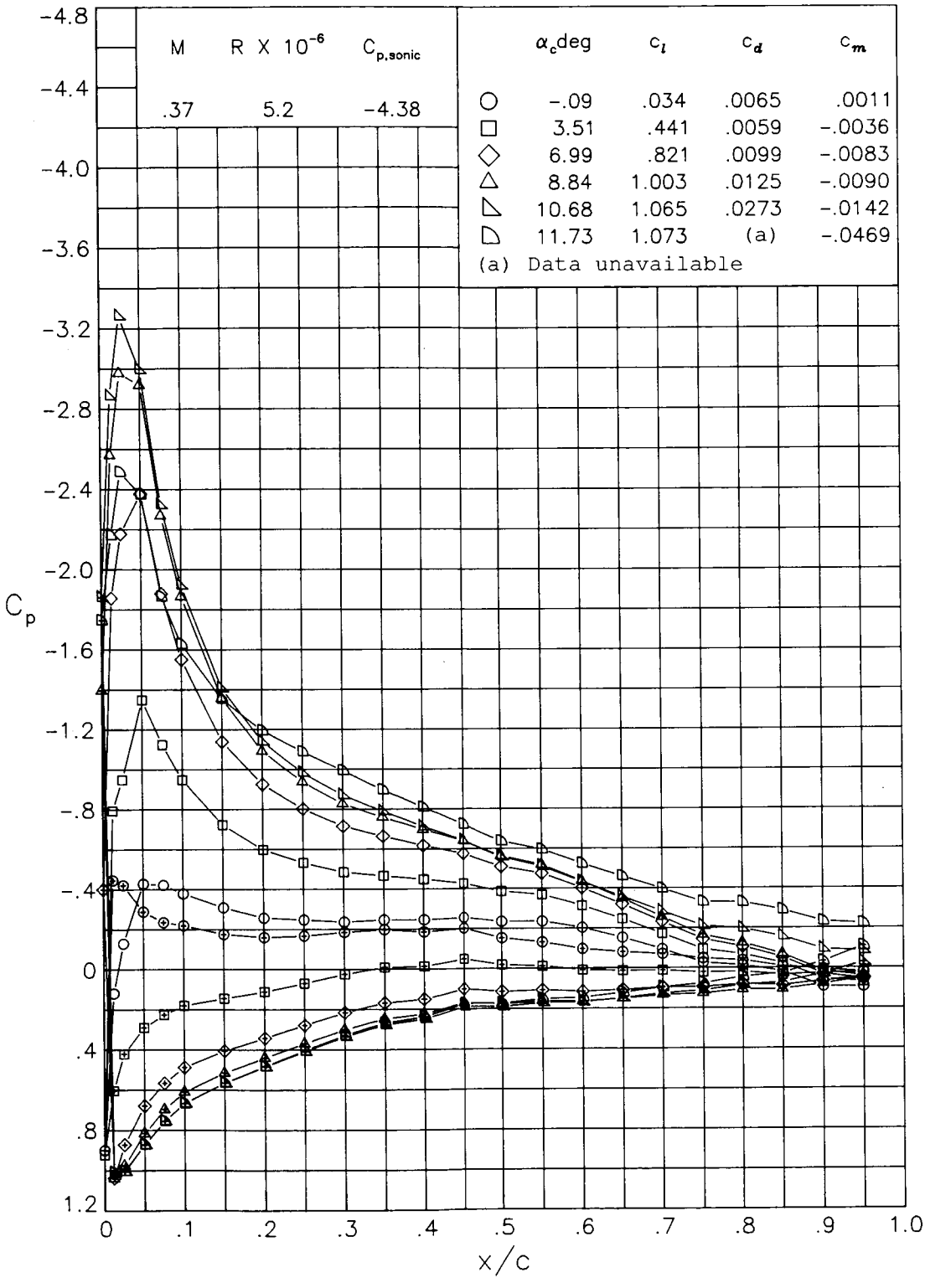

(a) $M = 0.37$; $R = 5.2 \times 10^6$.

Figure 14. Chordwise pressure distributions of the RC(6)-08 airfoil measured in the Langley 6- by 28-Inch Transonic Tunnel.

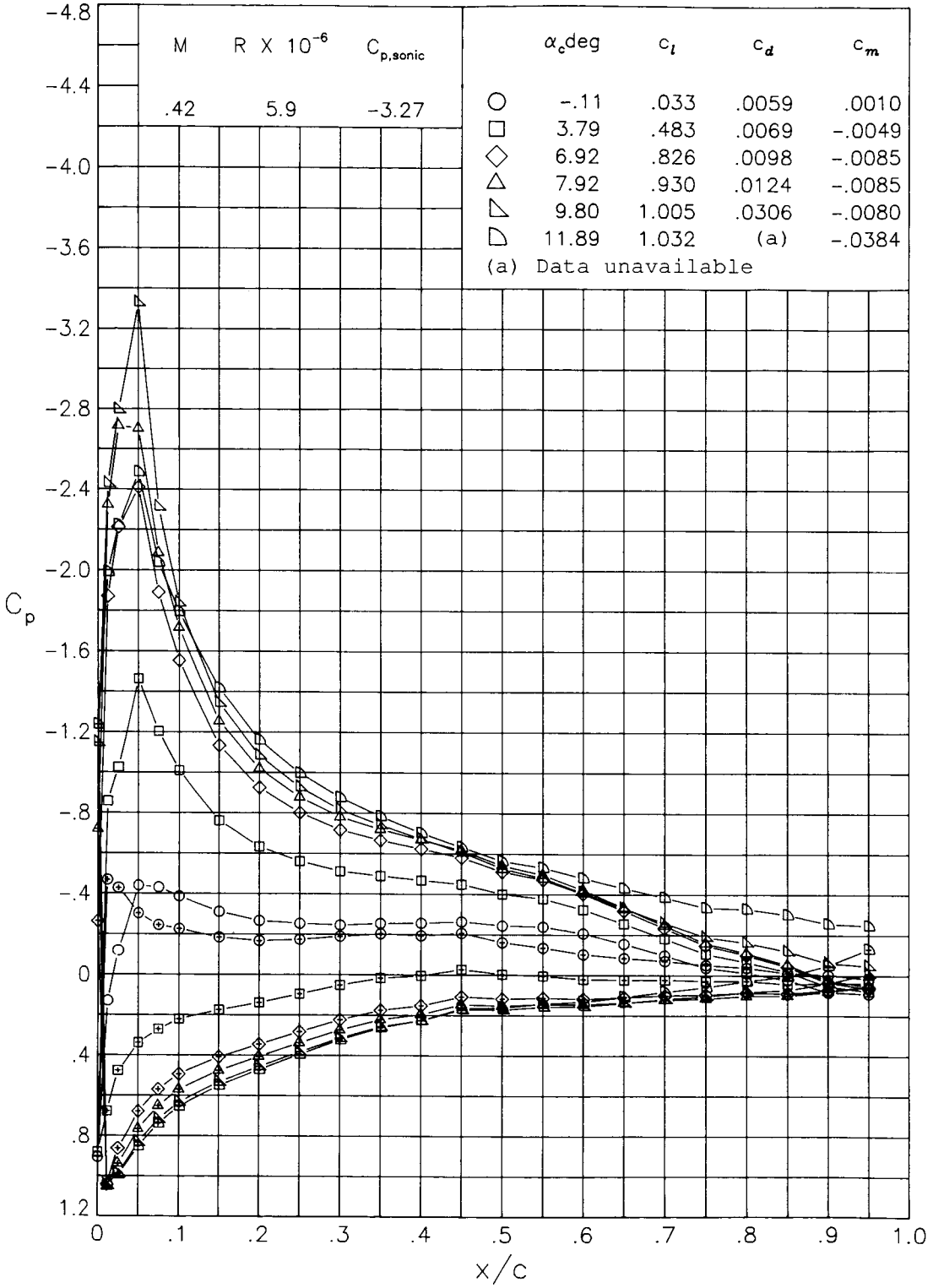

(b) $M = 0.42$; $R = 5.9 \times 10^6$.

Figure 14. Continued.

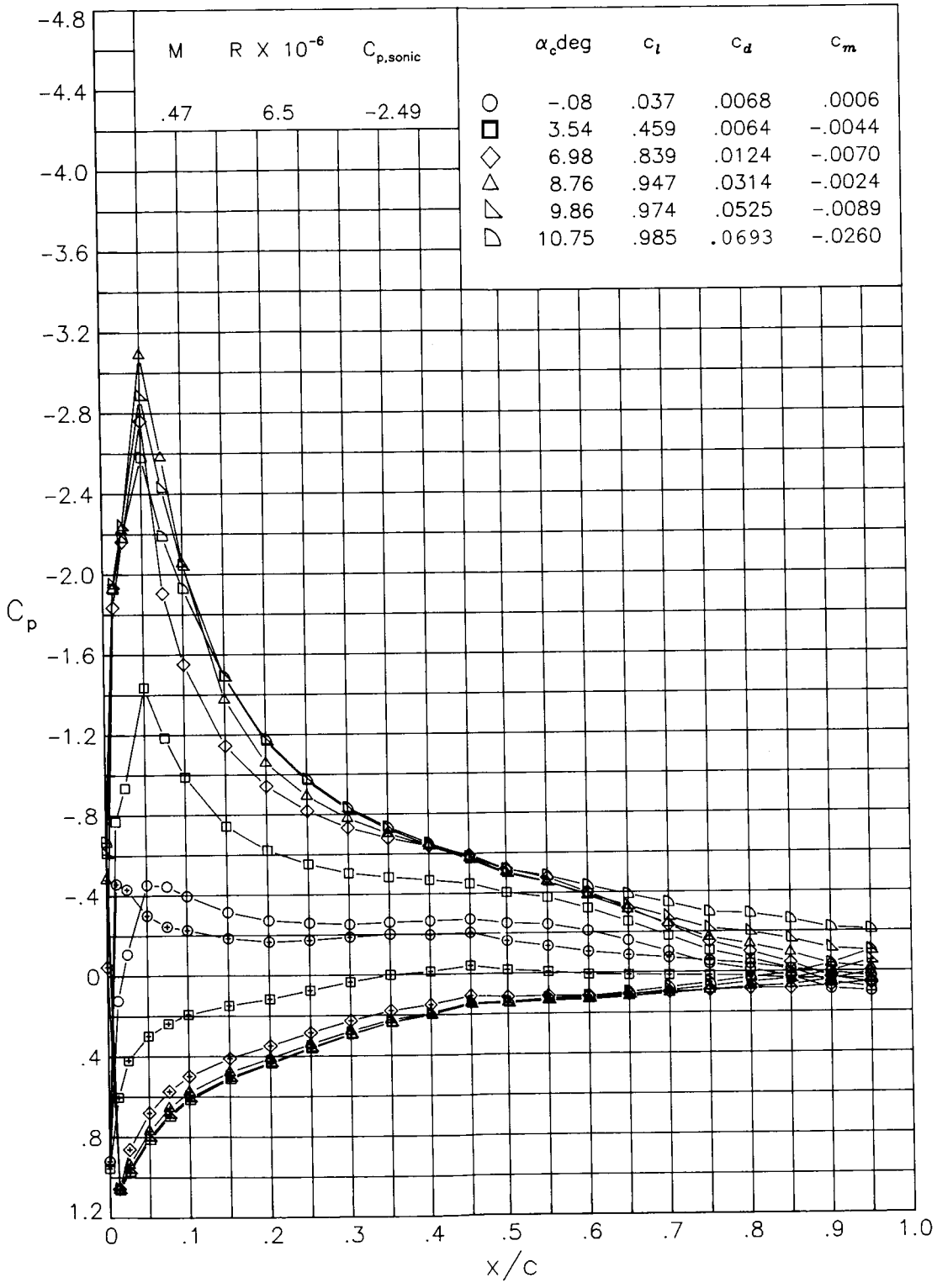

(c) $M = 0.47$; $R = 6.5 \times 10^6$.

Figure 14. Continued.

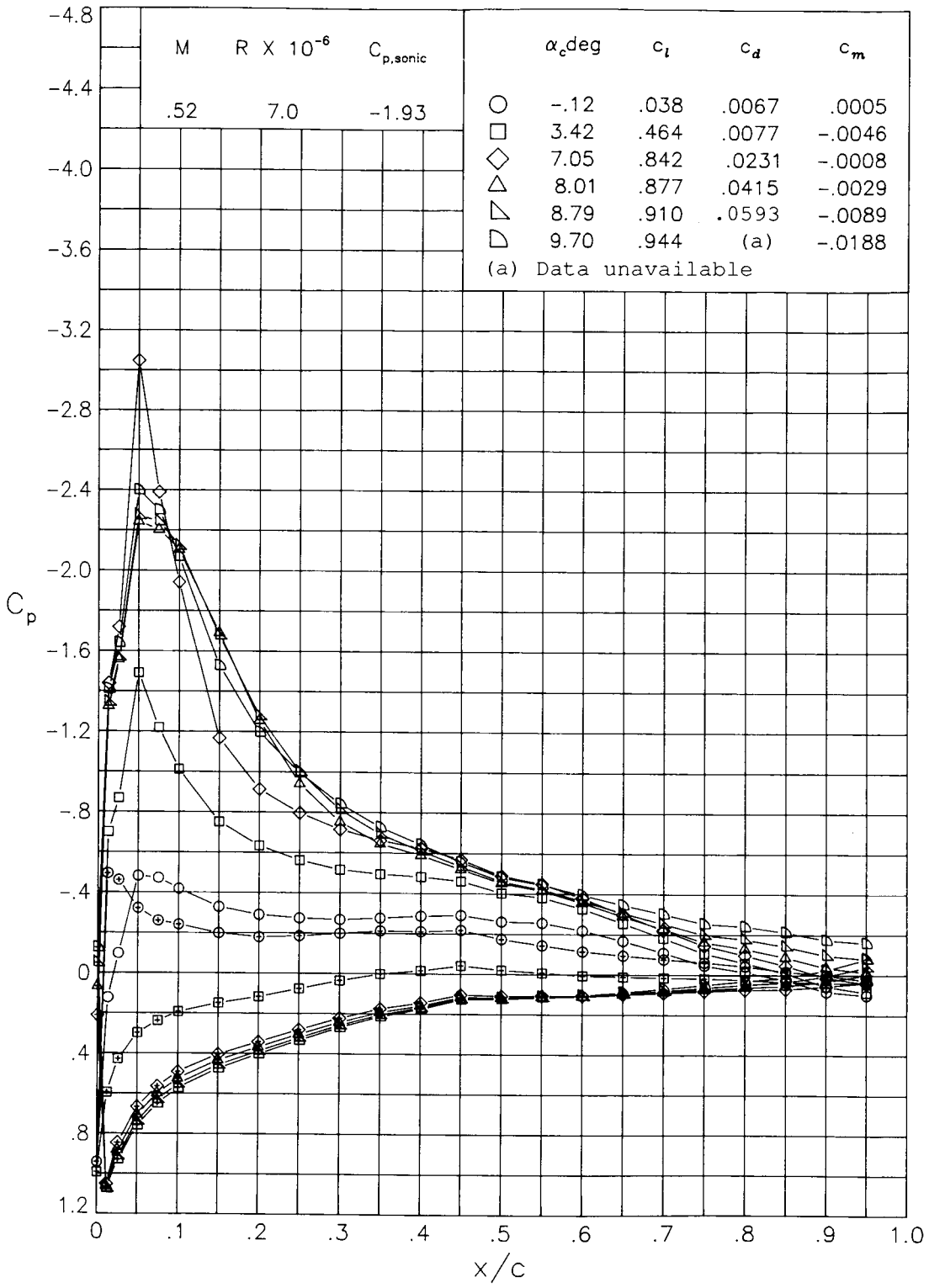

(d) $M = 0.52$; $R = 7.0 \times 10^6$.

Figure 14. Continued.

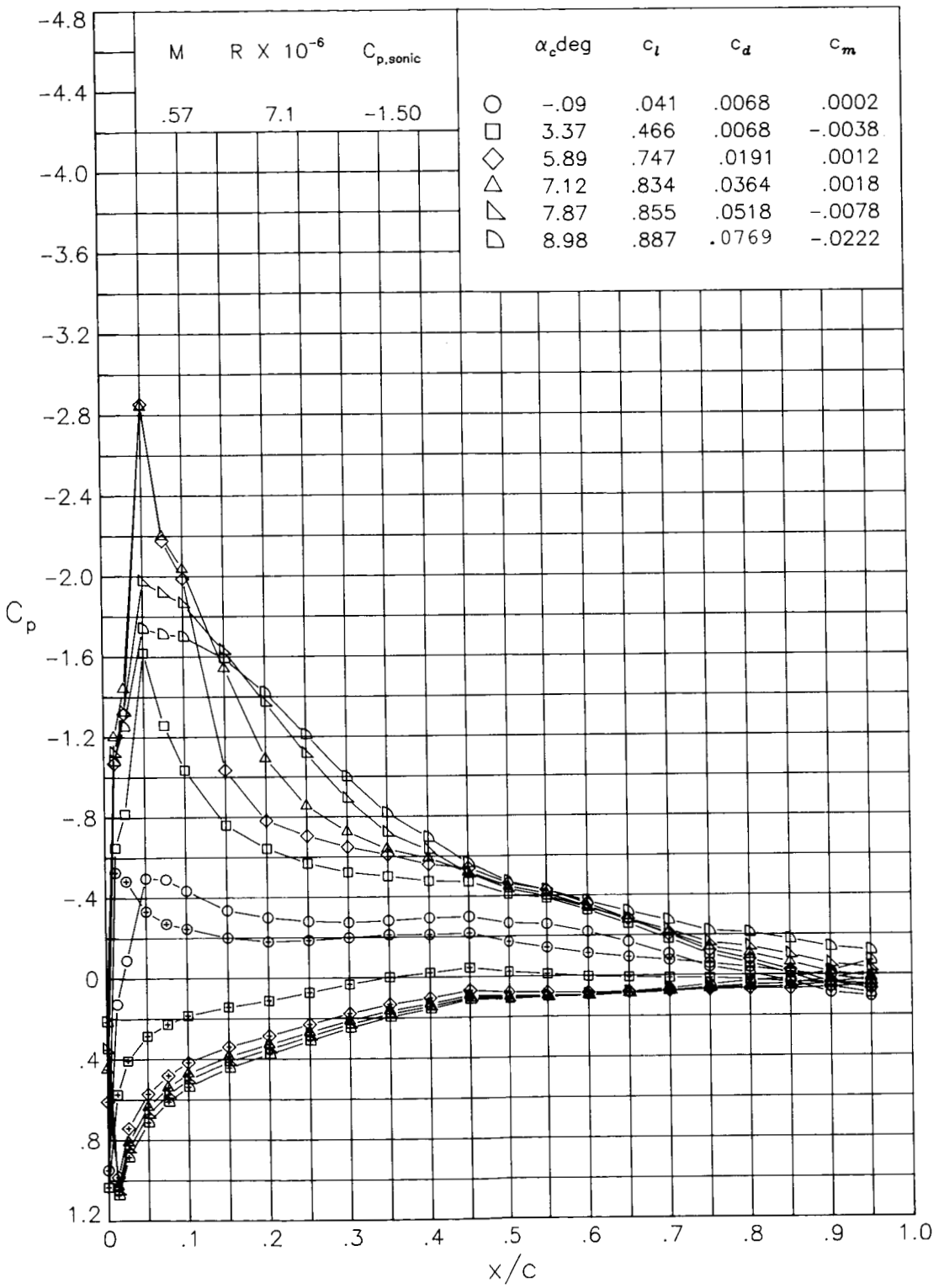

(e) $M = 0.57$; $R = 7.1 \times 10^6$.

Figure 14. Continued.

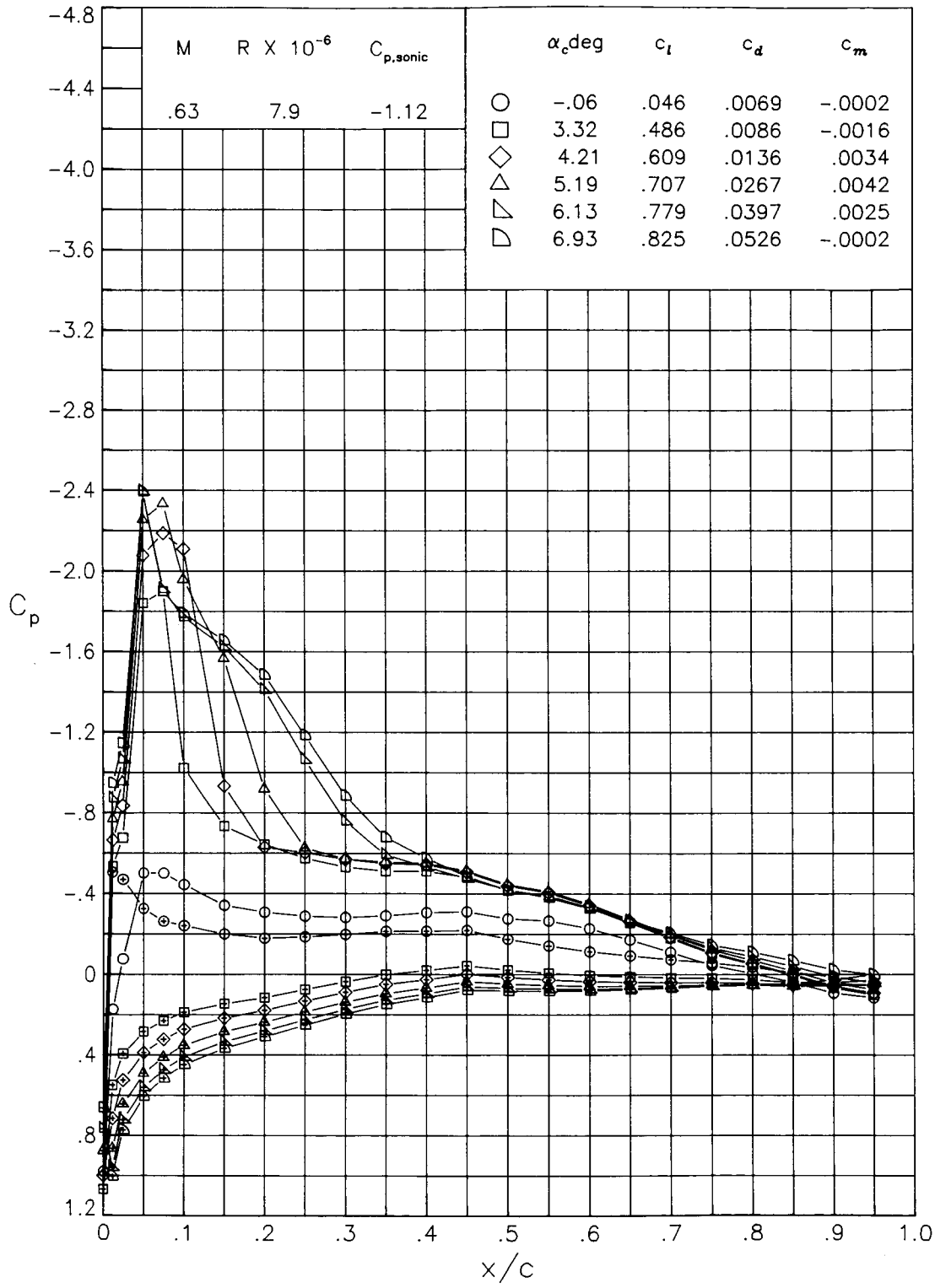

(f) $M = 0.63$; $R = 7.9 \times 10^6$.

Figure 14. Continued.

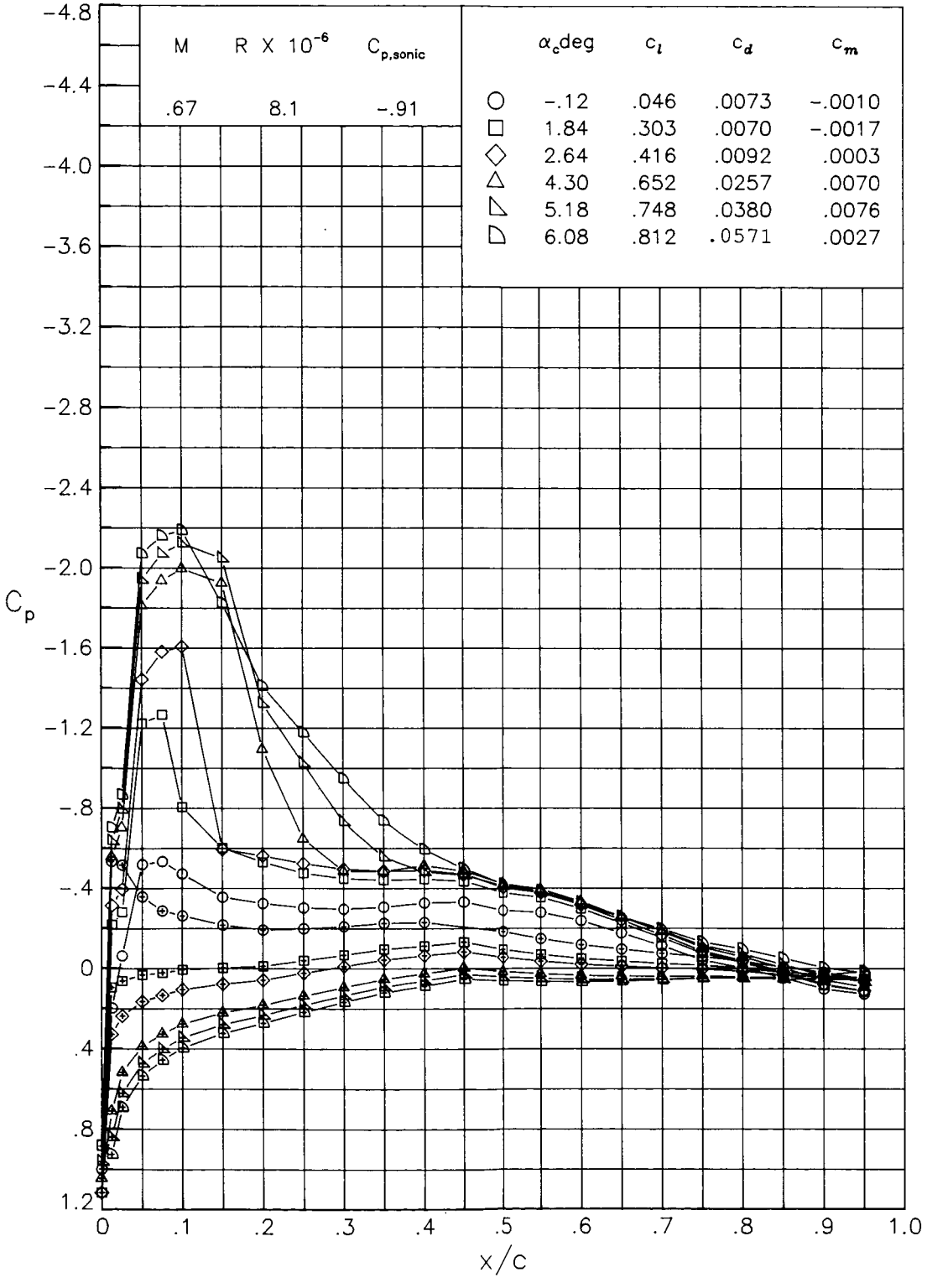

(g) $M = 0.67$; $R = 8.1 \times 10^6$.

Figure 14. Continued.

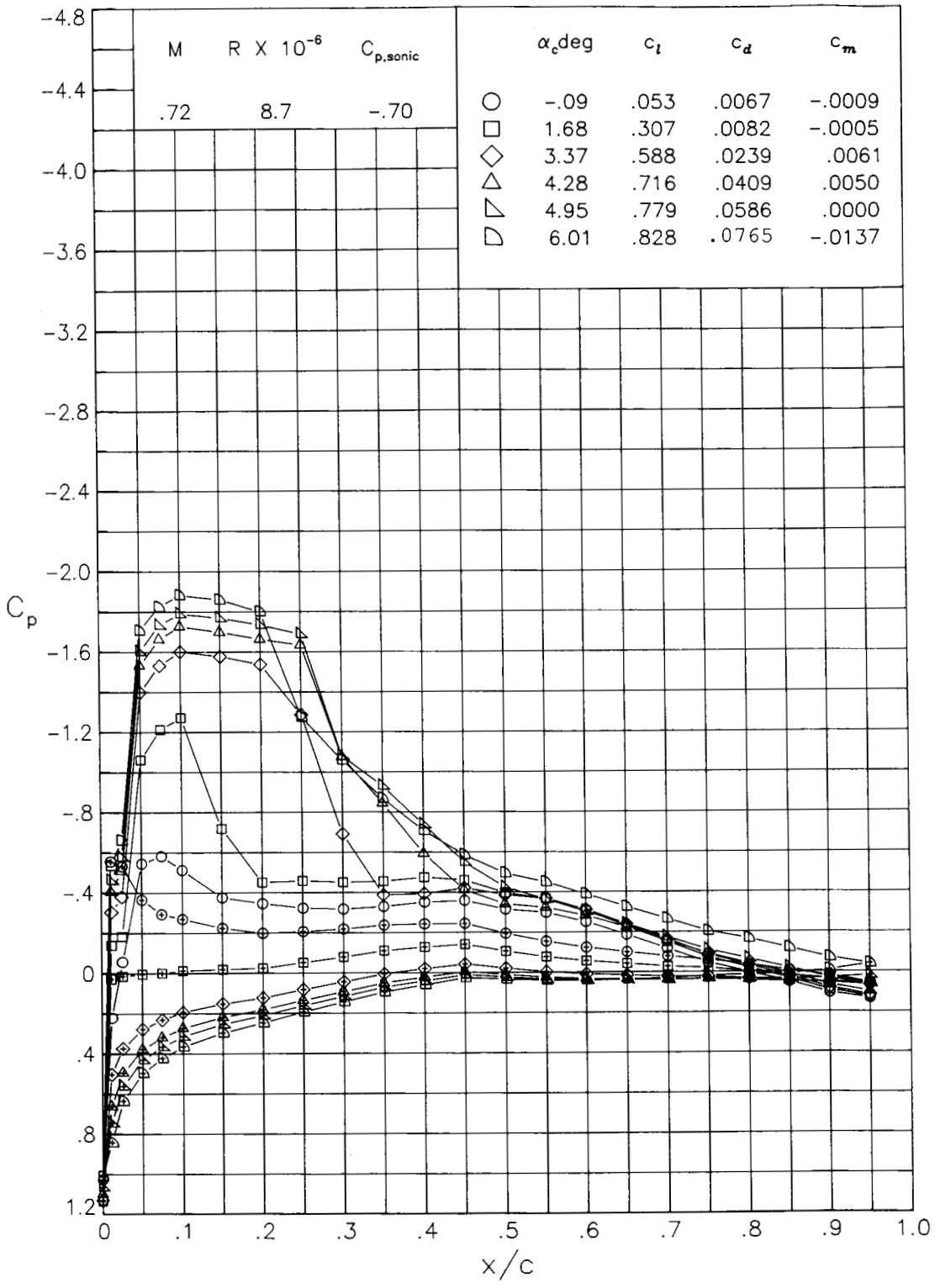

(h) $M = 0.72$; $R = 8.7 \times 10^6$.

Figure 14. Continued.

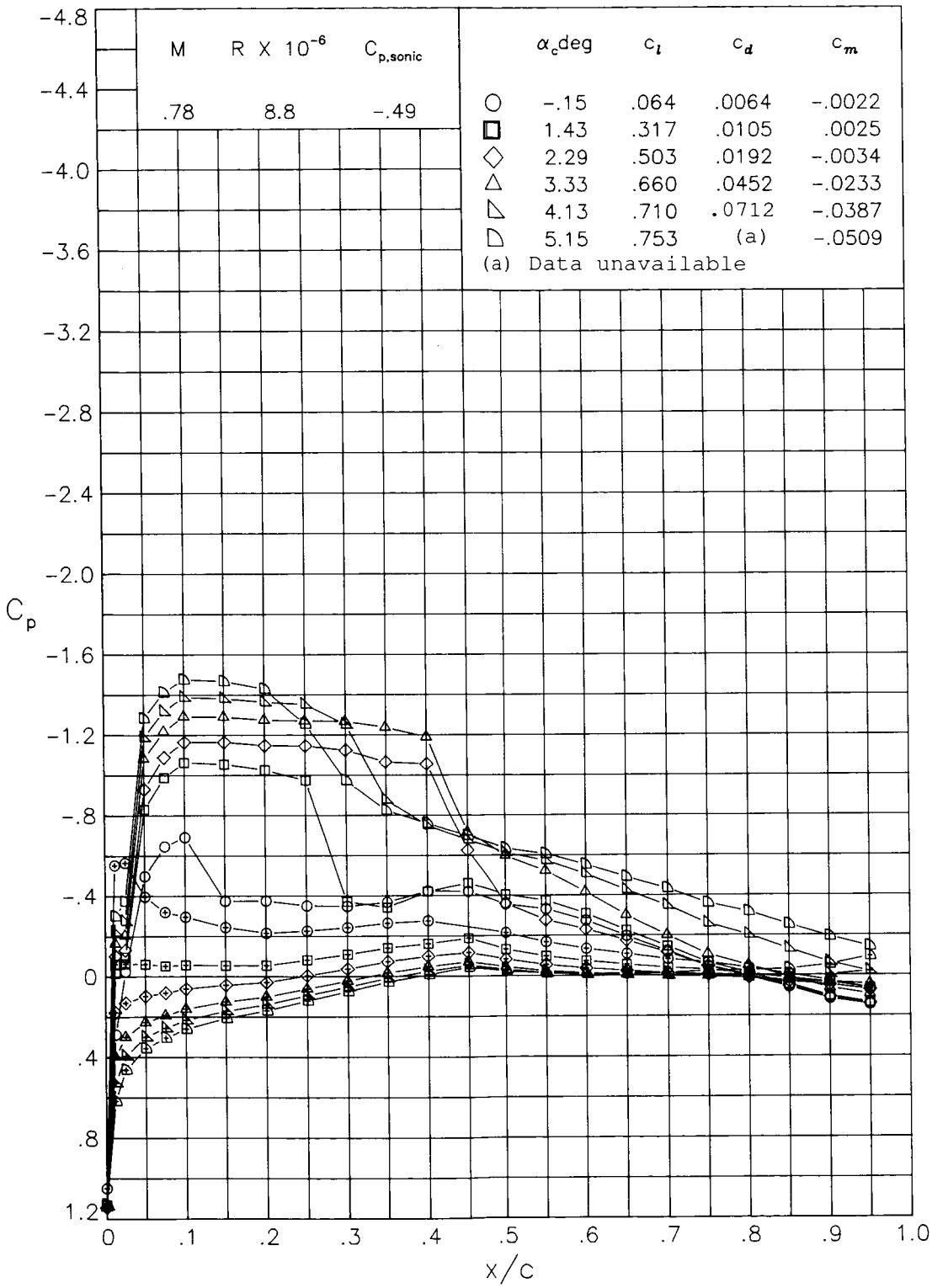

(i) $M = 0.78$; $R = 8.8 \times 10^6$.

Figure 14. Continued.

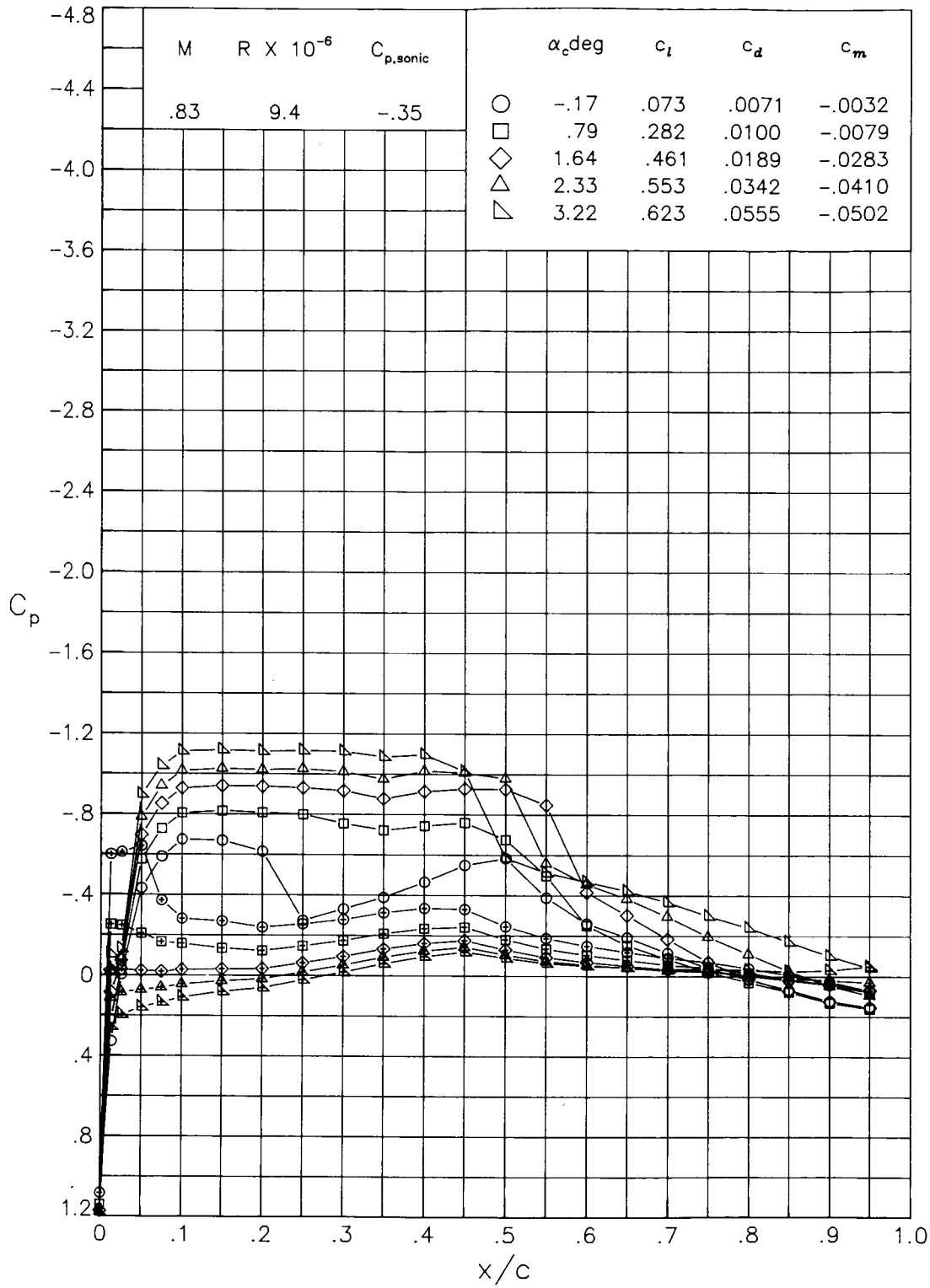

(j) $M = 0.83$; $R = 9.4 \times 10^6$.

Figure 14. Continued.

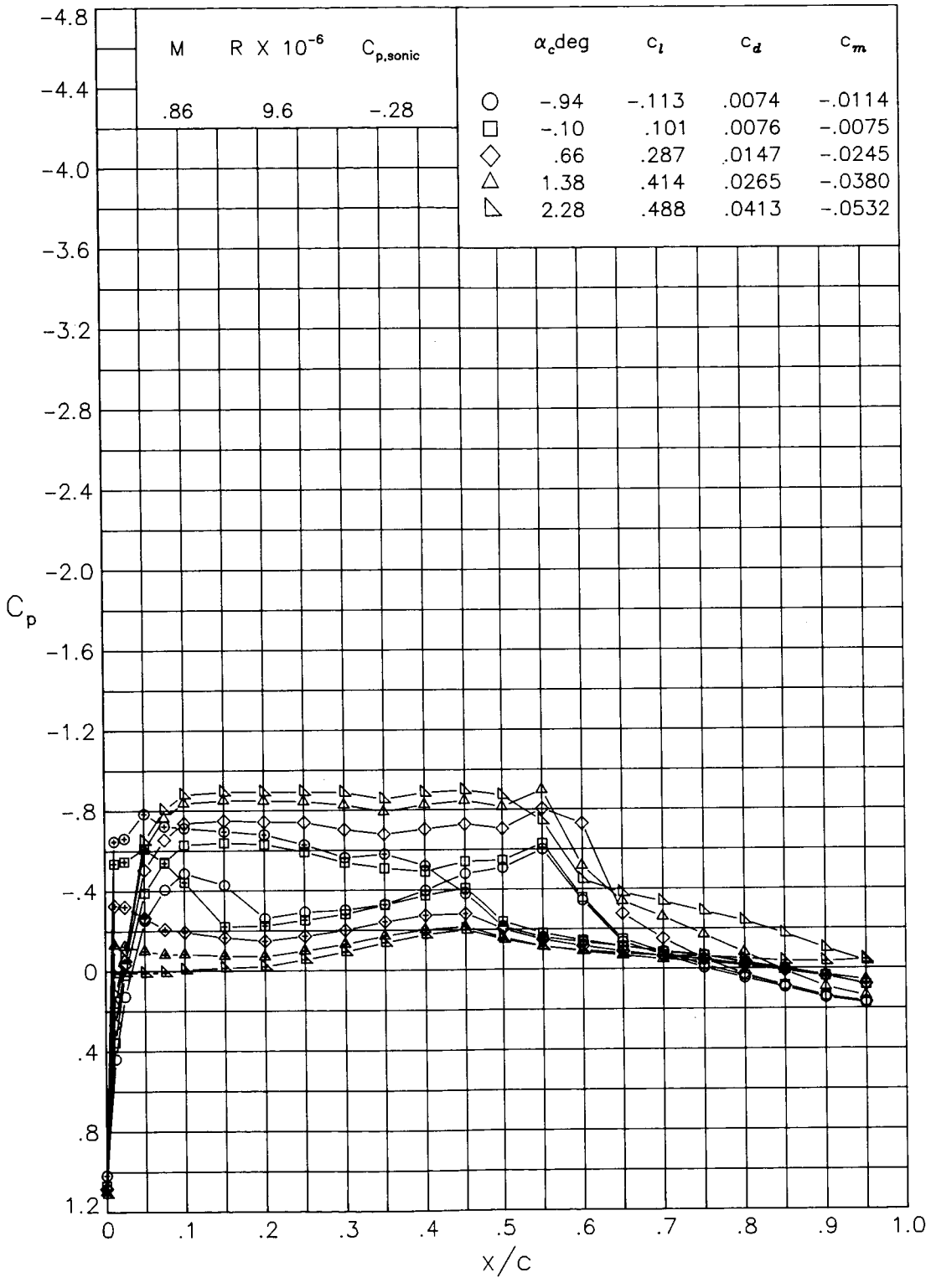

(k) $M = 0.86$; $R = 9.6 \times 10^6$.

Figure 14. Continued.

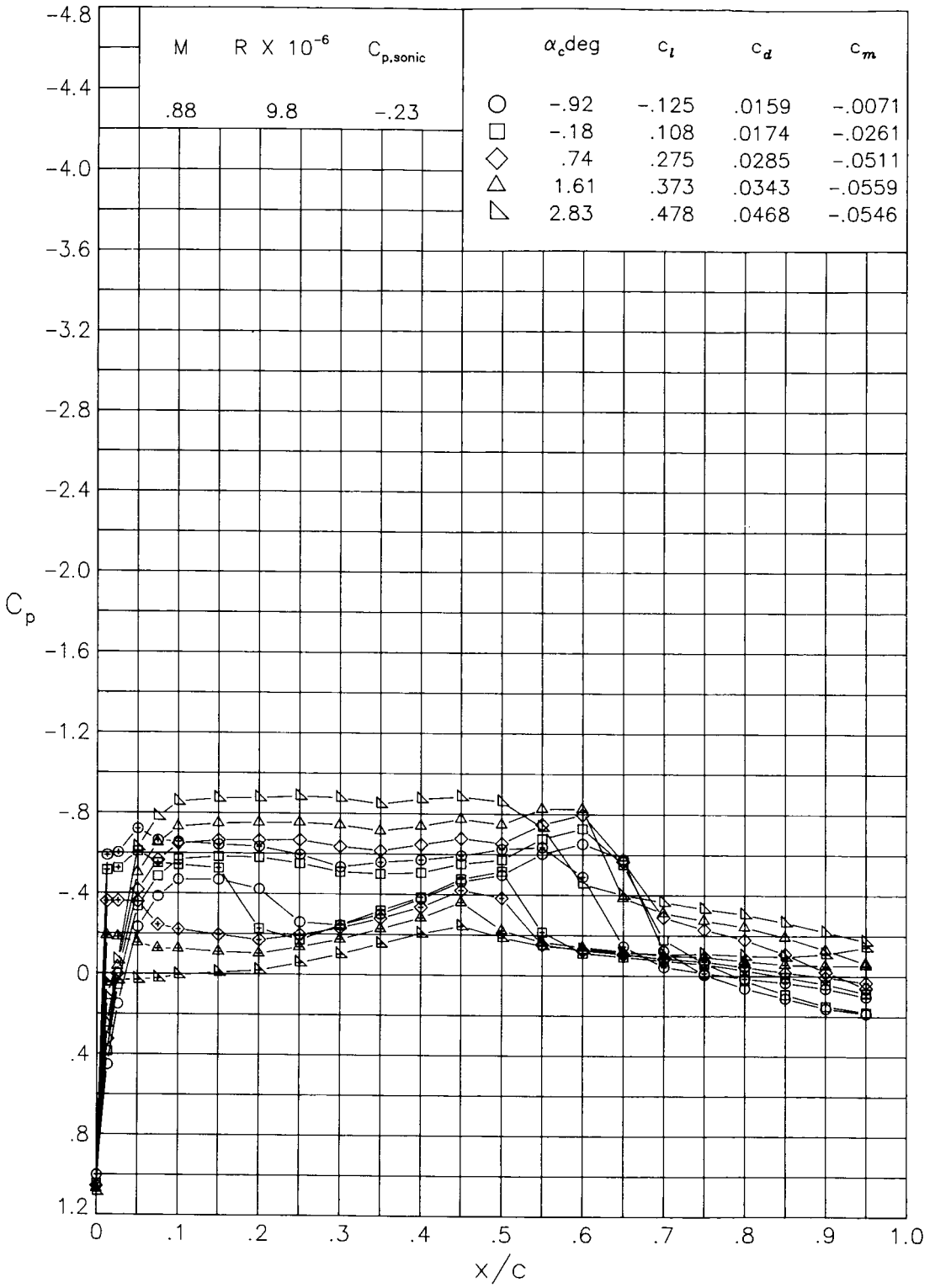

(l) $M = 0.88$; $R = 9.8 \times 10^6$.

Figure 14. Continued.

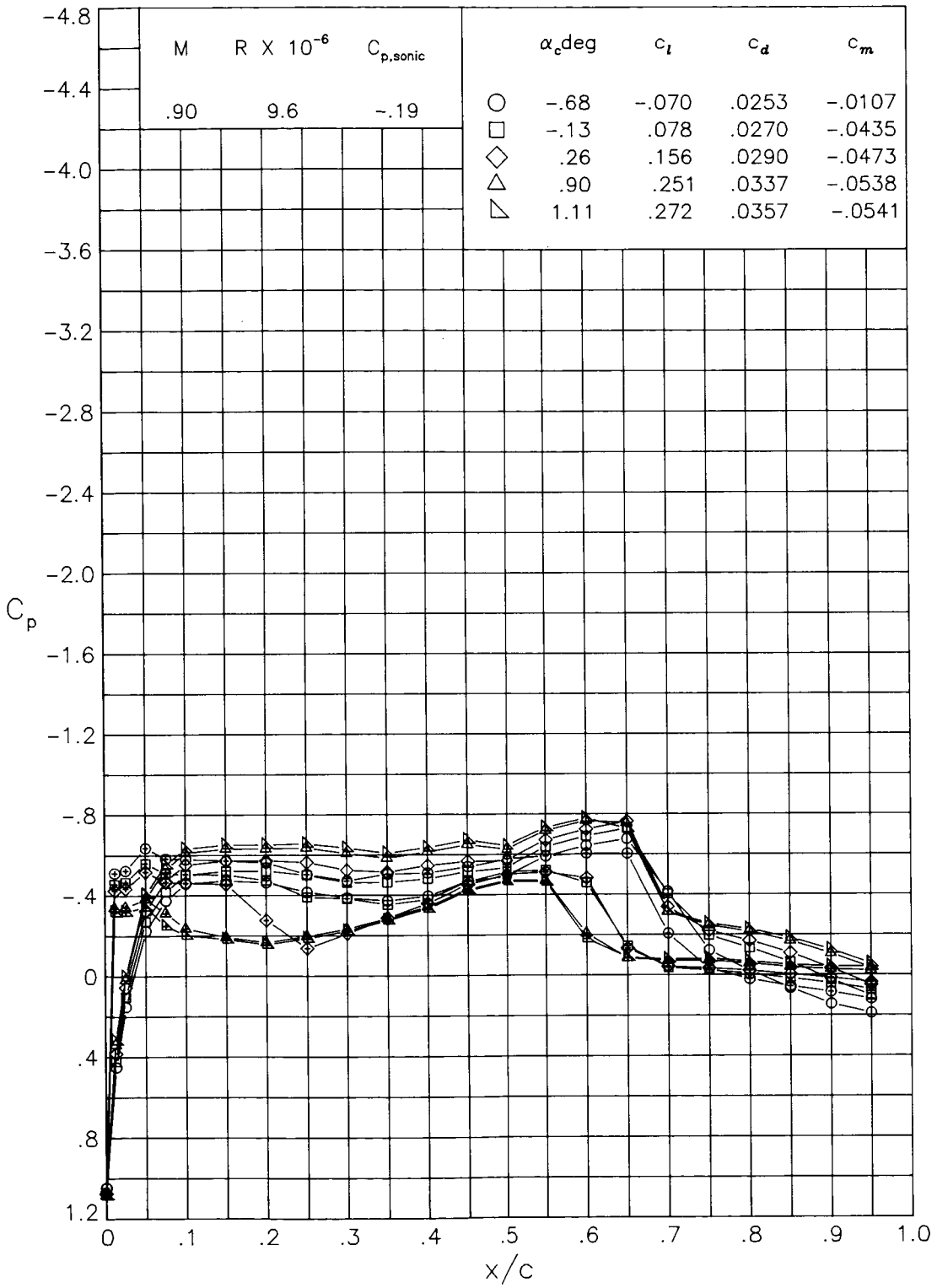

(m) $M = 0.90$; $R = 9.6 \times 10^6$.

Figure 14. Concluded.

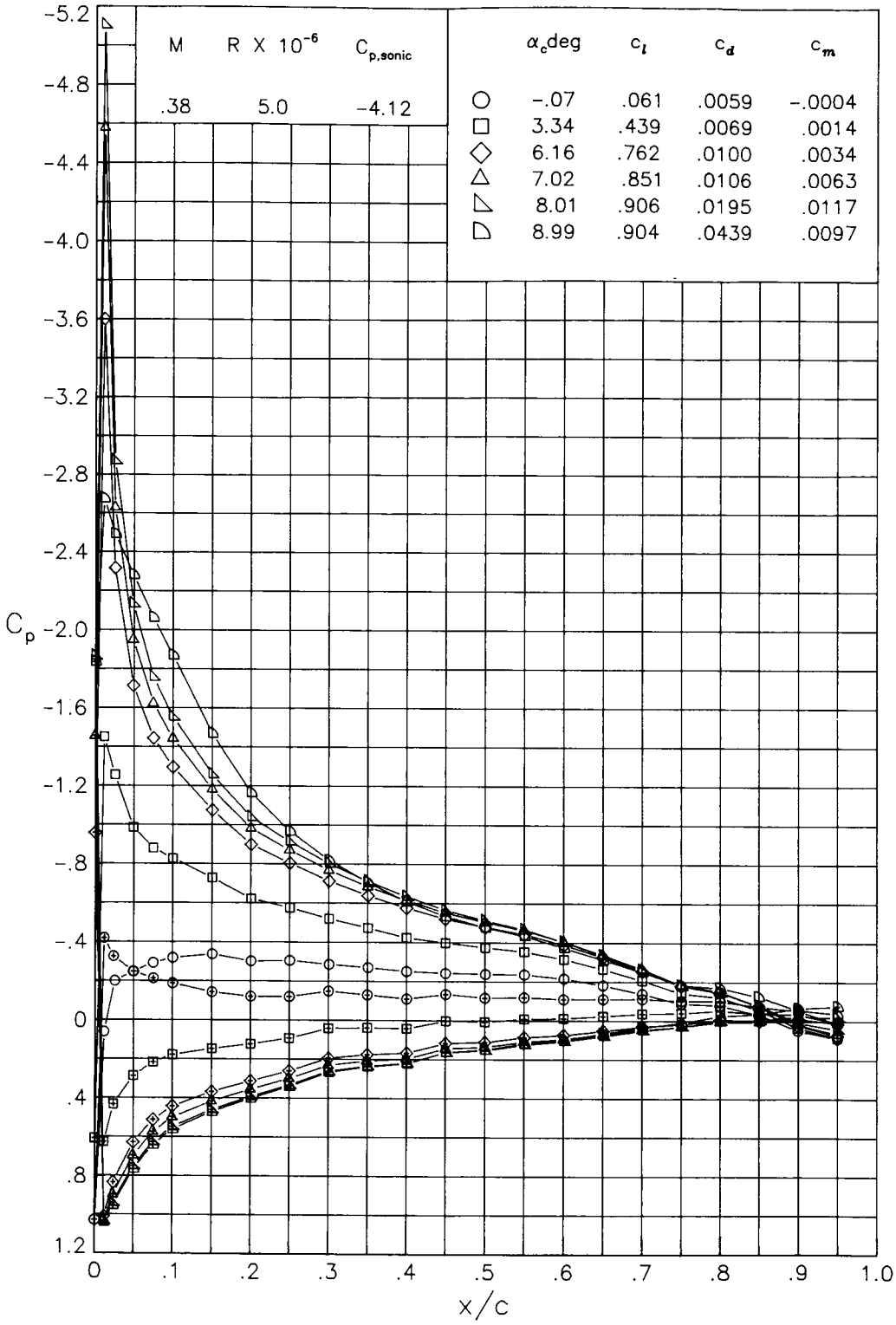

(a) $M = 0.38$; $R = 5.0 \times 10^6$.

Figure 15. Chordwise pressure distributions of the RC(3)-08 airfoil measured in the Langley 6- by 28-Inch Transonic Tunnel.

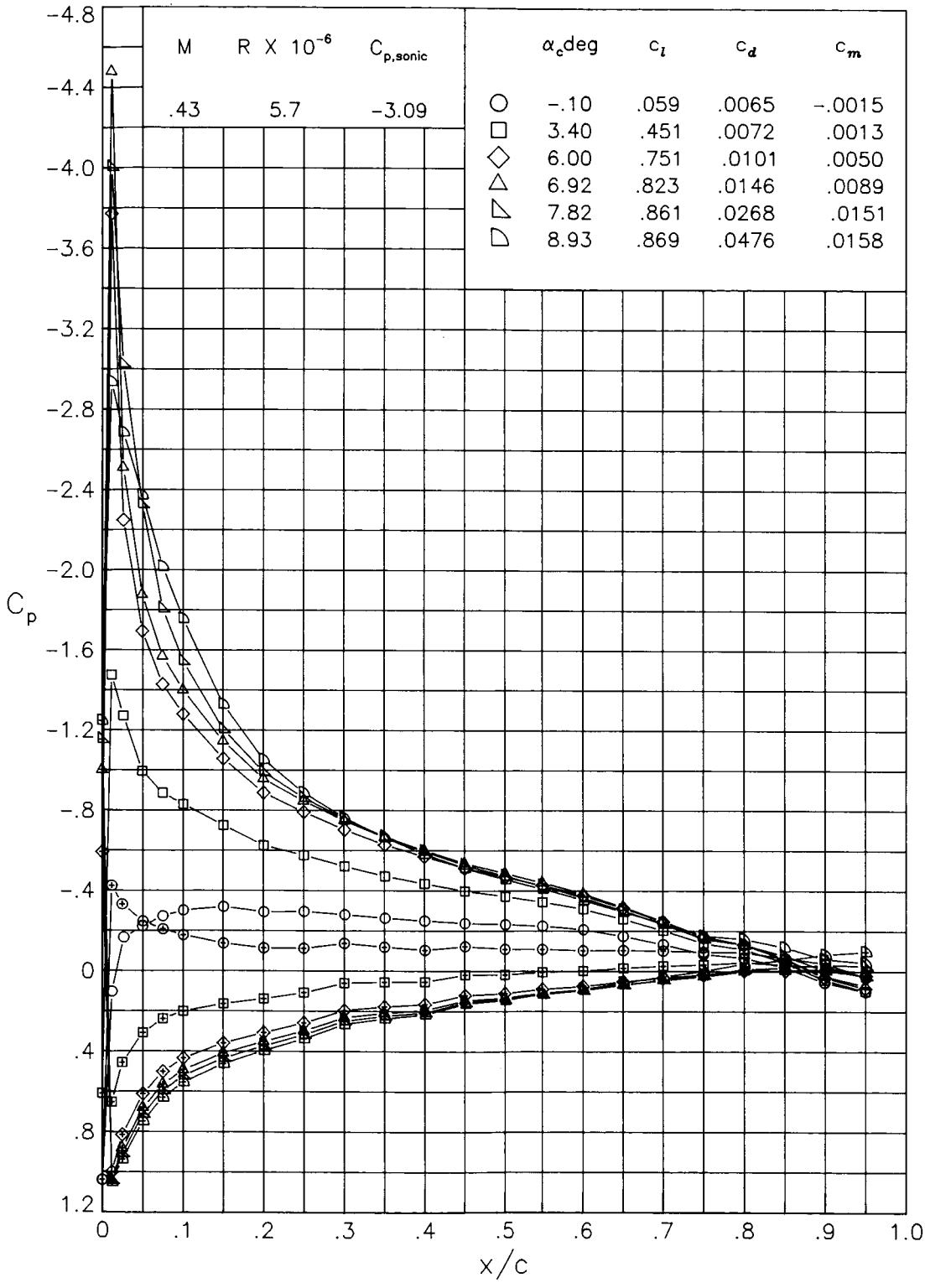

(b) $M = 0.43$; $R = 5.7 \times 10^6$.

Figure 15. Continued.

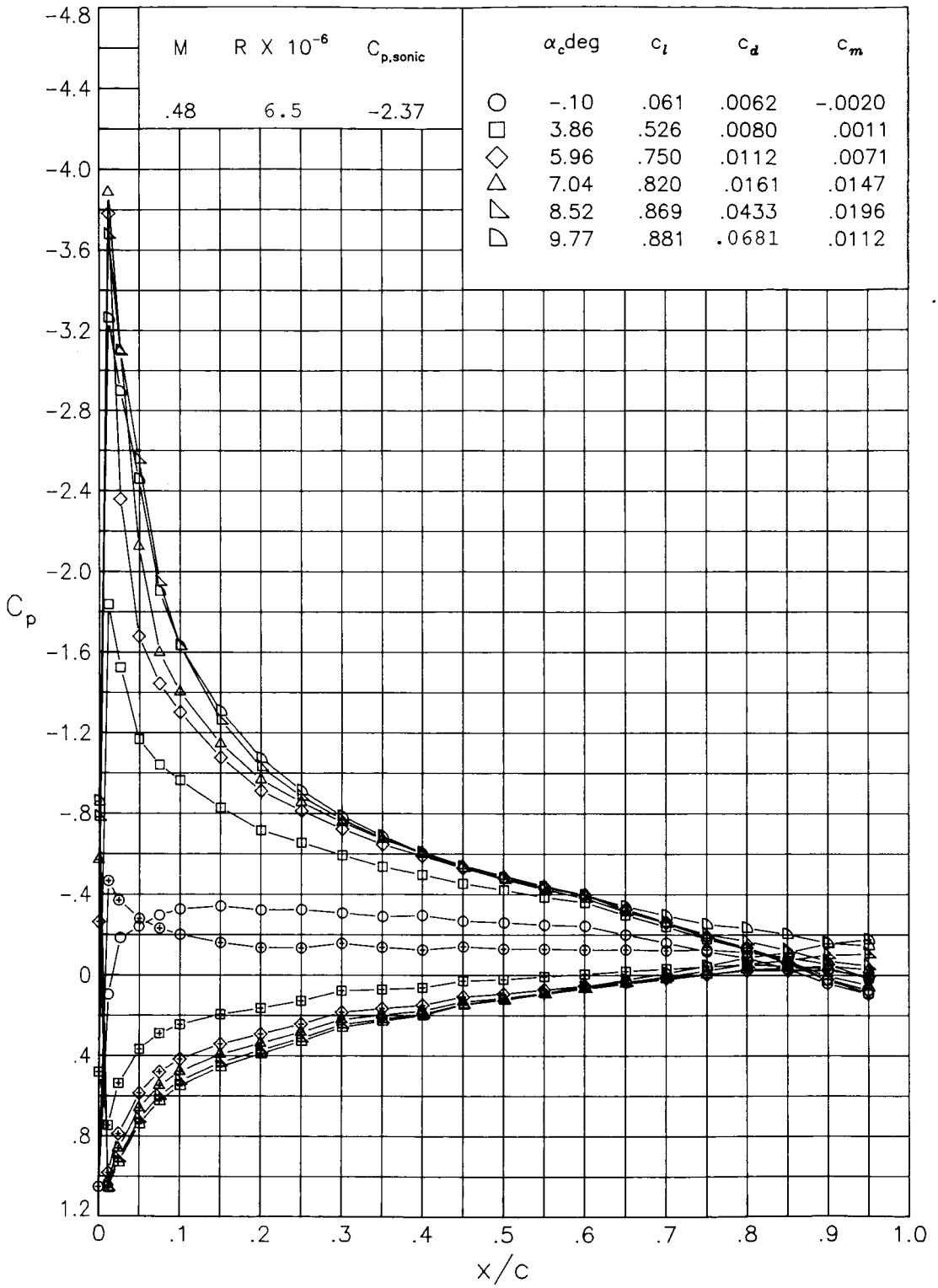

(c) $M = 0.48$; $R = 6.5 \times 10^6$.

Figure 15. Continued.

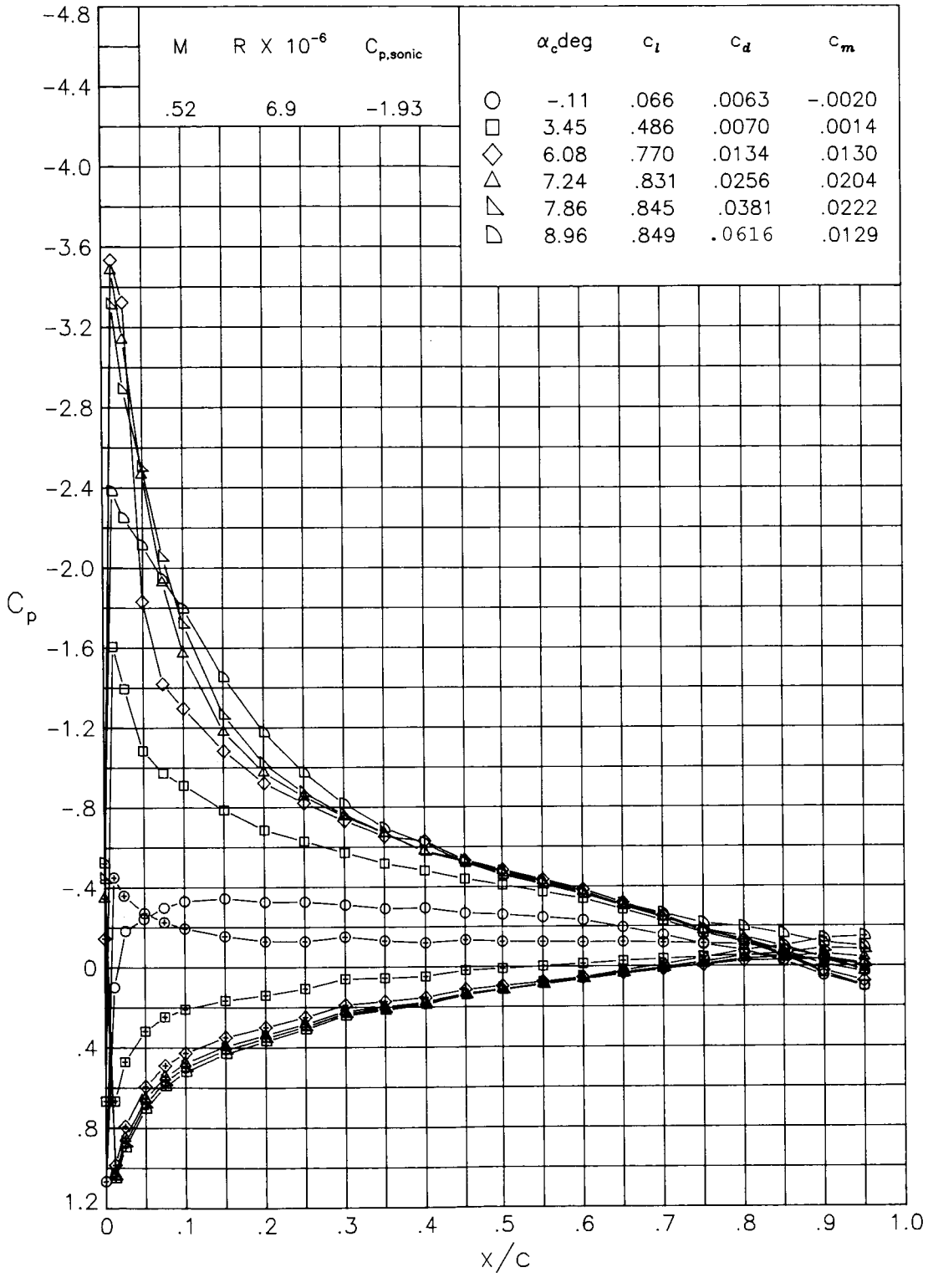

(d) $M = 0.52$; $R = 6.9 \times 10^6$.

Figure 15. Continued.

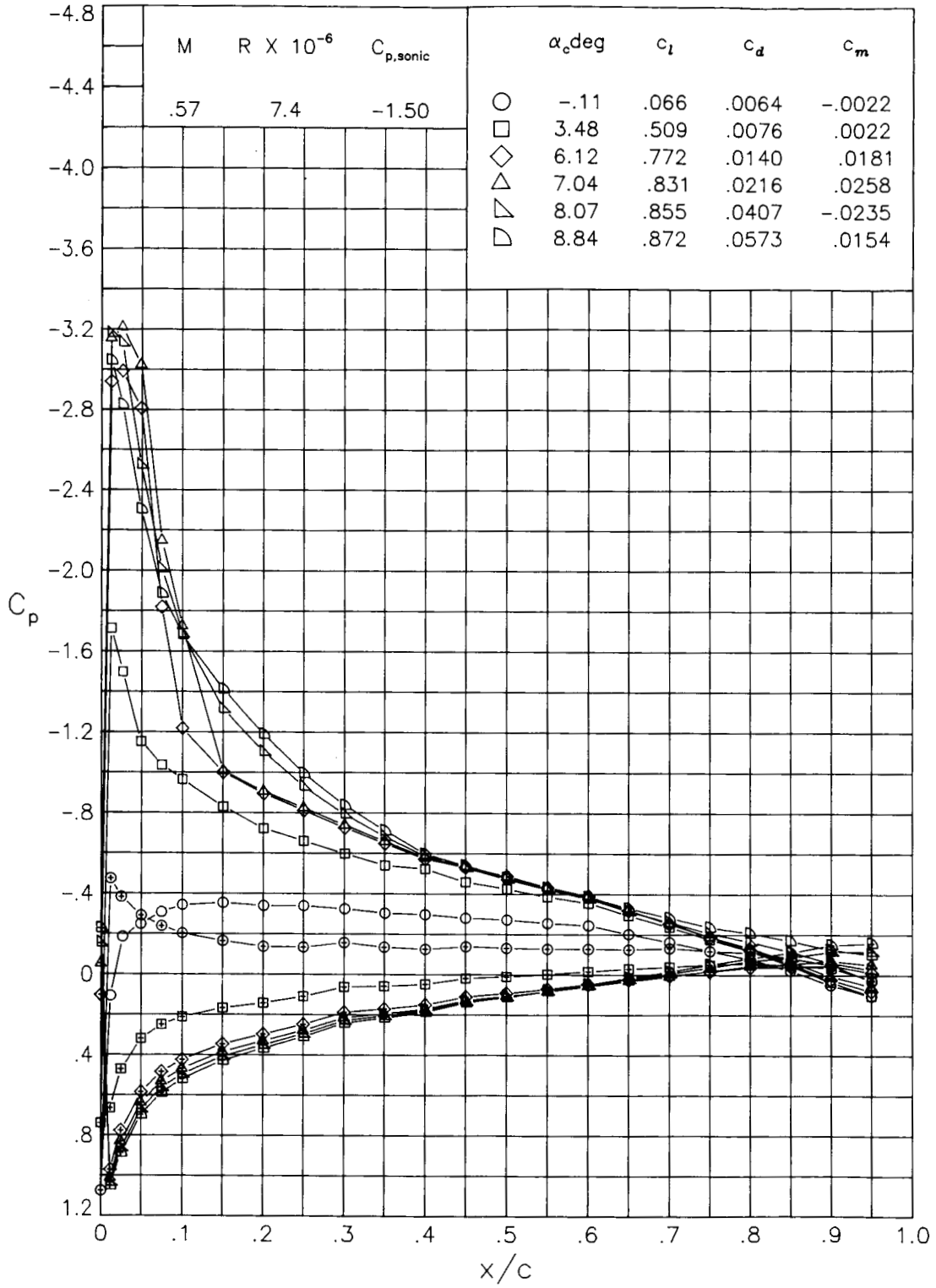

(e) $M = 0.57$; $R = 7.4 \times 10^6$.

Figure 15. Continued.

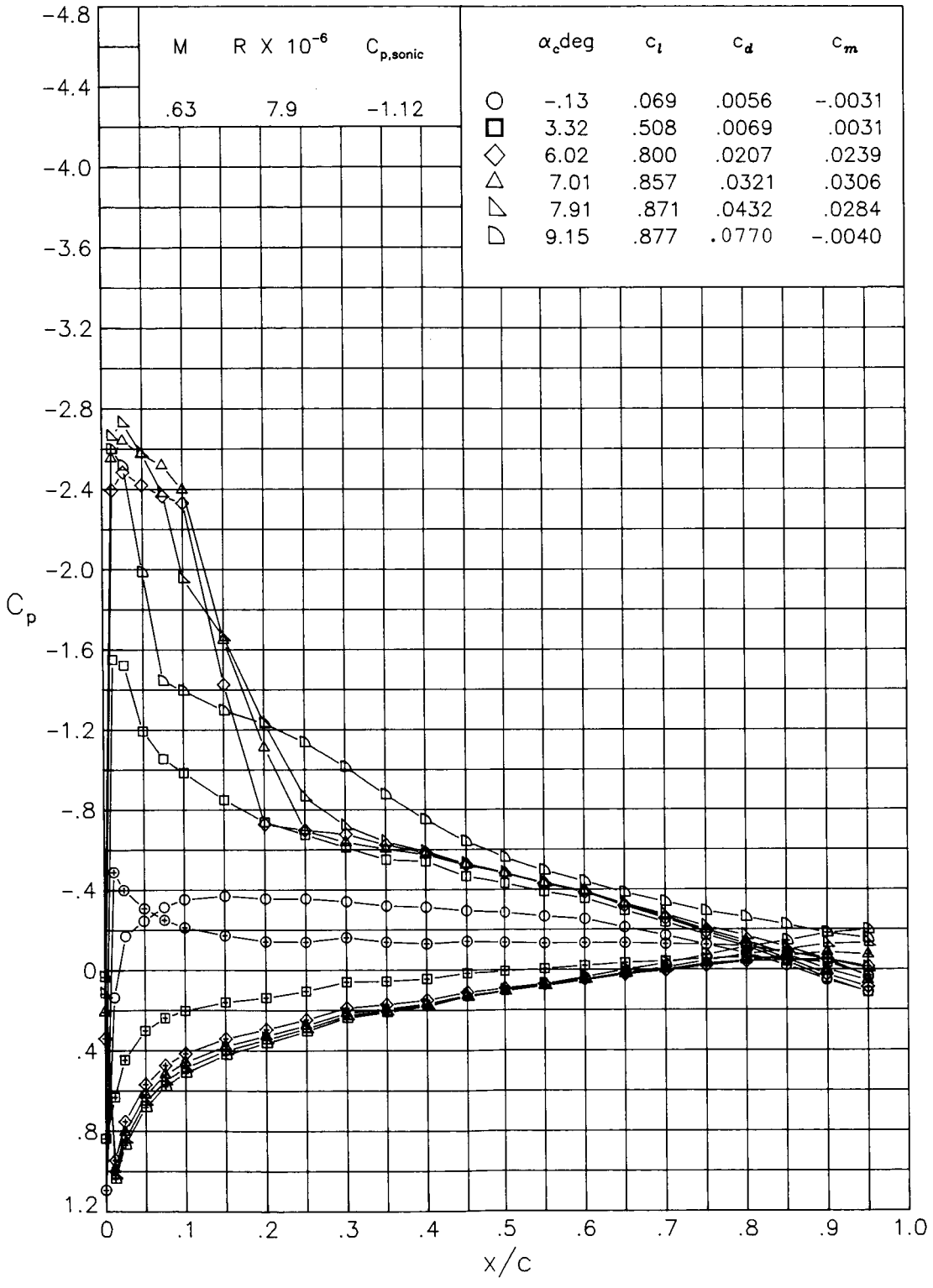

(f) $M = 0.63$; $R = 7.9 \times 10^6$.

Figure 15. Continued.

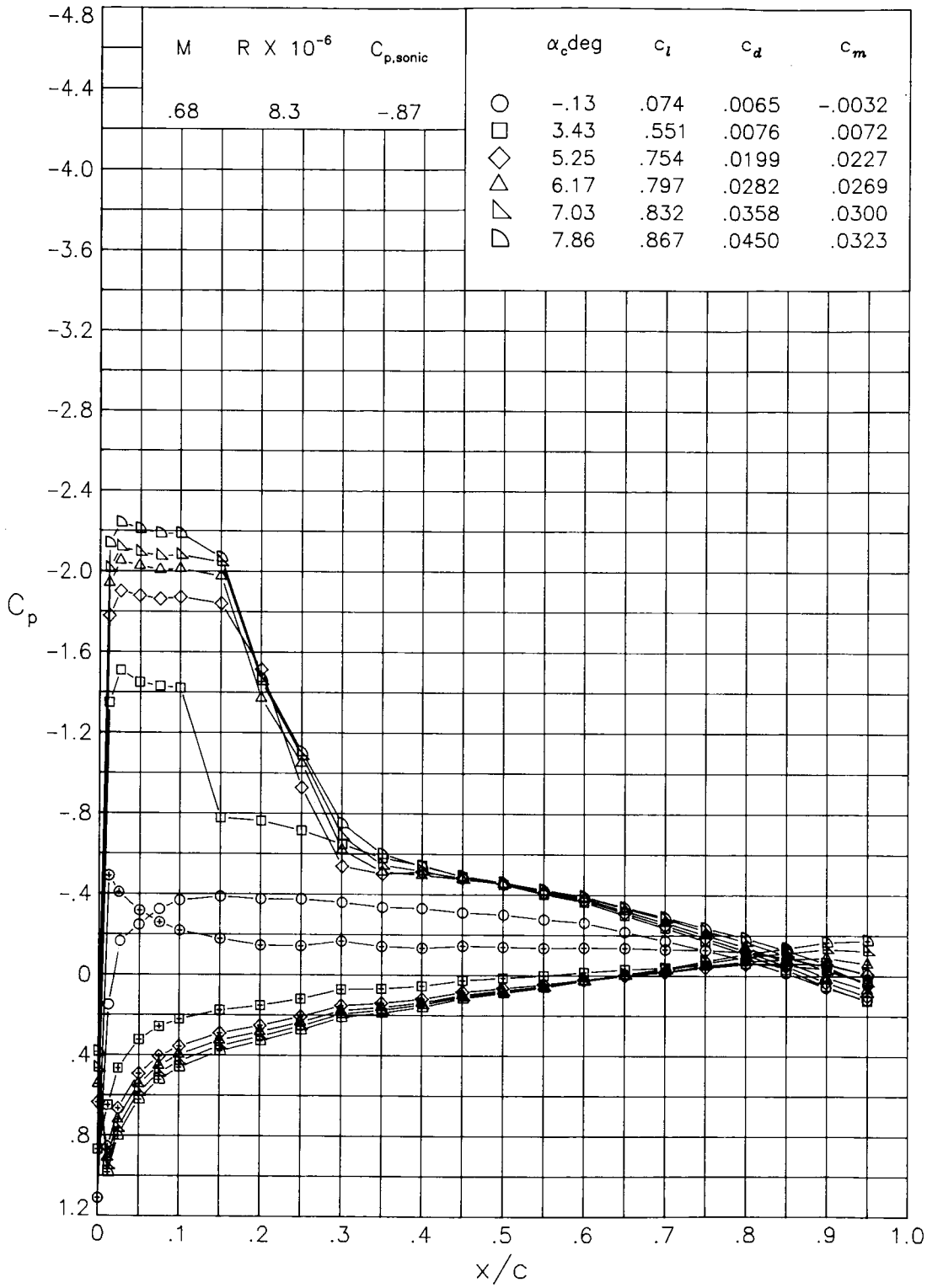

(g) $M = 0.68$; $R = 8.3 \times 10^6$.

Figure 15. Continued.

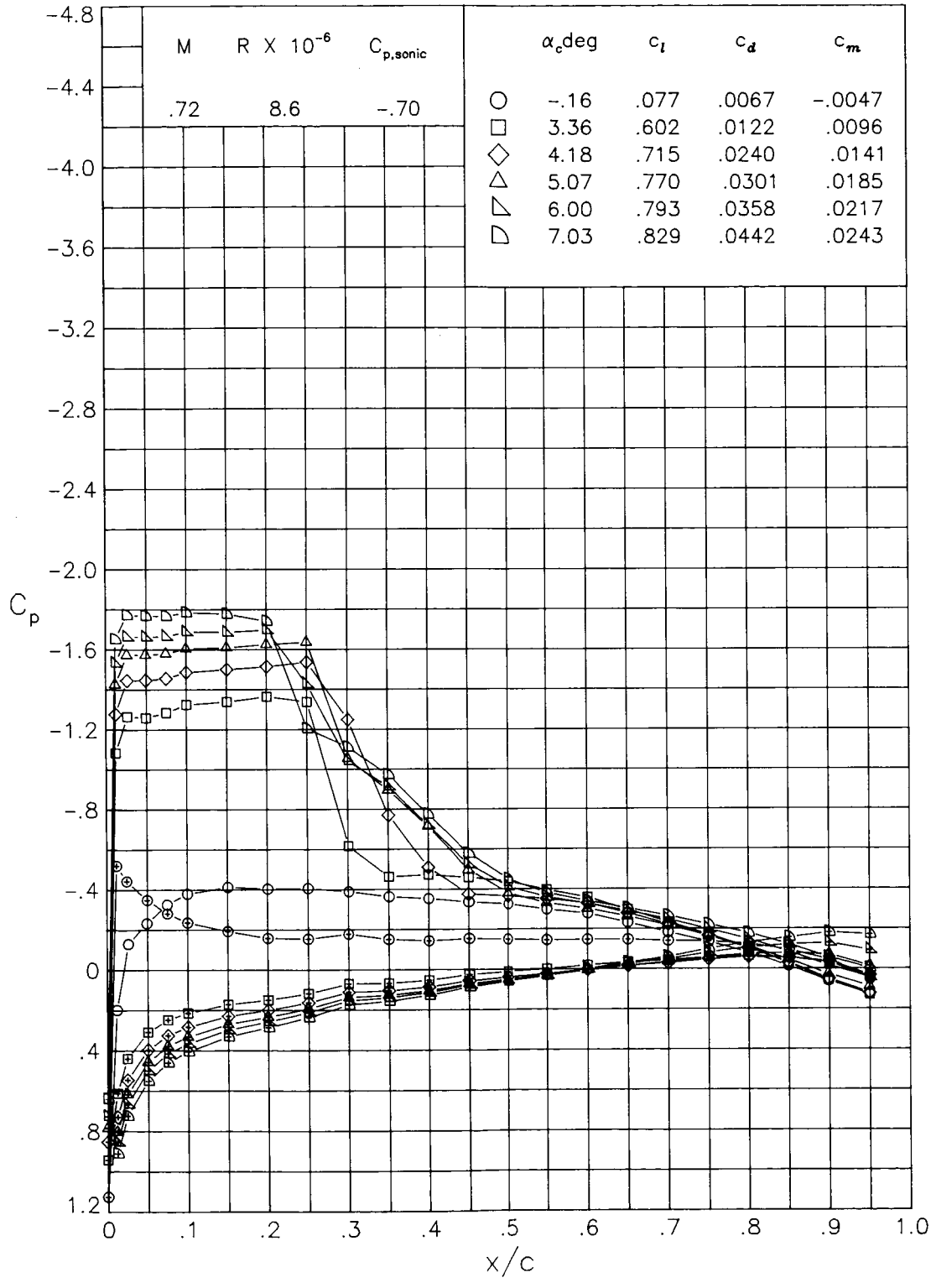

(h) $M = 0.72$; $R = 8.6 \times 10^6$.

Figure 15. Continued.

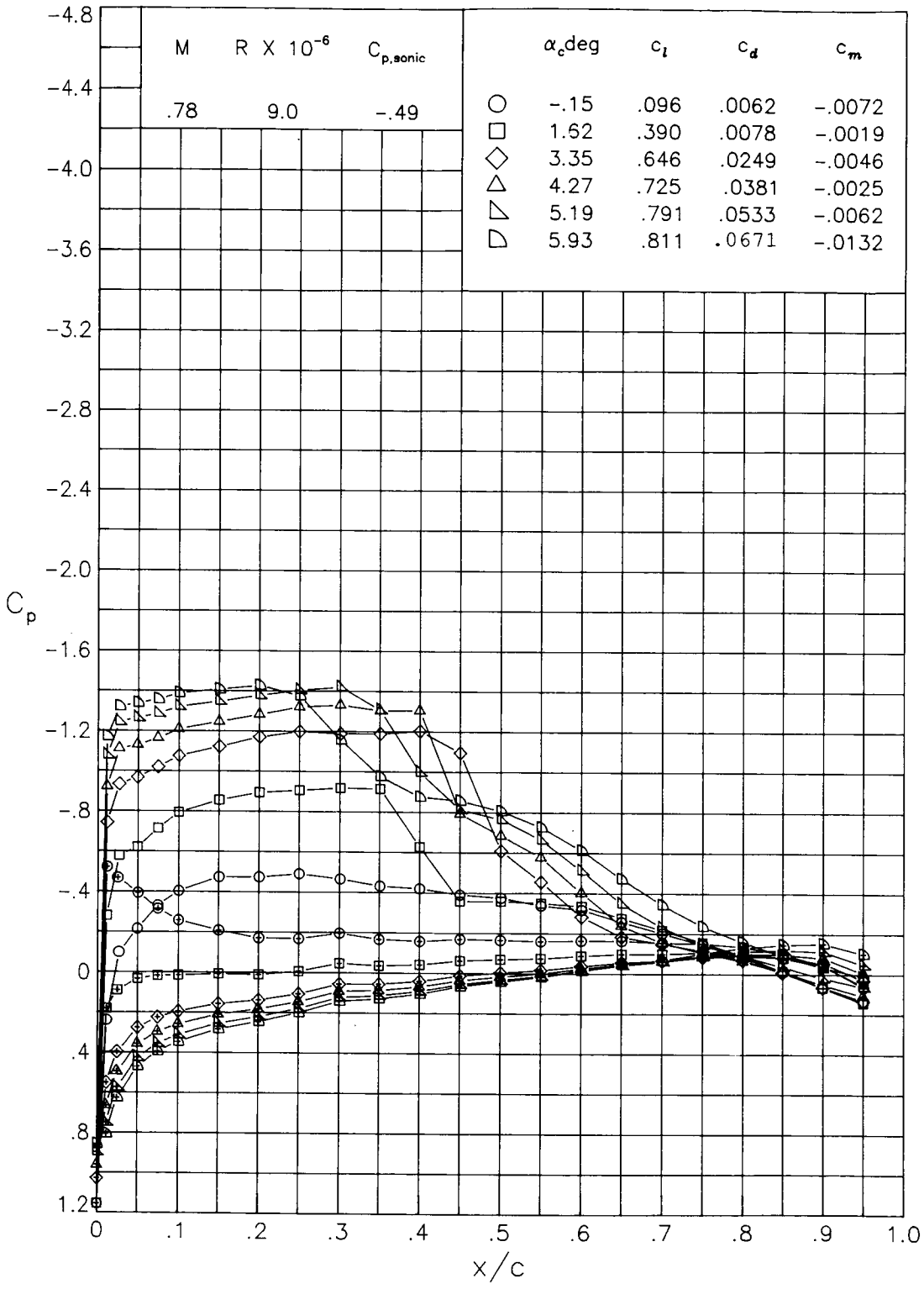

(i) $M = 0.78$; $R = 9.0 \times 10^6$.

Figure 15. Continued.

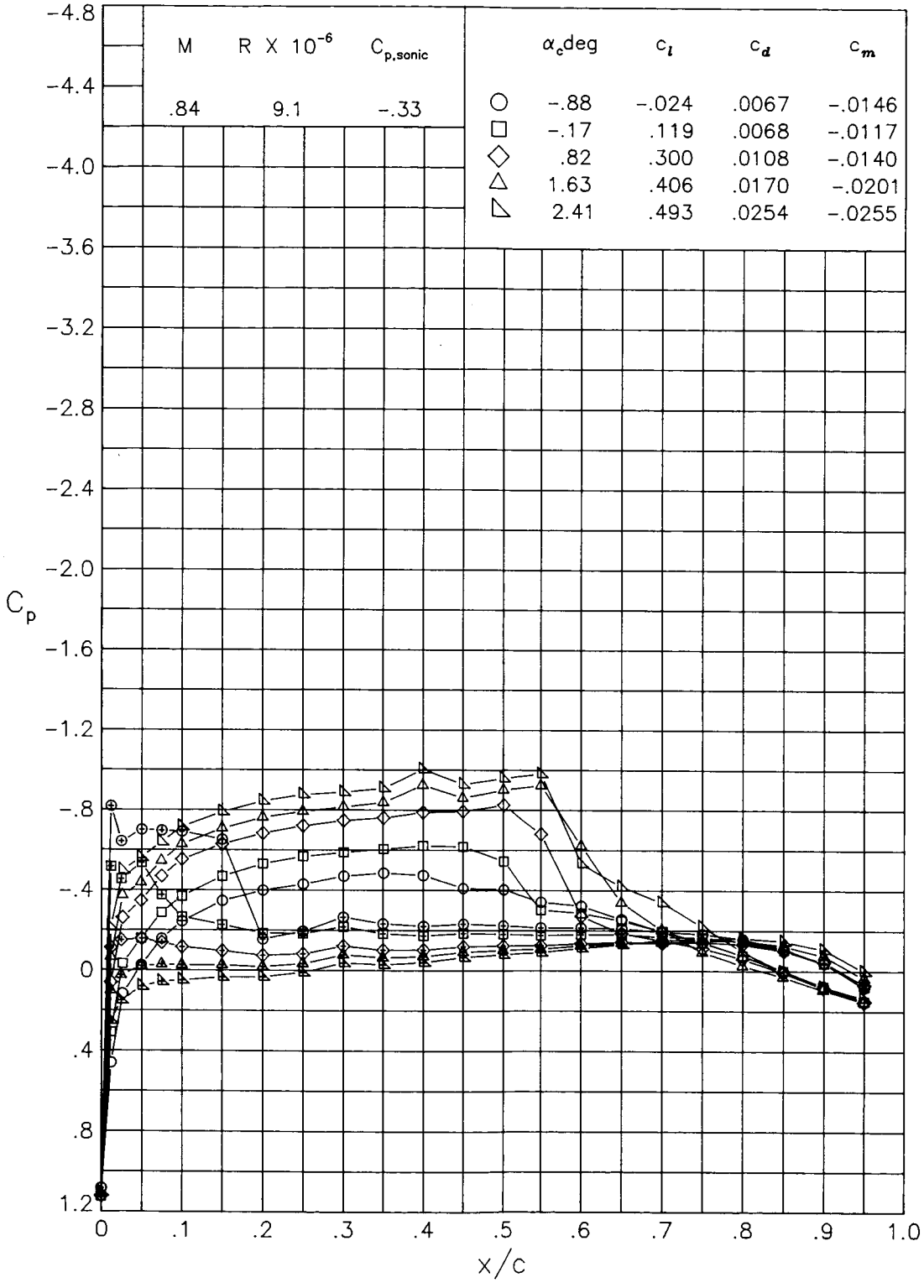

(j) $M = 0.84$; $R = 9.1 \times 10^6$.

Figure 15. Continued.

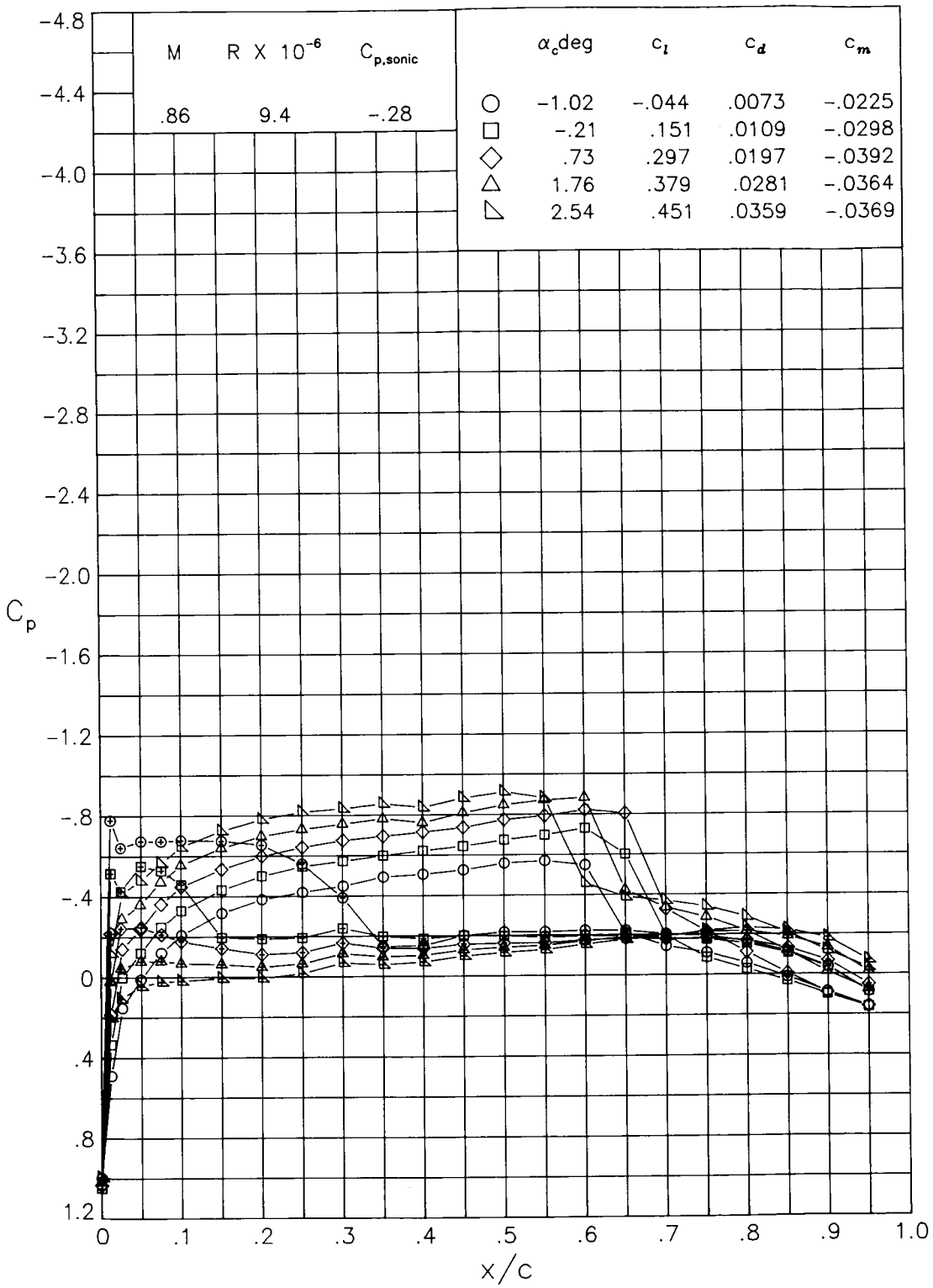

(k) $M = 0.86$; $R = 9.4 \times 10^6$.

Figure 15. Continued.

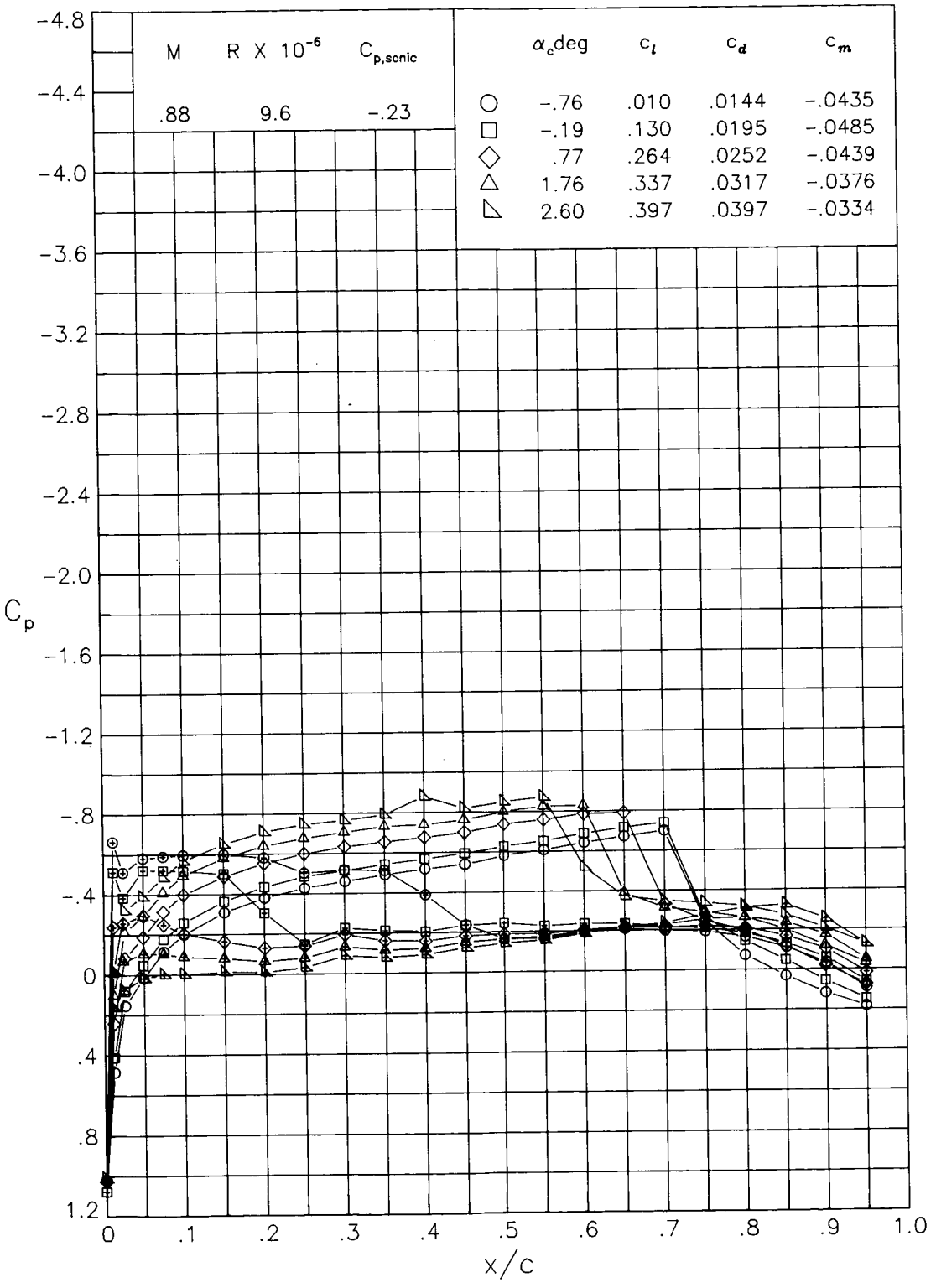

(l) $M = 0.88$; $R = 9.6 \times 10^6$.

Figure 15. Continued.

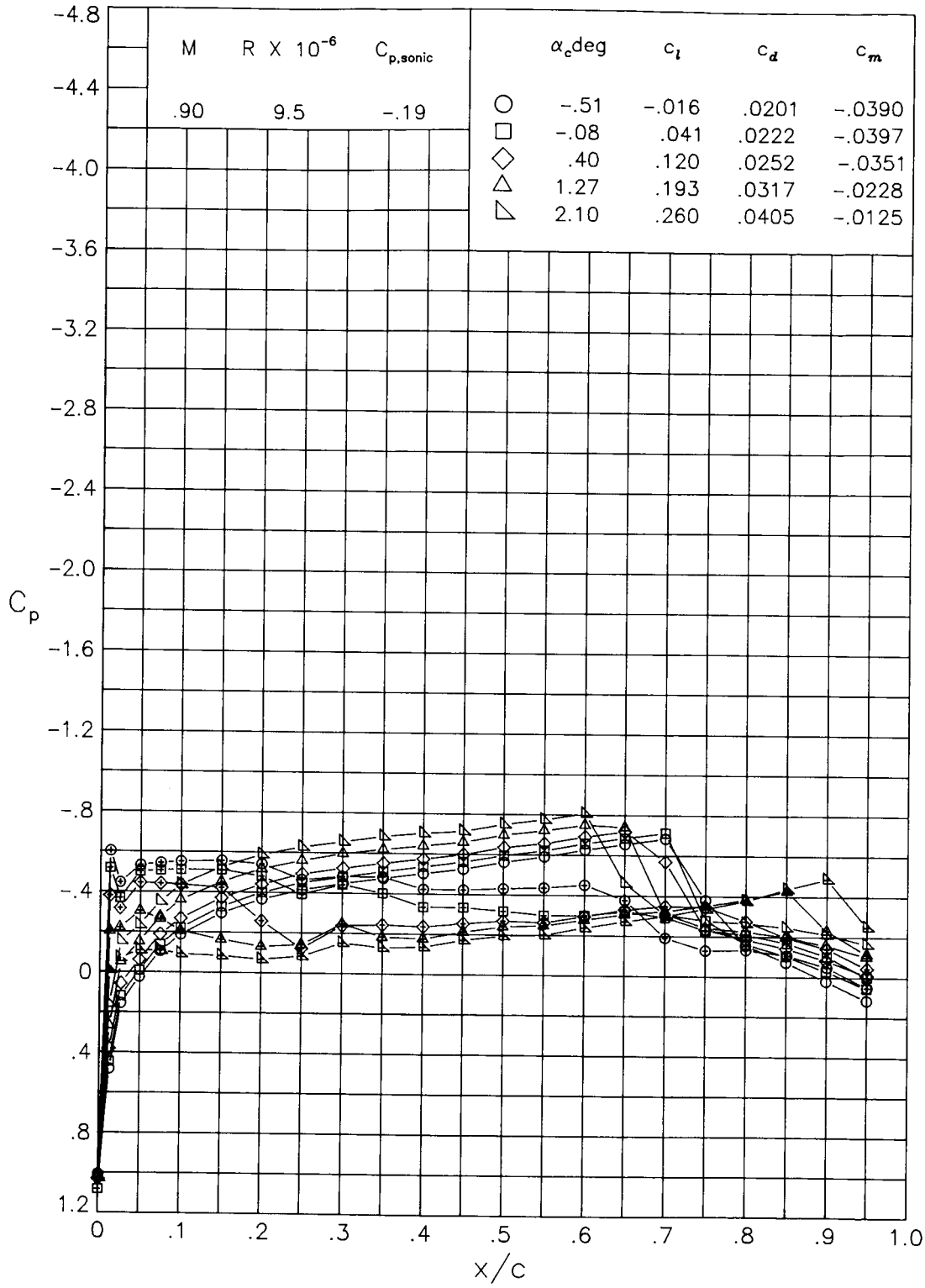

(m) $M = 0.90$; $R = 9.5 \times 10^6$.

Figure 15. Concluded.

NASA
National Aeronautics and Space Administration

Report Documentation Page

1. Report No.	2. Government Accession No.	3. Recipient's Catalog No.
NASA TM-4264 AVSCOM TR-91-B-003		

4. Title and Subtitle	5. Report Date
Aerodynamic Characteristics of a Rotorcraft Airfoil Designed for the Tip Region of a Main-Rotor Blade	May 1991
	6. Performing Organization Code
7. Author(s)	8. Performing Organization Report No.
Kevin W. Noonan	L-16855
9. Performing Organization Name and Address	10. Work Unit No.
Aerostructures Directorate U.S. Army-AVSCOM Langley Research Center Hampton, VA 23665-5225	505-61-59-76
	11. Contract or Grant No.
12. Sponsoring Agency Name and Address	13. Type of Report and Period Covered
National Aeronautics and Space Administration Washington, DC 20546-0001 and U.S. Army Aviation Systems Command St. Louis, MO 63120-1798	Technical Memorandum
	14. Army Project No.
	1L162211A47AA

15. Supplementary Notes

Kevin W. Noonan: Aerostructures Directorate, U.S. Army-AVSCOM, Hampton, Virginia.

16. Abstract

A wind-tunnel investigation was conducted to determine the two-dimensional aerodynamic characteristics of a new rotorcraft airfoil designed for the tip region of a helicopter main rotor blade. The new airfoil (RC(6)-08) and a baseline airfoil (RC(3)-08) were investigated at Mach numbers from 0.37 to 0.90. Reynolds number varied from 5.2×10^6 to 9.6×10^6. Comparisons were made of the experimental data for the new airfoil and the predictions of a transonic, viscous analysis code. The RC(6)-08 met the design goals of attaining higher maximum lift coefficients than the baseline airfoil while maintaining drag-divergence characteristics at low lift and pitching-moment characteristics nearly the same as those of the baseline airfoil. Maximum lift coefficients of the RC(6)-08 varied from 1.07 at Mach 0.37 to 0.94 at Mach 0.52 while those of the RC(3)-08 varied from 0.91 to 0.85 over the same Mach number range. At lift coefficients of -0.1 and 0, the drag-divergence Mach number of both airfoils was 0.86. Pitching-moment coefficients of the RC(6)-08 were less negative than those of the RC(3)-08 for Mach numbers and lift coefficients typical of a main rotor blade tip at high forward speeds on the advancing side of the rotor disk.

17. Key Words (Suggested by Author(s))	18. Distribution Statement
Rotor airfoils Airfoils Rotor Helicopter	[redacted] Subject Category 02

19. Security Classif. (of this report)	20. Security Classif. (of this page)	21. No. of Pages	22. Price
Unclassified	Unclassified	77	